Calhoun
Institutional Archive of the Naval Postgraduate School

Calhoun: The NPS Institutional Archive

DSpace Repository

Theses and Dissertations 1. Thesis and Dissertation Collection, all items

1976

Reduction of distortion in welded aluminum fram structures.

Brito, Victor Manuel Goncalves de

Massachusetts Institute of Technology

https://hdl.handle.net/10945/17923

Downloaded from NPS Archive: Calhoun

DUDLEY KNOX LIBRARY

http://www.nps.edu/library

Calhoun is the Naval Postgraduate School's public access digital repository for research materials and institutional publications created by the NPS community. Calhoun is named for Professor of Mathematics Guy K. Calhoun, NPS's first appointed -- and published -- scholarly author.

Dudley Knox Library / Naval Postgraduate School
411 Dyer Road / 1 University Circle
Monterey, California USA 93943

REDUCTION OF DISTORTION IN WELDED ALUMINUM FRAME STRUCTURES

Victor Manuel Gonçalves de Brito

DUDLEY KNOX LIBRARY
NAVAL POSTGRADUATE SCHOOL
MONTEREY, CALIFORNIA 93940

REDUCTION OF DISTORTION IN WELDED ALUMINUM FRAME STRUCTURES

by

Victor Manuel Gonçalves de Brito
B.S.,Escola Naval, Lisboa-Portugal(1968)

SUBMITTED IN PARTIAL FULFILLMENT OF THE REQUIREMENTS FOR
THE DEGREES OF OCEAN ENGINEER AND MASTER OF SCIENCE
IN NAVAL ARCHITECTURE AND MARINE ENGINEERING

at the

MASSACHUSETTS INSTITUTE OF TECHNOLOGY

May, 1976

Thesis
F2089

DUDLEY KNOX LIBRARY
NAVAL POSTGRADUATE SCHOOL
MONTEREY, CALIFORNIA 93940

REDUCTION OF DISTORTION IN WELDED ALUMINUM FRAME STRUCTURES

by

Victor Manuel Gonçalves de Brito

Submitted to the Department of Ocean Engineering on May 7, 1976, in partial fulfillment of the requirements for the degrees of Ocean Engineer and Master of Science in Naval Architecture and Marine Engineering.

ABSTRACT

Studies of angular distortion due to fillet welding of Aluminum stiffened plates, using GMA welding process.

Gathering of experimental data on thin plates and subsequent analysis. A procedure for predicting angular distortion is presented, using linear elastic analysis and correlation of the data. The calculation of the effects of angular distortion on plate behavior, when subjected to uniaxial compression and lateral pressure was done, allowing the prediction of loss of plate efficiency for given welding conditions, plate thickness and frame spacing. Plate preheating before welding

showed small angular distortion.

This work includes a summary and conclusions.

Thesis Supervisor: Dr. Koichi Masubuchi

Title: Professor of Ocean Engineering and
Materials Science

ACKNOWLEDGEMENT

I would like to thank the United States Government for sponsoring my three year program at the Massachusetts Institute of Technology.

I would like to thank the Portuguese Navy the opportunity of coming to the U.S. and to study in such a fine Institute.

I would like to express my appreciation to Professor Masubuchi, my thesis supervisor, for his suggestions, guidance and support during the execution of this thesis.

Finally, it would not be possible to proceed in a reasonable manner without the support and understanding of my wife Isabel. I am very grateful to her.

TABLE OF CONTENTS

Page

Abstract 2

Acknowledgment 4

Table of contents 5

List of Tables 9

List of Figures 10

1. INTRODUCTION 12

1.1 General 12

1.2 Scope of the present study 15

2. IDENTIFICATION OF DEFECTS AND IMPERFECTIONS DUE TO FUSION WELDING 17

2.1 General 17

2.2 Defects and imperfections due to fusion welding 20

2.2.1 Dimensional defects 20

2.2.2 Structural defects 23

2.2.3 Property deficiencies 29

3. THE EFFECT OF WELDING FABRICATION DEFECTS ON SHIP DESIGN AND SHIP PLATING BEHAVIOR 30

3.1 Effects of initial distortion 30

3.2 Effect of out-of-plane angular distortion using theory of orthotropic plates 32

3.3 Actual plate distortion for displacement type ships, in service 34

3.4 Collapse of shell plating due to compressive loads and lateral pressure 35

Page

3.4.1 Basic definitions of structure and stresses .. 35

3.4.2 Collapse modes 36

3.5 Plating for Surface Effect Ships (SES) 39

4. EXPERIMENT 43

A - PHASE I 43

4.1 Description and results of the experiment 43

B - PHASE II 64

4.2 Description and results of the experiment 64

5. ANALYSIS OF OUT-OF-PLANE DISTORTION DUE TO FILLET WELDING IN ALUMINUM ALLOY PLATING 70

5.1 Summary of previous work 70

5.2 Correlation of data from present experiments with previous analytic models 74

5.3 Analysis of out-of-plane distortion after welding 75

5.3.1 General 75

5.3.2 Development of a relationship between the equivalent uniform moment M_o induced during fillet weld and the central deflection 81

5.3.3 Generation of empirical values for the equivalent uniform moment M_o 82

5.4 Relationship between parameters M_o and C 87

5.4.1 Derivation of relationship 87

5.4.2 Numerical calculations 89

5.5 Allowable out-of-plane distortion 90

5.5.1 General 90

5.5.2 Aluminum structures and the US Navy permissible plate unfairness standard 96

Page

5.6 Design of a grillage subjected to a lateral load 98

5.7 Effect of initial out-of-plane deflection on plate element design, using Marguerre's theory of plates and the equivalent elastic moment concept 102

5.7.1 Analysis 102

5.7.2 Effect of initial distortion on the inplane load and lateralpressure 108

6. CONTROL AND REDUCTION OF DISTORTION 115

A - General 115

B - Methods of reducing distortion in fillet welding 116

6.1 Choice of welding process 116

6.2 Welding sequence 117

6.3 Forced cooling 117

6.4 Plate preheating 118

6.5 Use of external constraints 121

6.5.1 General 121

6.5.2 Analysis of distortion reduction in orthogonally framed plates using pre-bending 122

6.6 Flame heating 124

6.7 Other methods 125

7. SUMMARY AND CONCLUSIONS 127

7.1 Summary 127

7.2 Conclusions 128

LIST OF REFERENCES 131

APPENDICES 135

Page

1. Materials used in experiments and their properties 135
2. Guidelines for GMA welding process 137
3. Relationship between M_o and C 139
4. Plate behavior under longitudinal compression and lateral pressure 142
5. Analysis of distortion reduction on orthogonally framed plate, using pre-bending 145
6. Parameters included in figure 3.3 148
7. Computer program developed to calculate the dimensional parameters AA1, AA2, TT, used in section 5.4 and appendix 3 149

LIST OF TABLES

Page

2.1 Welding processes 18

2.2 Common forms of distortion and shrinkage 21

3.1 Relationship between N and q for achieving w/h = 1.6 33

3.2 Parametric variations of design input for concept SES design 42

4.1 Experiment dimensions 45

4.2 Experiment welding conditions 45

4.3 Plate displacement (w) due to distortion 54

4.4 Mean value of the steepest angle 63

4.5 Mean value of the angle between the horizontal reference (1 inch) and the secant s (on the weld line) 63

4.6 Experiment dimensions 65

4.7 Experiment welding conditions 65

4.8 Plate displacement (w) due to distortion 69

5.1 Welding parameters 74

5.2 Values of M_o for experimental data 84

5.3 Summary for parameters TT, AA1 and AA2 for several frame spacing (h = 1/2 in) 91

5.4 Calculation of revised values of C using the concept presented in section 5.4 93

5.5 Welding distortion (w_o) vs. USN specs.(tol) 99

5.6 Allowable σ_A and p for several plate dimensions . 106

5.7 Calculation of w/h max 111

5.8 Loss in load carrying capacity ε (percentage) .. 114

6.1 Reduction of distortion due to pre-heating 120

LIST OF FIGURES

Page

2.1 Welding defects 24

2.2 Effect of porosity on tensile properties of Al 5083/5356 welds 27

2.3 Fatigue life vs. fracture porecount 27

2.4 Effect of depth of incomplete penetration on ultimate tensile strength 27

3.1 Relationship between N and q for achieving w/h = 1.6 33

3.2 Initial welded plate distortions 35

3.3 Modes of failure in uniaxial compression 38

3.4 Loads on SES 42

4.1 Experiment plate dimensions and configuration ... 44

4.2 Welding sequence 46

4.3 Clamping system 46

4.4 Measurement of plate displacement 49

4.5 Ideal measurement system 49

4.6 Profile of plate displacement w due to angular distortion 51

4.7 Measurement stations 56

4.8 Plate profile at the weld lines 57

4.9 Profile stations 62

4.10 Schematic of plate pre-heating 66

4.11 Schematic of plate pre-heating 66

4.12 Profile of plate displacement w due to angular distortion 67

Page

5.1 Free and constraint joint 71

5.1a Calculation of the angle at the weld lines, using the FEM computer program (10) 76

5.2 Experimental and predicted deformation 77

5.3 Plate configuration 79

5.4 Calculation of k (γ) 85

5.5 Calculation of M_o 86

5.6 Coefficient C as function of θ_o, M_o, b, γ (h= 1/4") 92

5.7 Comparison between calculated, predicted and experimental central plate deflection 94

5.8 Experimental and allowable distortion 97

5.9 Load and plate configuration 104

5.10 Yielding criterion 104

5.11 Effective width b_e 104

5.12 Allowable compressive longitudinal stress in function of lateral pressure and frame spacing .. 109

6.1 Forced cooling 120

6.2 Pre-bending systems 121

6.3 Pre-bending system for orthogonally framed plate 123

1. INTRODUCTION

1.1 - General

Ship Structures are designed for containing whatever payload, propulsion and functional systems were sought to be necessary for the ship's mission and also for sustaining the loads induced by the interaction of the whole Ship System with the environment, during the ship's life time.

These loads are static and dynamic. Dynamic loads are random in nature and may be due to impact from waves, wind action, explosion, collision, etc..

For displacement hull type ships - slender ships -, the primary strength of a ship, if evaluated by a deterministic method, is usually calculated by modelling the ship as a free-free beam, in which the load distribution curve is the difference between weight and buoyancy distribution curves. Integrating this load twice over the length, we get the bending moment distribution curve; this, in general, has its maximum around the midship section. This allows the calculation of the scantlings for the structural elements contributing to the longitudinal strength, i.e., those elements that are continuous well after and forward of amidships.

Amongst these structural elements, the envelope made by the strength deck, bottom and side shell represents a major part in weight and in strength.

For reducing weight but keeping the same strength, these flat plates, and curved shells that make up the hull envelope, are reinforced with stiffners welded to the main plate, thus allowing reduction of thickness of the shell.

The interaction between the ship and the sea,produces alternating stresses in the hull girder and these tensile and compressive stresses are particularly important in the calculation of the scantlings of the strength deck and bottom, which are the members farthest apart to the neutral axis. The designer needs to account for this fact, making the calculations in such a way that failure by compressive buckling or tensile yielding of a grillage or inter-stiffener panel won't occur. Also the hull girder must be designed to avoid failure due to fatigue caused by the forementioned alternated compressive and tensile stresses occurring during the ship's life.

Displacement hull type ships with small length to depth ratio and Advanced Concept vehicles like Air-Cushion Vehicles, Hydrofoil Ships, Semisubmersibles and Catamarans, can't be modeled as a simple beam, for the purpose of calculating the primary strength because the stresses due to transverse bending becomes important and must be considered. The use of Finite Element Analysis is adequated for this calculation.

The calculation of the scantlings obeys to the design criteria by specifying the allowable stresses accordingly to the location of the members and its dimensions as we

will develop later. The allowable stresses are a percentage of the yielding stress or of the ultimate tensile stresses, and represent the limit tolerated for the service stresses.

Under this criteria the full properties of the material aren't completely used because a safety factor must be included, allowing for uncertainties in analysis, material properties, fabrication, and in loading schedule along the ship's lifetime.

Considering a typical ship flat panel, we may say that it is subjected to longitudinal inplane loads due to bending and torsion of the hull girder and normal loads due to hydrostatic pressure, cargo, etc.. It has been observed that for displacement hull type ships the hogging bending moment is generally much larger than the sagging bending moment, therefore the combination of compressive inplane stresses and lateral loads on the ship bottom becomes critical and must be investigated for avoiding plate instability or plate buckling.

Ideally, this refered panel should be flat, but because of moments induced during the welding of the stiffeners to the main plate, an initial distortion is produced, which reduces the efficiency of the plate to withstand the loads and the resistence against buckling is greatly reducing. This is undesirable mainly from the structural and weight carrying standpoint, because more material needs to be added for achieving the same strength;

this additional weight would not be necessary on the absence of imperfections and defects; it also may create hydrodynamic disturbances during the ship motion in the bottom and side shell; the appearance of this distortion in recreation boat fabrication may also require cosmetic work to cover it.

1.2 - Scope of the present study

The above mentioned out-of-plane angular distortion do to fillet welding of stiffeners to plates, which is an imperfection due to fabrication methods, is the main interest on the development of this thesis. As mentioned in ref. 17 angular distortion in steel erection has been studied and design rules have been developed; in Aluminum, there is already a large amount of work done by former students at the M.I.T.'s Department of Ocean Engineering, under the supervision of Professor K. Masubuchi (ref.4,5,10). In this thesis their work will be extended by gathering data in some large dimension plates and subsequent analysis, in order to possibilitate the creation of a satisfactory mathematical model for predicting angular distortion due to fillet welding and also the study of effective means of reducing this distortion.

Experiments will be conducted in Aluminum alloys - series 5xxx- weldable magnesium-aluminum alloys, largely

used in marine applications given their good characteristics for service in ocean environment.

2. IDENTIFICATION OF DEFECTS AND IMPERFECTIONS DUE TO FUSION WELDING

2.1 - General

Welding is, by far, the most common joining technique used in today's shipbuilding; for each ship constructed, joining by fillet welding accounts for about 80% of the total structural joining fabrication using welding. (21) Repair of welding defects, structural mismatching and misalignment may weight high in the construction cost. This factors make the study of fillet welding in flat plates and curved shells, necessary for understanding and predicting the effect of this fabrication process on the behavior of the structure, and for developing techniques conducent to the avoidance of its damaging effects on the structural strength.

From the most common welding processes used in structure joining - summarized in table 2.1, we must restrict ourselves to continuous fusion welding processes and with these, we will select the ones used in Aluminum Alloys because this is the structural material we are more interested in investigating, both by the experimental and by the analytic point of view.

The processes used today for welding Aluminum are Gas Shielded Arc welding, either Gas Metal Arc (GMA) or Gas Tungsten Arc (GTA); energy sources like Laser Beam

Welding Processes	Plastic Welding	Forge W.	Hammer, Die, Roll
		Resistence W.	Spot, Seam, Projection Flash, Upset,Percussion
		Pressure W.	
		Cold W.	Pressure,Ultrasonic Vibrations
	Fusion Welding	Gas W.	Air-acetylene, Oxy-acetylene, Oxy-hydrogen Gas-pressure
		Thermit W.	
		Induction W.	
		Braze W.	Torch, Dip, Furnace, Induction, Resistance, Carbon-arc
		Arc W.	Metal electrode: Shielded arc, Inert-gas arc, Submerged arc, Shielded stud Unshielded Metal arc and Stud Carbon electrode: Shielded arc, Inert-gas arc

Table 2.1 - Welding Processes (14)

and Electron Beam are also being used in a developmental state and information about this two processes is scarce.

Using GMA or GTA welding processes, the base plate, or workpiece and the filler wire are melted to the welding point due to heat generated by an electric arc established between the end of one metallic electrode and base plate material. This melting process is envolved in inert gas shielding for avoiding oxidation.

We must emphasize that Aluminum and Aluminum Alloys rapidly develop a tenacious refractory oxide film, when exposed to air. This film must be removed or broken up to permit proper coalescence of the base and filler material in fusion welding. The oxide film may be removed by fluxes or by action of welding arc in an inert gas atmosphere or by mechanical or chemical means.

As the melting is proceeding, a molten pool is formed, the temperature raises in the adjacent material that tends to expand, but it is prevented of a free expansion by the remaining plate still colder because the heat flow is not instantaneous. As the temperature distribution is not uniform and the plate, hereby assumed to be continuous and restrained by the structural boundaries (frames, other components etc.), a nonuniform transient stress field is generated. Depending on the stress level and temperature at any particular point, plastic and elastic material behavior takes place. The plate will then start to cool down, again stresses and

strains will be building up, but in a reverse sense, shrinkage takes place and finally when the plate reaches room temperature, an energy balance is achieved. When strain energy due to deformation (out-of-plane) or change of dimensions (shrinkage - planar), equates the energy absorbed by the plate in the form of locked in stresses, equilibrium is achieved. This strain energy is the difference between the heat input and the sum of heat lost by radiation, heat energy necessary to melt the filler material and heat lost by conduction to the working plate or other connected external structures.

2.2 - Defects and imperfections due to fusion welding

A systematic classification of this welding defects are mentioned in reference 14 and they are grouped in three main categories:

Dimensional and Structural defects and Property deficiencies.

These effects are dependent on the welding process, welding parameters and material and filler wire properties and correct balance of these will ensure the least damaging effect regarding the service.

2.2.1 - Dimensional defects

Includes Warpage, Mismatching, and incorrect weld

Table 2.2- Common Forms of Distortion and Shrinkage

TRANSVERSE SHRINKAGE 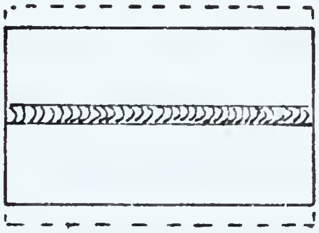	LONGITUDINAL SHRINKAGE 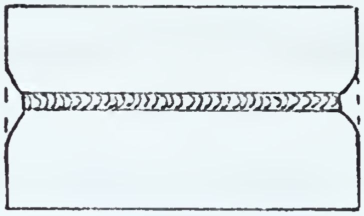
LONGITUDINAL BOWING 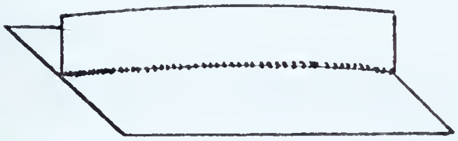	OUT-OF-PLANE OR ANGULAR DISTORTION 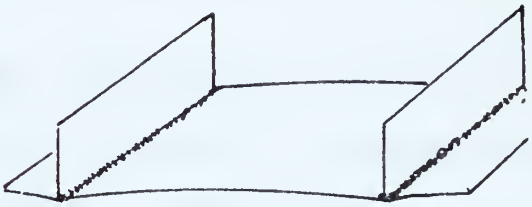
BUCKLING 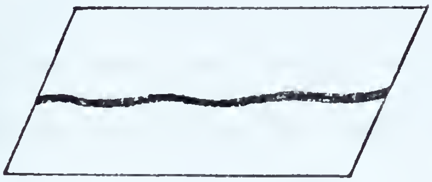	ROTATION DISTORTION 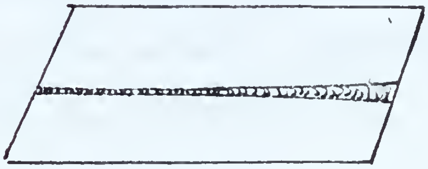

size and profile.

i) Warpage is an overall twisting and bending of the structure.

Mismatching is an incompatibility of dimensions and misalignment when joining subassemblies previously independently welded.

These two defects or fabrication imperfections are due to thermal stresses due to the transient behavior of the welding process as mentioned in 2.1 . They are very complex and breakdown of these defects is required for better understanding of the effect of fusion welding.

We may say that warping and mismatching is due to deformation and shrinkage generally referred as distortion, whose most common forms are included in table 2.2 .

Distortion and the residual or locked in stresses built up during welding will alter the structure capability to withstand loads, as will be mentioned in section 3.

ii) Incorrect weld size and profile (weld size is specified as the length of the leg of the largest isosceles triangle that can be inscribed in the cross section of the weld - L - in fig. 2.1).

Under size welds will fail to satisfy the structural requirements of the joint and may be corrected by additional beads of filler metal.

Oversize welds will tend to create a notch effect and introduce additional shrinkage.

Weld profile defects - fig.2.1- include excessive concavity and insufficient leg that result in defficient strength in the fillet; undercut and overlap that produce a notch effect which tends to lower the overall joint strength by stress concentration; excessive convexity that is more sensitive to the entrapment of slag inclusions, the formation of voids, and shrinkage in the weld metal.

2.2.2 Structural defects: figure 2.1

Include porosity, non metalic inclusions, incomplete fusion of the parent metal, lack of penetration, cracking, surface defects, metallurgical discontinuities.

Porosity is spherical, all the others are planar defects.

These defects may reduce the mechanical properties of the weld metal, some are neither visible, nor detectable using non-destructive testing, therefore the prediction of welding conditions for avoiding them is of the most interest and may save repair work necessary to fix the weldment.

i) Porosity, that is caused by gaseous products of chemical reactions taking place in the molten weld metal, or by release of dissolved gases,is one big concern in aluminum welding.

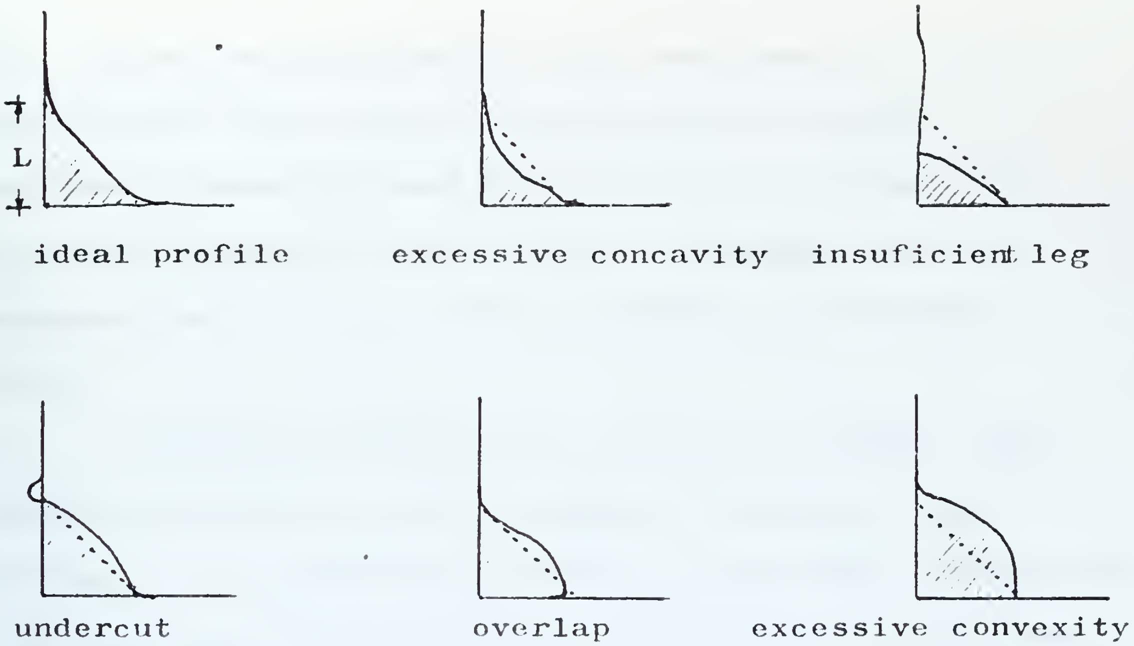

ideal profile excessive concavity insuficient leg

undercut overlap excessive convexity

Dimensional Defects

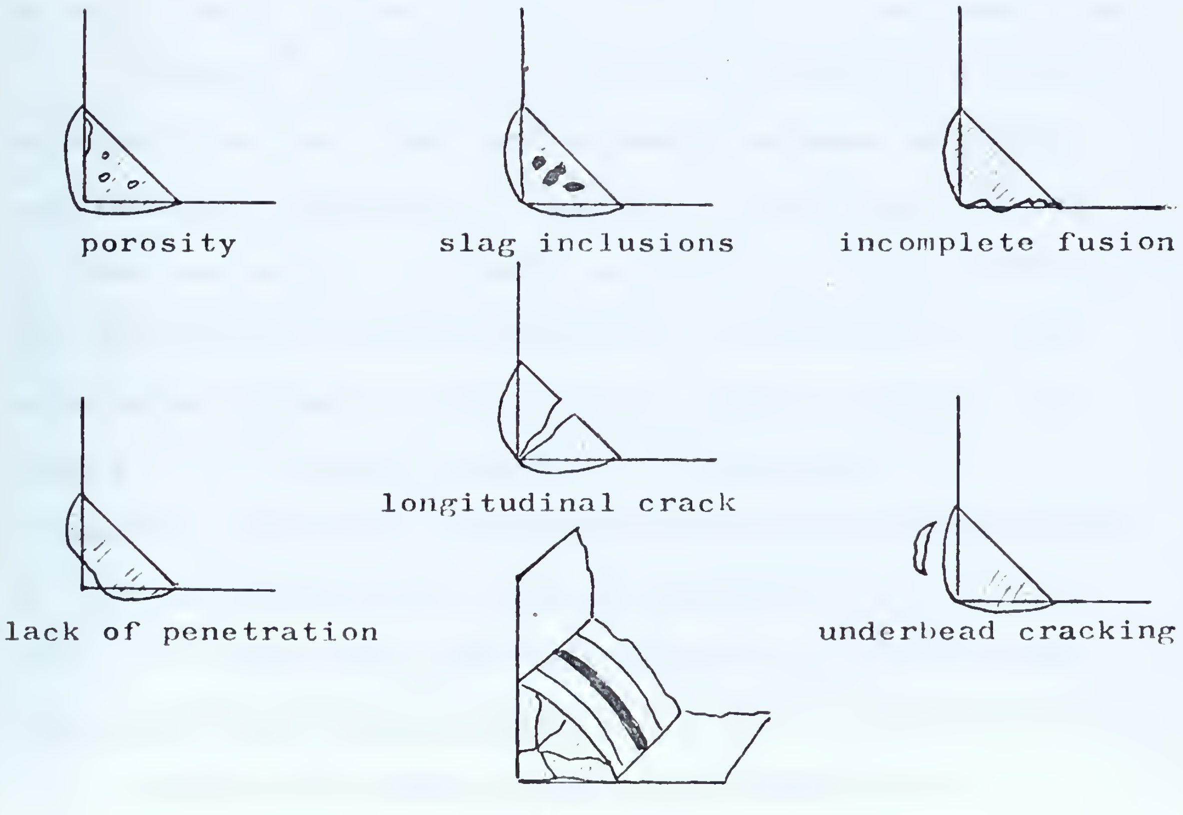

porosity slag inclusions incomplete fusion

longitudinal crack

lack of penetration underbead cracking

crater cracks

Structural Defects

Figure 2.1- Welding Defects (from reference 14)

Oxygen and hydrogen are the most harmful contaminants, thus these elements must be kept to acceptable concentrations at the site of welding. It has been documented (2,20) that is hydrogen the entrapped gas, forming voids or porosity in aluminum alloys.

Atmospheric humidity as a source of hydrogen has a significant effect on the formation of porosity (20). Although in low atmospheric humidity conditions variations in porosity are not significant with humidity variations, and the absolute number of porosities is small, the porosity increases in high atmosperic humidity. With humidity over 85% porosity can be attributed to condensation of water vapor on the external surface of electrode wire.

Porosity affects the mechanical properties of the weldment, but the exact relationship between porosity and tensile properties or others, is difficult, because it does not exist a reliable way of evaluating porosity. The best known is the percentage of void space in the weld metal volume of cross section area. Figure 2.2 from (2) gives a trend of the variation of elongation and yield strength with porosity for weldment of 5083 Aluminum Alloy using using GMA and 5356 filler wire. It seems that moderate amounts of porosity does not affect these properties.

Fatigue strength is much more sensitive to porosity. Fig. 2.3 shows the relationship for 1/4 inch

thick 2219 and 2014 Aluminum Alloy using GTA. Porosity at or near the surface is more harmful to fatigue strength than deep seated pores.

The effect of porosity on notch toughness is not determined yet.

ii) Lack of penetration, reduces the tensile strength of the weld metal. Figure 2.4 shows the trend of the effect of depth of incomplete penetration on the tensile strength for an Aluminum Alloy with 3.5 to 5.5% Mg using GMA process.

Because of the notch effect exerted by lack of penetration, the fatigue strength is markedly lowered.

iii) Incomplete fusion, is resultant from oxide inclusions, has similar effect to that of porosity. It was not found to be seriously damaging unless the defects are numerous or appreciable in size. If the incomplete fusion is extensive enough to generate a planar-shaped flaw, it will act much like lack of penetration.

iv) Weld reinforcement, verified in butt joints has characteristics of an increase in the cross section of the weld metal, and a discontinuity in the metal section acting as a local stress raiser. If the weld metal is the weakest link in the chain of microstructures across the joint, the presence of reinforcement is beneficial because will enhance the transverse strength

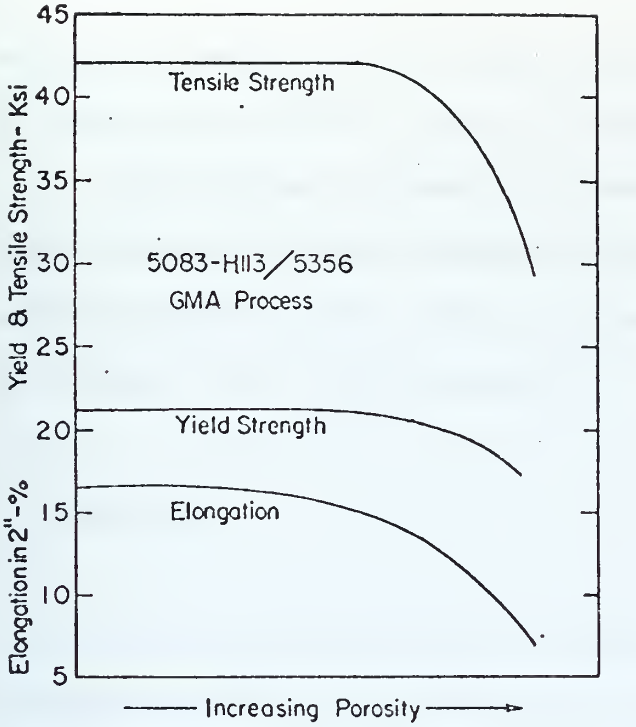

Fig.2.2—Effect of porosity on tensile properties of 5083/5356 welds(2)

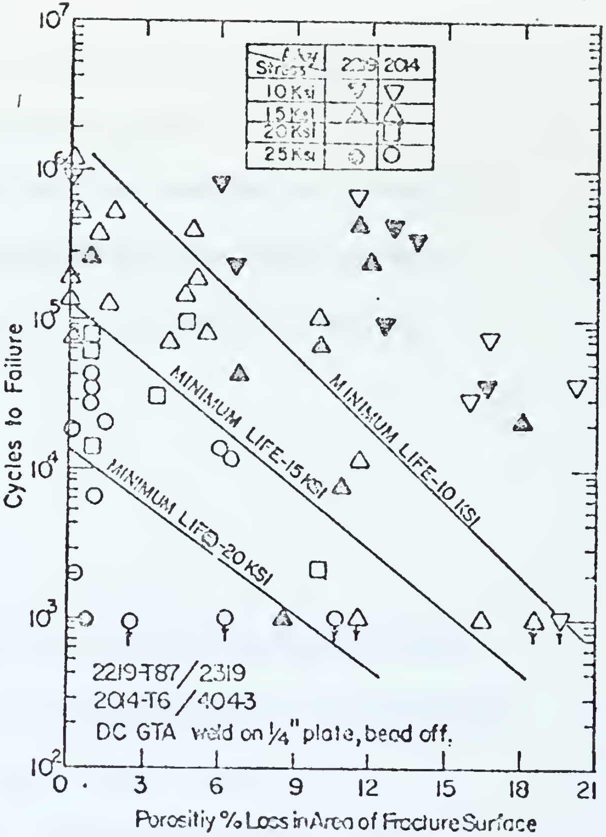

—Fatigue life vs. fracture pore count for ¼-inch thick 2219 and 2014(2)

FIG. 2.3

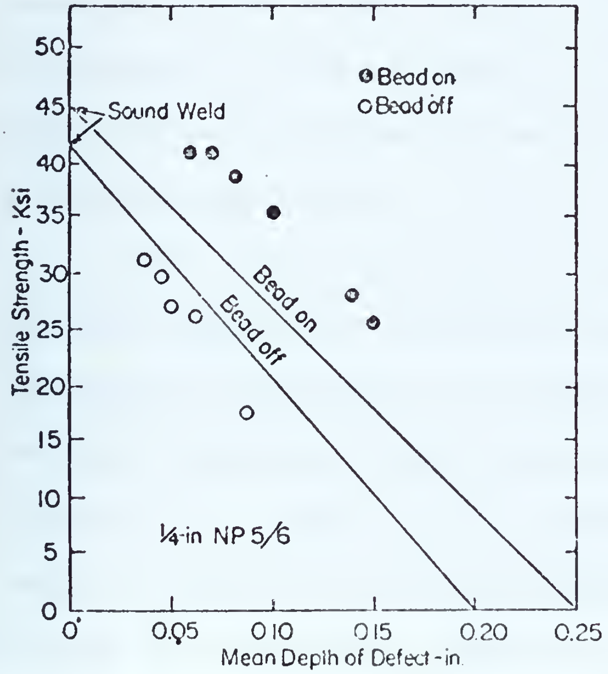

—Effect of depth of incomplete penetration on ultimate tensile strength: ¼-inch NP 5/6 specimens(18)

FIG 2.4

NOTE: All these 3 figures are from reference 2.

of the weldment and the locus of failure may be transfered to the heat affected zone of the base plate.

The fatigue strength is lowered as the reinforcement angle becomes sharper because of raising of notch effect, but undercut or under fill is found to be more damaging to fatigue than reinforcement.

v) Cracking

Cracking damages the integrity of the weldment and it can be either hot cracking (cracking above the solidus) or cold cracking (cracking below the solidus).

Hot cracking is minimized by proper choice of the welding filler metal, which frequently results in sacrifice of weld strength. In the Heat Affected Zone (HAZ) it is minimized by reducing the number of passes and heat input (21).

Cold cracking depend on composition, microstructure and the degree of restraints imposed on the cooling weld, therefore distortion and locked-in stresses, directly produce cracking, which are known as shrinkage welding cracks (14). They can be transverse, longitudinal or crater cracks (associated with high heat concentration in the arc welding), figure 2.1. Underbead cracking is believed to be related with hydrogen and takes place in shielded arc welding.

vi) Surface defects

Includes surface irregularities, holes etc.. They are due to poor workmanship or improper welding technique and may cause loss of strength if in large extension.

2.2.3 - Property deficiencies

Includes inadequate mechanical properties or corrosion resistence in comparison with the parent metal, may result from improper selection of filler metal or welding process.

3. THE EFFECT OF WELDING FABRICATION DEFECTS ON SHIP DESIGN AND SHIP PLATING BEHAVIOR

Thermal stresses due to welding, induce stress fields and deformations on the hull structural elements, that complicate the design procedure and are likely to reduce the structure efficiency for withstanding the loads.

The purpose of this section is to relate the structural design and distortion, and to assess the effect of the later on the former.

3.1 - Effects of initial distortion

The distortion we are interested in is the resultant from the fabrication process, i.e., imperfections arising from the joining and building up operations, namely welding.

These distortions are associated with reactions, or locked in stresses, been all built up from thermal stresses generated during welding due to non-uniform transient heating, of the structure.

Our main concern is the structural resistance against buckling, when compressive forces and normal loads are present, and once it was found (3) that buckling is much more sensitive to out of plane angular distortion,

rather than residual stresses, we may pursue without further reference to these reaction stresses by themselves, therefore considering only the stiffeness and the strength of a stress free but distorted plate.

An initially deformed plate loses stiffeness immediatly after a load be applied, therefore the efficiency of a plate, defined as the ratio of the total contraction of a perfectly plane plate to that of a deflected plate, is continually reducing as the load increases, even before buckling occurs. It has been recognized that this loss of efficiency is small until buckling loads are approached, particularly in plates which are longer than they are wide. Even for wide plates, it has been shown (3), by using elastic analysis that initial deflection does not, in general, lower the efficiency of plating significantly, unless the plating is very thin. It was suggested that this initial deflection should not exceed 0.30 of the thickness if great loss of efficiency is to be avoided.

Unfortunately progress of buckling and deflection growth are often present in the bottom of transversly framed and welded construction ships, and the best remedy known so far is to alter the system of framing to longitudinal framing. Other way would be the reduction of the distortion (wide plates).

This reduction of distortion may be achieved either by changing of design, or prewelding mesures or post

welding distortion removal techniques and we will try to develop systematic guidelines convenient for aluminum, by performing experimental tests and subsequent analysis.

3.2 - Effect of out of plane angular distortion using theory of orthotropic plates

From a parametic study, using the theory of orthotropic plates developed in ref. 8 for plates with initial distortion and with inplane and transverse loads we can see the influence of a initial distortion of 0.50 of the thickness vs. no initial distortion. Fig. 3.1 represents the relationship between the inplane forces N and the uniformly applied transverse loads q (both in form of nondimensionalized quantities for simplicity). These plottings are made for two different boundary conditions and frame spacing as we can see in the description of the Fig 3.1and Table 3.1 .

The curves represented are the locus of the limiting values for N and q if we want to achieve a final value of the initial distortion w to thickness h ratio of 1.6.

For a constant value of q a initially flat plate will allow about 20% more of inplane force.

Allowing the same inplane N a initially flat plate will carry a much larger transverse load.

Relationship between N*and q* for achieving w/h=1.6

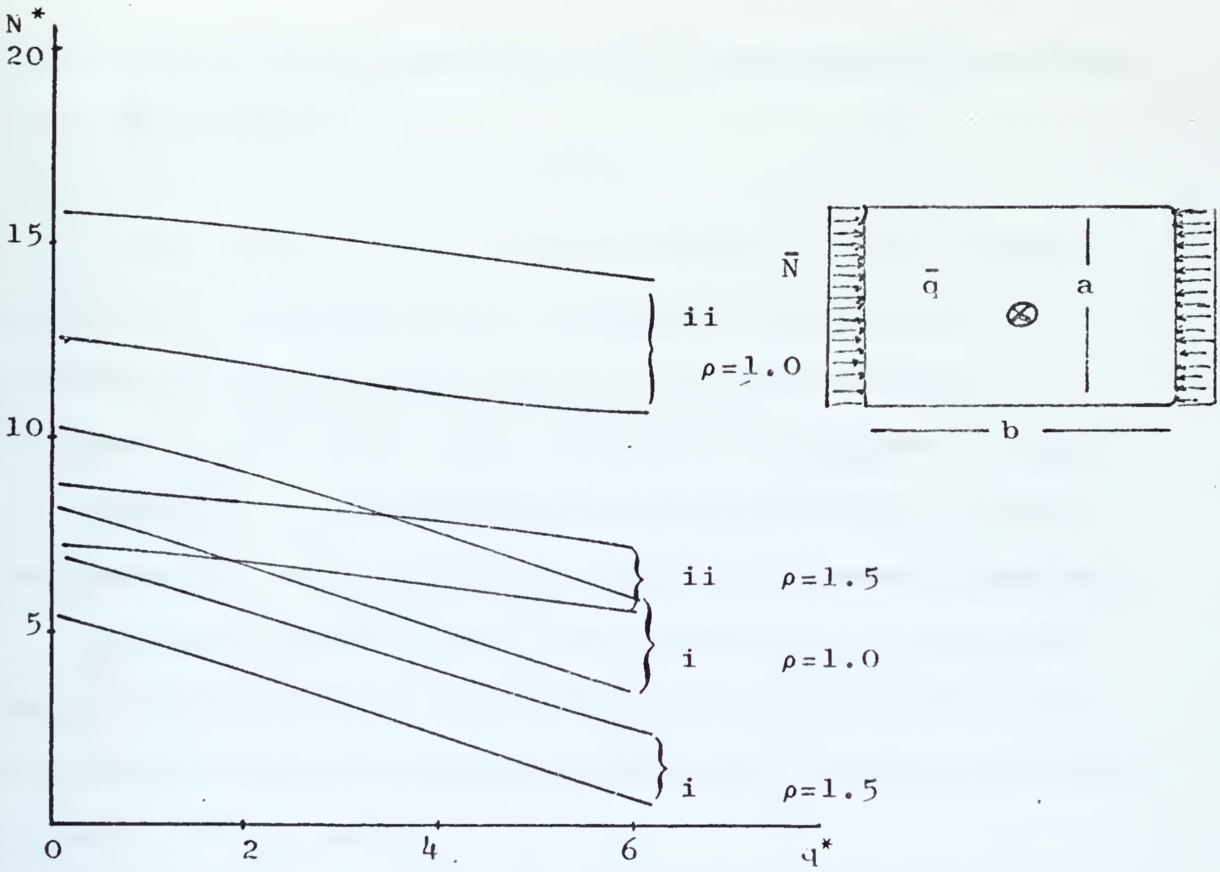

Figure 3.1

bc's		i				ii			
	ρ	1		1.5		1		1.5	
q*	w	0	.5h	0	.5h	0	.5h	0	.5h
0		10.58	8.24	7.10	5.30	15.60	12.50	8.72	7.17
2		9.02	6.67	5.40	3.90	15.30	11.91	8.18	6.70
4		7.49	4.94	3.90	2.34	14.72	11.05	7.75	6.00
6		5.88	3.50	2.46	.58	14.19	10.66	7.07	5.49

$\gamma=1$ $\eta=1$ boundary conditions
i ±b/2 edges clamped
±a/2 edges simply supported
ii all edges are clamped

Table 3.1

(explanation of q , N etc. is included in Appendix 6).

3.3 - Actual plate distortion for displacement type ships, in service

The author of (3) collected data of actual plate deformation in several U.K. frigates and plotted a statistical curve of the plate central deformation referred to the plate width factor or slenderness factor $(\beta = \frac{b}{h}\sqrt{\frac{\sigma}{E}}$, b = stiffener or frame spacing, h = plate thickness, $\sigma_0 =$ material yield stress, E = Young's Modulus).

We must mention that this deflection is not only due to fillet welding, but also includes permanent set due to ship operation (hydrostatic load, bending stresses, slamming, wave loads).

The curve representing the RMS values of the central deflection is plotted in figure 3.1.It was found that all the deformations were of mode 1. It is suggested that the stiffener web thickness (H) influences the central deflection and two equations taken from regression analysis are proposed as follows:

$$\frac{w}{t} = k\beta^2\left(\frac{H}{h}\right)^2 \qquad \text{if} \quad H<h \qquad \begin{cases} k = .12 \text{ if} & \beta \leqslant 3 \\ k = .15 \text{ if} & \beta \leqslant 3 \end{cases}$$

$$\frac{w}{t} = k\beta^2 \qquad \text{if} \quad h \geqslant H \qquad k \simeq .12 - .15 \qquad (3.1\ a,\ b)$$

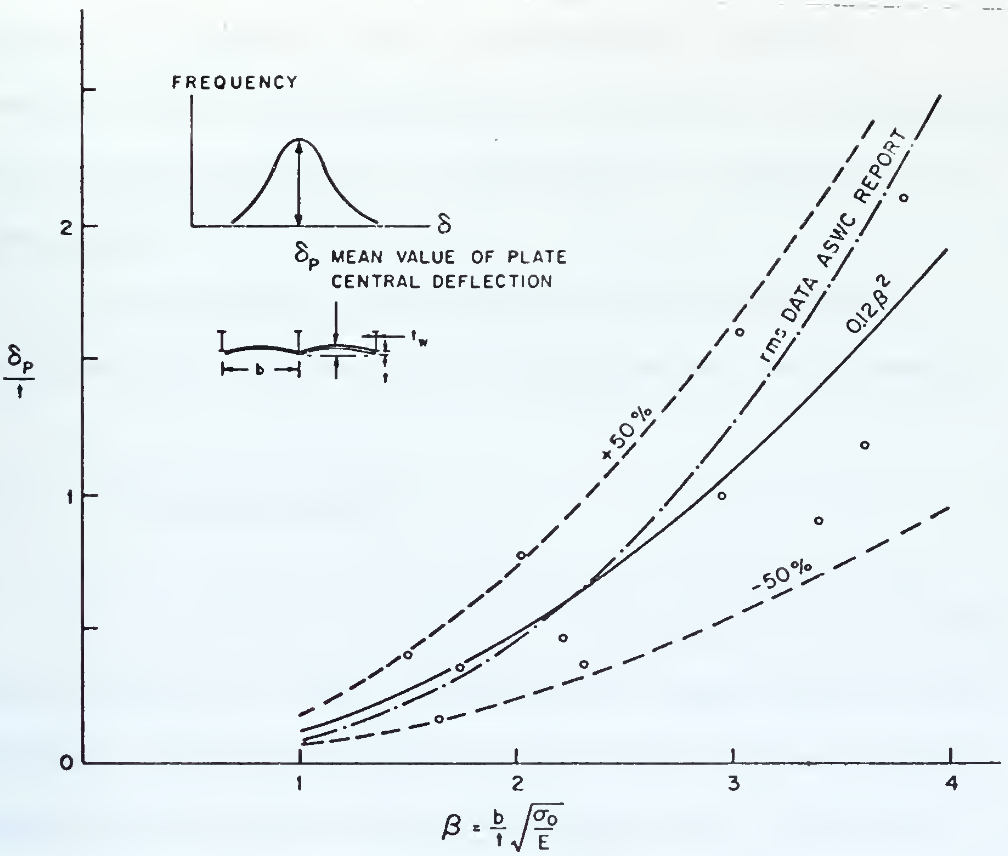

FIG 3.2 Initial welded plate distortions (3)

3.4 - Collapse of shell plating due to compressive loads and lateral pressure

3.4.1 - Basic definitions of structure and stresses

Before enumerating the collapse modes, we must refer to a widely used classification of ship structure and related stresses (15) that will help use to situate the collapse modes:

i) Primary: the hull when considered in its totality

ii) Secondary: stiffened gross panels of plating bounded by side shell, transverse and longitudinal

bulkheads or other lines of orthogonal support. Commonly they are denominated grillages (if orthogonally stiffened) or panels (if stiffened or framed in one direction).

iii) Tertiary: unstiffened plate elements. Supported by transverse and longitudinal stiffeners.

3.4.2 - Collapse modes

The collapse behavior of orthogonally stiffened welded grillages under compressive loads and lateral pressure, situation found in the outer hull, can be assumed to fall into the following four categories:

i) Plate failure

ii) Interframe flexural buckling of stiffeners and plating

iii) Interframe tripping of stiffeners and plating

iv) Overall grillage instability

i) Plate failure

In this case, the ultimate strength of the plate panel , the tertiary structure, is exceeded before extensive yield occurs in the stiffeners. The reduction of load in the plating proceeds more rapidly than the increase of load in stiffeners so that the ultimate load for the stiffened plate is reached before stiffener

failure occurs.

Out-of-plane distortion directly influences this mode of failure ; the lateral pressure carrying capability is diminished, but as membrane tension stresses are building up, the plate might carry a larger compressive load (if the welded edges remained straight and if they do not move by translation).

ii) Interframe flexural buckling of longitudinals

Failure in this case occurs by beam-column like flexural buckling of stiffeners and plating between transverse frames. Initial flexural deformation of the stiffeners, resultant of longitudinal shrinkage of the weldment and (or) resultant of transverse shrinkage due to welding in the normal direction, will reduce the column flexural buckling strength.

This deformation, along with the lateral pressure on the plate, will produce the type of buckling illustrated in figure 3.3b .

iii) Interframe tripping of stiffeners and plating

This form of failure - figure 3.3c - is likely to occur in short flexurally stiff girder and in stiffeners with low lateral - torsional rigidity (flat bars, bulb plates). The eccentric longitudinal load will make the

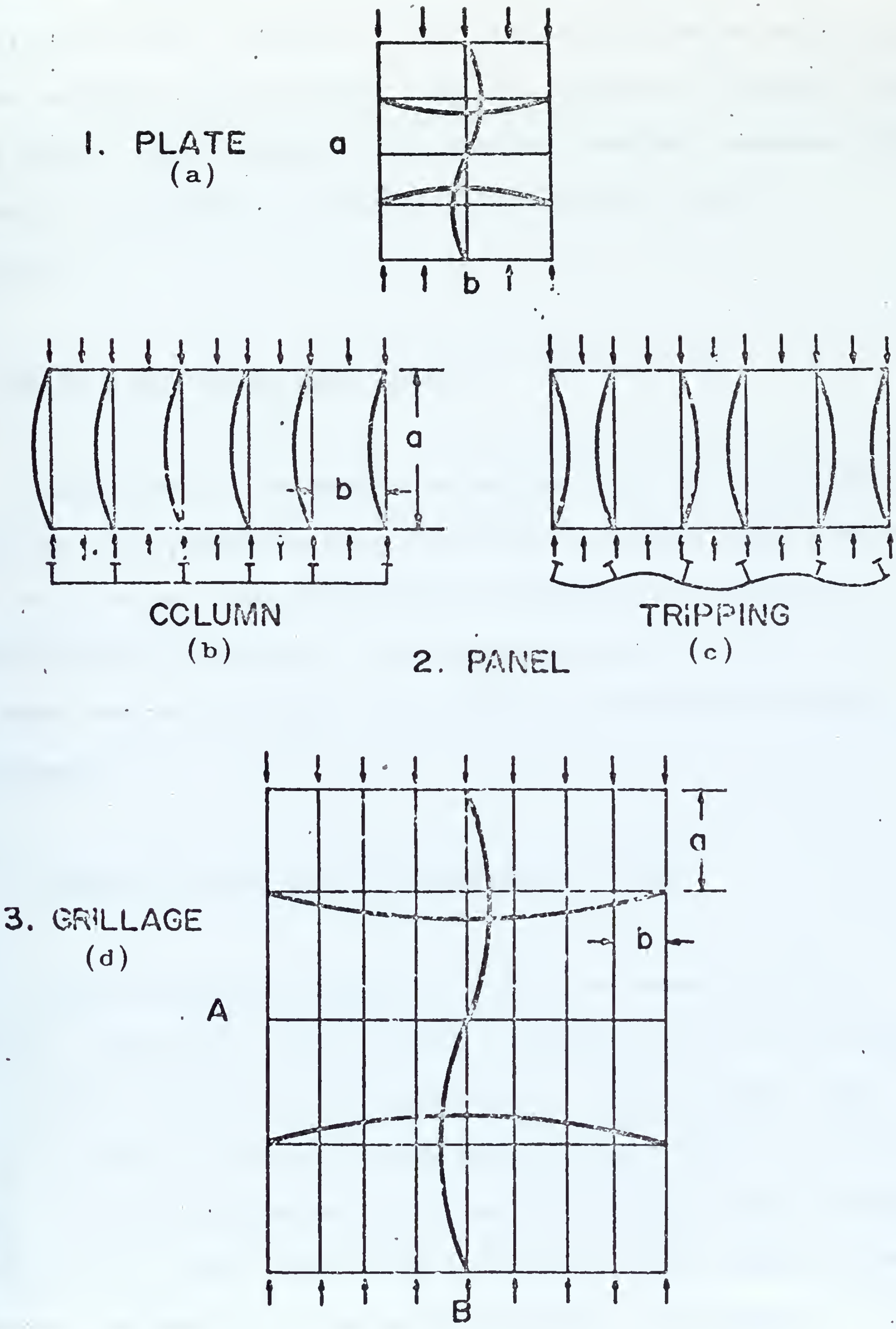
1. PLATE
(a)
a
b
COLUMN
(b)
a
b
TRIPPING
(c)
2. PANEL
3. GRILLAGE
(d)
a
b
A
B

MODES OF FAILURE IN UNIAXIAL COMPRESSION
FIGURE 3.3 (15)

grillage susceptible of tripping. It can take place in association with flexure of the stiffeners where buckling occurs towards the plating. This a release of energy when the lateral load, inplane compressive bending stresses and locked-in residual stresses combine and reach buckling.

iv) Overall grillage instability - figure 3.3b

This form of secondary structure failure, involves buckling of a grillage over its entire length into one or more half waves with bending of transverse as well as longitudinal stiffeners. In this case, as in iii), collapse may be strongly influenced by reduced plating stiffeness.

3.5 - Plating for Surface Effect Ships (SES)

The structural weight of a SES as constrained by current technology and economic considerations represents 25 to 30% of full load displacement. Light weight can go up to 55% of the full load displacement which is very high. It is antecipated that the most significant single reduction in light ship weight fraction will result from improved methods of structural analysis, increased understanding of allowable safety factors, improved production techniques and economic feasibility of utilizing

materials with high strenght to weight ratio, materials like high strength marine grade aluminum alloy materials.

The first step in the structural design process is to predict the loadings which will be encountered, which are not available at present. The difficulty lies in the complex nature of the interaction between the moving ship and the sea. This is further complicated by the presence of the flexible seals.

Three different modes of operation must be considered: cushion borne, hull borne and emergency and ship handling.

i) Cushion borne

The forces due to wave impact are the most significant and also the most difficult to assess. The forces vary with: the altitude of the craft relative to the oncoming wave; the ship velocity relative to the water; the ship characteristics at the point of impact including the hull configuration and stiffeness; and the presence of the flexible seals. The design pressures on the exposed surface due to the impact are corrently estimated based on experience with seaplane and planning hulls, and a limited amount of operational data from existing air cushion vehicles.

Static design loads or pressures on the hull structure, are included on table 3.2 It seems that for this operational mode, bending stresses do not have a

important role as they have for displacement hull type ships, because the portion of sidewall immersed is small and hogging and sagging bending moments are not high. Impact and lateral static loading are more important. Depending on the plate location and use, permanent set due to angular distortion or other cause may or may not be allowed.

ii) Hull borne

Similar to a displacement ship. All the design practices used with displacement ships can be applied.

It has been observed that for small crafts, the hull borne mode is less critical then the cushionborne, however, in large craft the situation is reversed. The cross over occurs at about a ship length of 250 ft, depending upon the magnitude of the impact loads used in the design for the cushionborne case.

iii) Emergency and shiphandling

A failure of the lift system or a loss of stability, while operating cushionborne at high speed, may result in the SES crashing into the sea. Impact loads would de high and the plating must be designed for a established chance of survival.

Ship handling that includes towing, mooring and drydocking loads will produce concentrated loads at certain

locations that must be locally strengthened.

Parametic Variations of Design Input for Concept SES Design

(taken from the Conceptual Design Handbook for SES - SES Program Office, Washington DC, Feb 6, 1973)

L/B (length beam ratio) 2, 3, 4

P_c (cushion pressure) lbs / ft^2 50, 100, 150, 200, 300

h_w (wave height) ft 0, 2.9, 6.0

w_G (gross weight) short tons 100, 1000, 2200, 3500, 5000

V_k (design speed) knots 60, 80, 100

w_{pp}/hp (power plant specific weight) lbs/HP 1.5, 2.0, 2.5

s (specific fuel consumtion) lbs/HP.hr .35, .4, .45, .5

Table 3.2

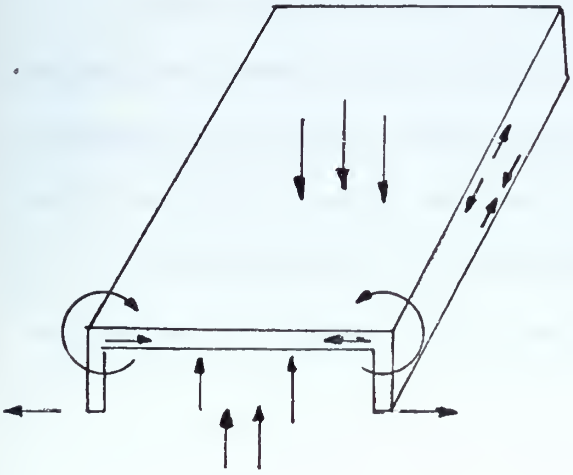

Fig. 3.4 - Loads on SES

4. EXPERIMENT

A - PHASE I

The aim of the experiment is to get data on out-of-plane or angular distortion due to fillet welding of orthogonal stiffeners on aluminum flat plate. As basic set up it was used the one shown in figures 4.1 a, b and it was thought to be an aproximate model of grillages used in ship structures.

The base plate material is 5052-H32 Aluminum Low Magnesium Alloy, whose chemical and mechanical properties are included in Appendix 1.

4.1 - Description and results of the experiment

The first phase of the experiment included four boxes whose set up is shown in figures 4.1 a, b, and whose dimensions are described in table 4.1, with the simbols referring to the previous figure.

The main interest goes to the central box(es), being the remaining plate a simulation of the natural extension of what would be a larger structure like a ship deck or a ship bottom.

The sequence of welding was done in a balanced way shown in figure 4.2, using semi-automatic GMA

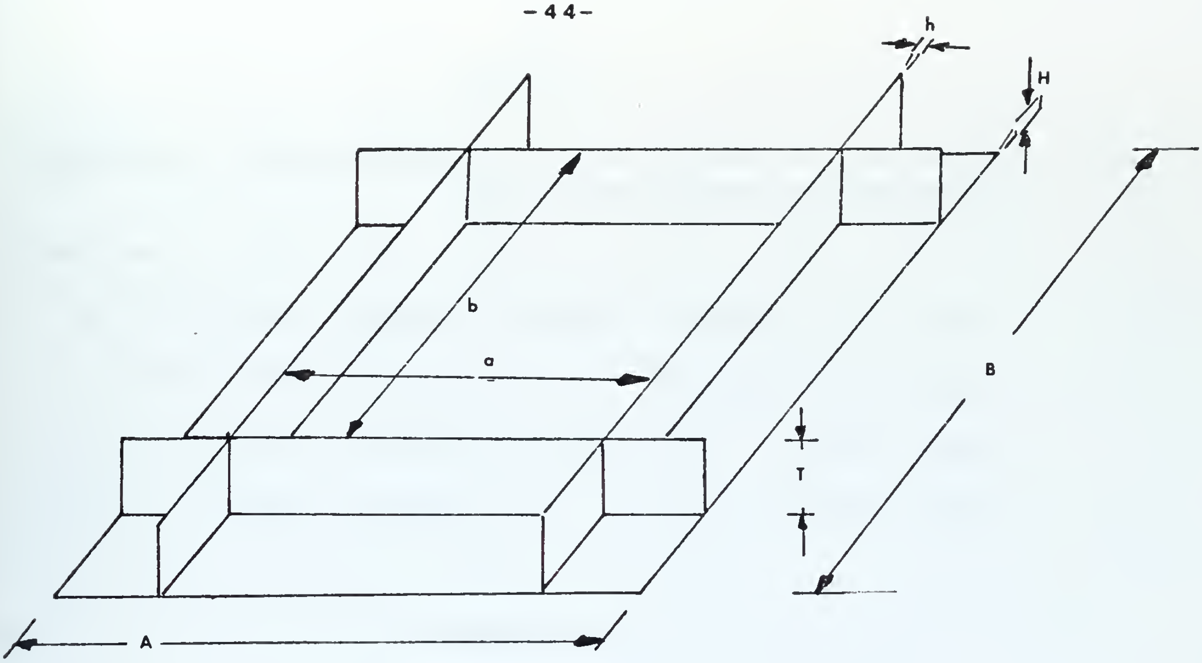

Figure 4.1.a

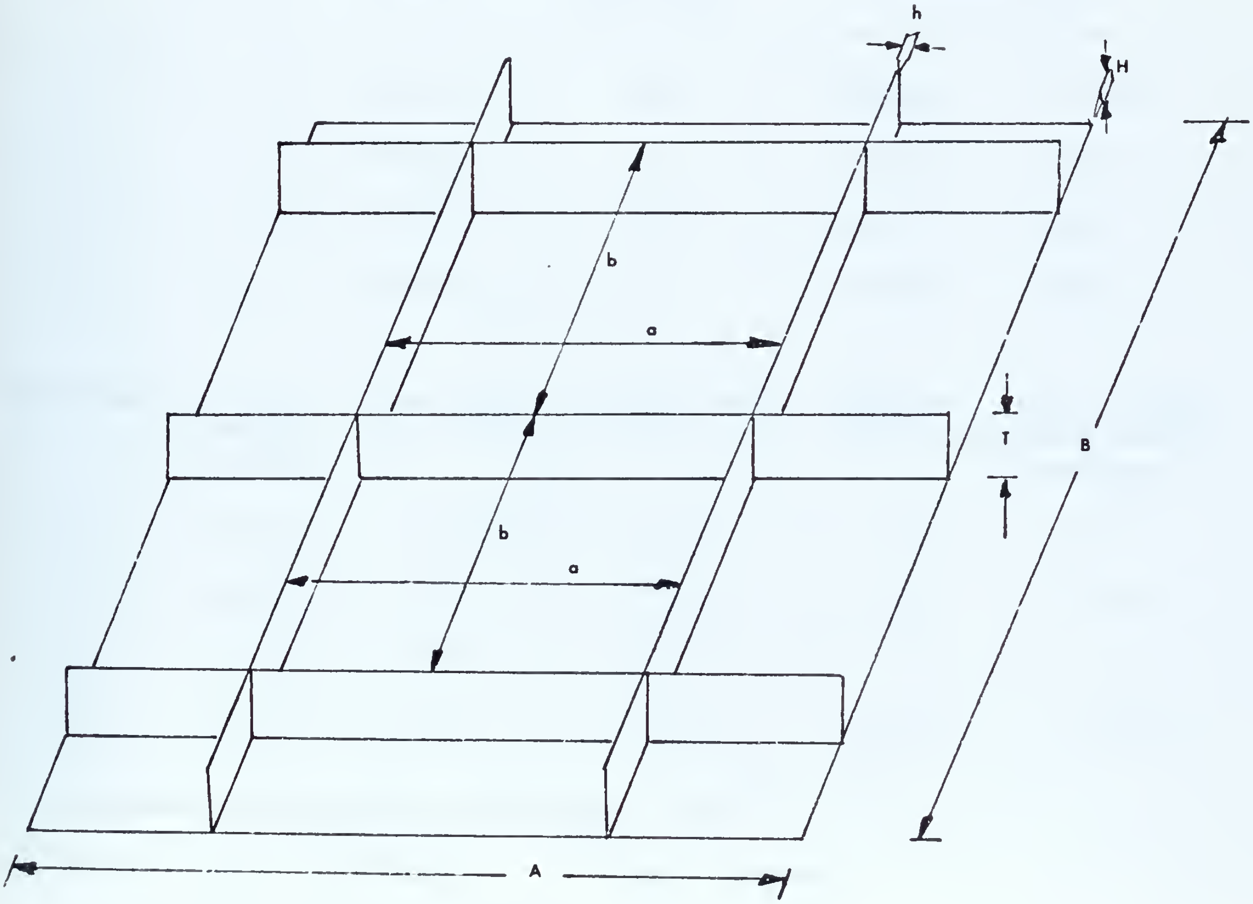

Figure 4.1.b

Experiment plate dimensions and Configuration

TABLE 4.1

Experiment dimensions (refer to figure 4.1 a and 4.1 b)
(all dimensions in inches)

Exp no.	A	B	a	b	T	h	H
1	48	48	23 1/2	23 1/4	4 5/8	1/4	1/4
2	48	48	23 1/2	16	4 5/8	1/4	1/4
3	48	48	23 5/8	23 5/8	5	3/16	3/16
4	48	48	23 5/8	16	5	3/16	3/16

TABLE 4.2

Experiment welding conditions

Exp no.	Voltage Volts	Current Amp	Mean travelling arc speed inch/sec	Mean filler wire consumption	
				lbs/inch	gr/cm
1	24	200 205	.32	.006468	1.1535
2	24	200 205	.31	.006676	1.190
3	22	185 195	.32	.005433	.969
4	22	185 195	.35	.004849	.865

Exp no.	Weldment length L (in)	Gas flow cu ft/hour	Filler wire diameter	Number of passes	Mean wire feed speed inch/sec
1	.35	40	3/64	1	12.5
2	.36	40	3/64	1	12.5
3	.32	30	3/64	1	10.5
4	.31	30	3/64	1	10.25

Assumed deposition efficiency 95%

Filler wire Al 4043 gas argon

Average ambient temperature 68°F

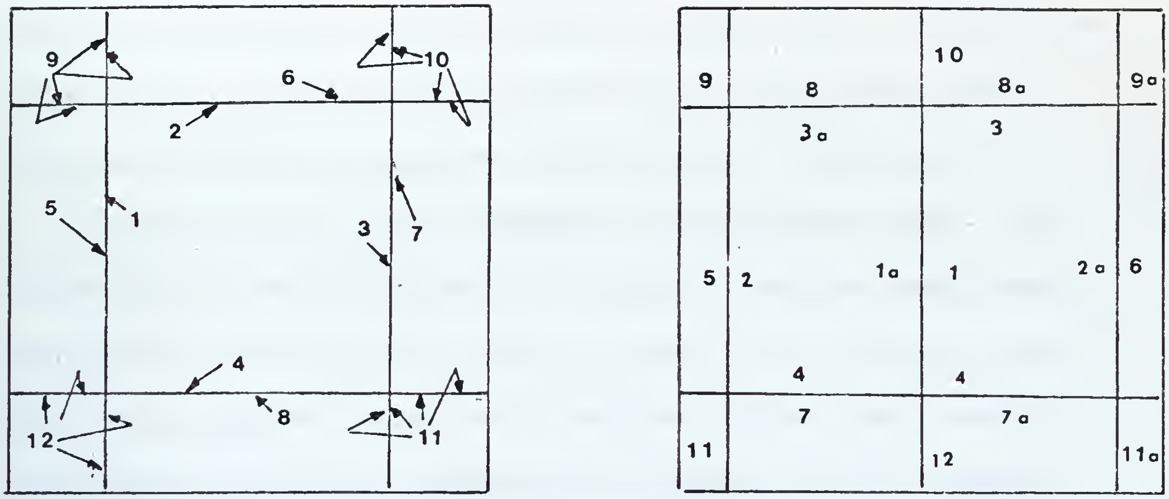
9
6
10
2
5
1
3
7
4
8
12
11
9
8
10
8a
9a
3a
3
5
2
1a
1
2a
6
4
4
7
7a
11
12
11a

Figure 4.2 - Welding sequence

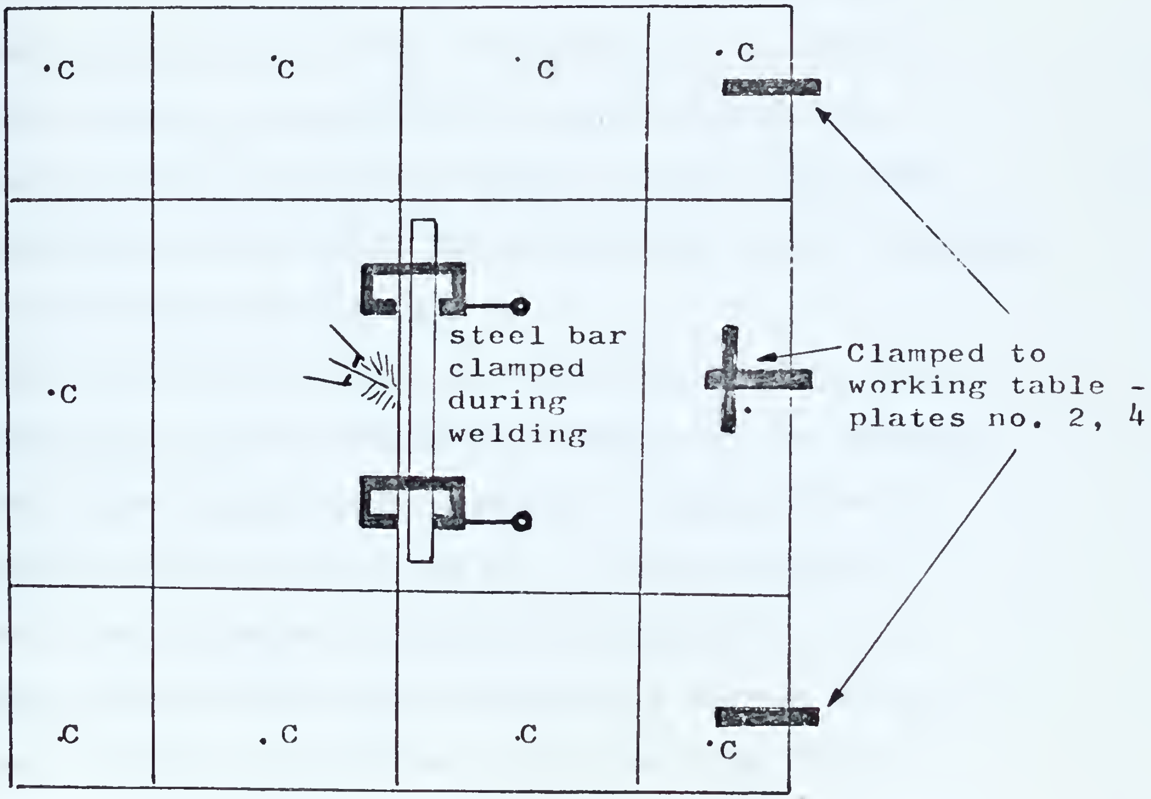
C
C
C
C
C
steel bar clamped during welding
Clamped to working table - plates no. 2, 4
C
C
C
C

Figure 4.3 - Clamping System

welding process, in the shop of Atomic Ltd. 27 Tudor St.-Cambridge. The welding parameters, electrode wire characteristics, etc, are mentioned in table 4.2.

Initially it was thought to built the box, i.e., to weld all the stiffeners together, before hand and then place them on the plate, clamp and fillet weld, procedure called "egg-box" joining system and used in mass fabrication in Japanese shipyards - but it was verified that for such a thin plate this would produce bending of the plate in the longitudinal direction during the welding of the several weldments, and it would produce increasing gap between the plate and the stiffener lower edge, being this difficult to avoid. Instead, the job was built up by tack welding the stiffeners to the plate and together, being this done very carefully, preserving the orthogonality and flatness of the stiffeners and plate.

All the work was done in a horizontal flat table. The continuous fillet weldments sequence no. 1 through no.8 were done without any clamping or other type of constraint in plates no.1 and no. 3 and plates no. 2 and no. 4 were clamped as shown in figure 4.3. The stiffener being welded was clamped to a strong steel bar for avoiding the bending of its top edge during the welding and partial cooling (see figure 4.3). The remaining fillets were done with the plate clamped to

the working table at the regions indicated by C - figure 4.3.

During the welding of set up no. 2 and no. 4, buckling (instantaneous overall twisting and torsion) was verified on the entire structure when the plate was moved, after fillet welding no. 7 and 7a, but the forementioned clamping system and the subsequent fillet welds corrected this and by the end of the welding the plates were stable.

The longitudinal shrinkage, producing longitudinal bending or rotation of the stiffeners was more notorious in the 3/10" thick plate, showing the stiffeners measurable curvature in the longitudinal sense.

The distortion measurements were taken by using a Vernier Calliper , dial gage and straight bars as shown in figure 4.4. Due to lack of an absolute reference and due to stiffener bending, the measurements taken were not absolute, therefore it was taken the mean value of measurements in several sequences and direction and it is believed that the results presented represent a reliable piece of data to the present experiment.

The measurement set up shown in figure 4.5 is generally more accurate but it could not be used because the long arm (A) would require a light weight rigid bar that was not available, otherwise its flexibility and the instability of the whole set up could not give accurate results; also a flat reference surface could

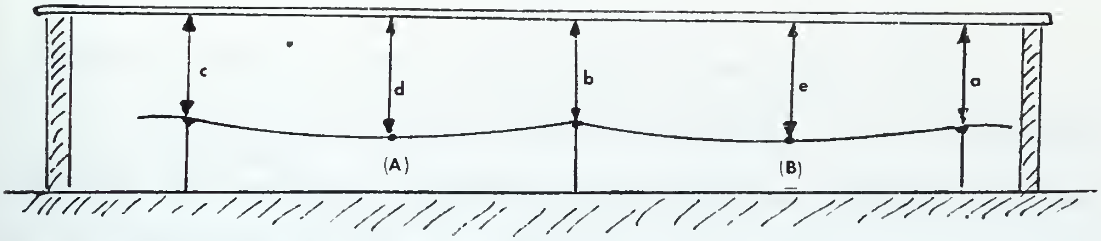

Plate displacement at centre of plate (A) = w_A

$$w_A = d - \frac{c+b}{2}$$

Plate displacement at centre of plate (B) = w_B

$$w_B = e - \frac{a+b}{2} .$$

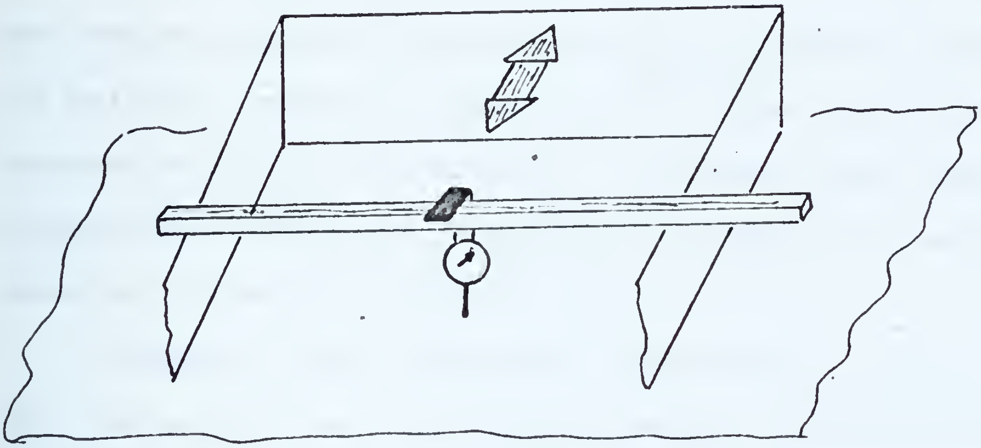

Figure 4.4 - Measurement of Plate Displacement

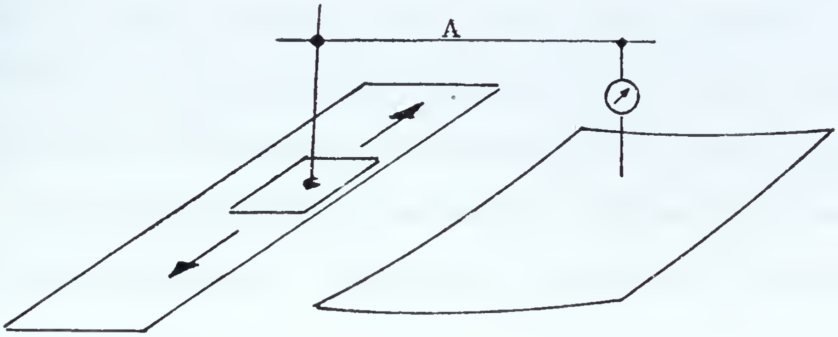

Figure 4.5 - Ideal Measurement System

not be found to cover the whole experiment plate.

Initially it was tried to monitor the distortion during the welding sequence, but due to the difficulty in handling the plate and the time consumed this was abandoned after the first plate.

Regardless of the existence of other welding defects like longitudinal bending of the stiffeners and torsion, it is believed that the procedure for taking the measurements produced results that reflect the out-of-plane distortion decoupled from the other effects.

The plate displacement curves due to the distortion are represented in figure 4.6 a, b, c and the values to get this curves are mean values taken using the method explained beforehand. The points where the values were taken are encircled in figure 4.7 and the data is collected in table 4.3.

Figures 4.8 a through e represent an attempt to get the profile of the plate normally to the welding line in several stations mentioned in figure 4.9.

Values of the steepest gradient were written in table 4.4 and values of the angle made between the horizontal reference and the secant to the displacement values most far apart are written in table 4.5.

From the profiles shown in figure 4.8, we see that underneath the fillet the gradient is steeper

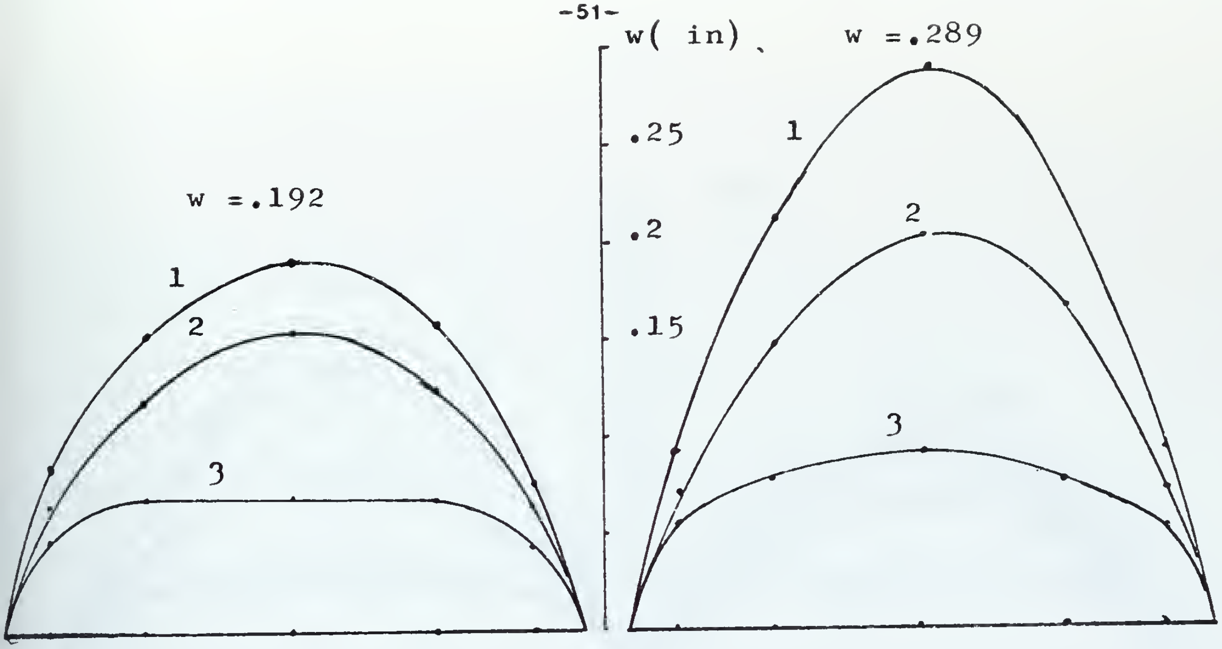

plate no. 1

plate no. 3

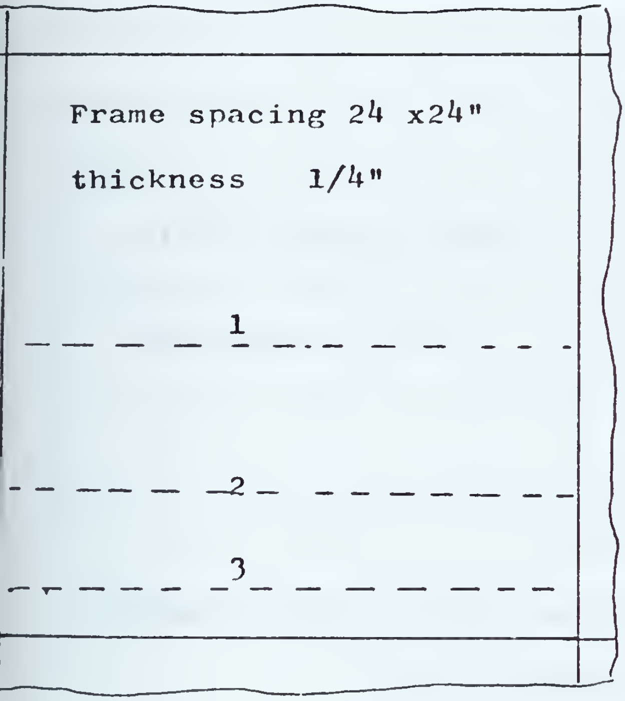
Frame spacing 24 x24"
thickness 1/4"
1
2
3

Frame spacing 24 x24"

thickness 3/16"

Figure 4.6a -Profile of Plate Displacement w due to Angular Distortion

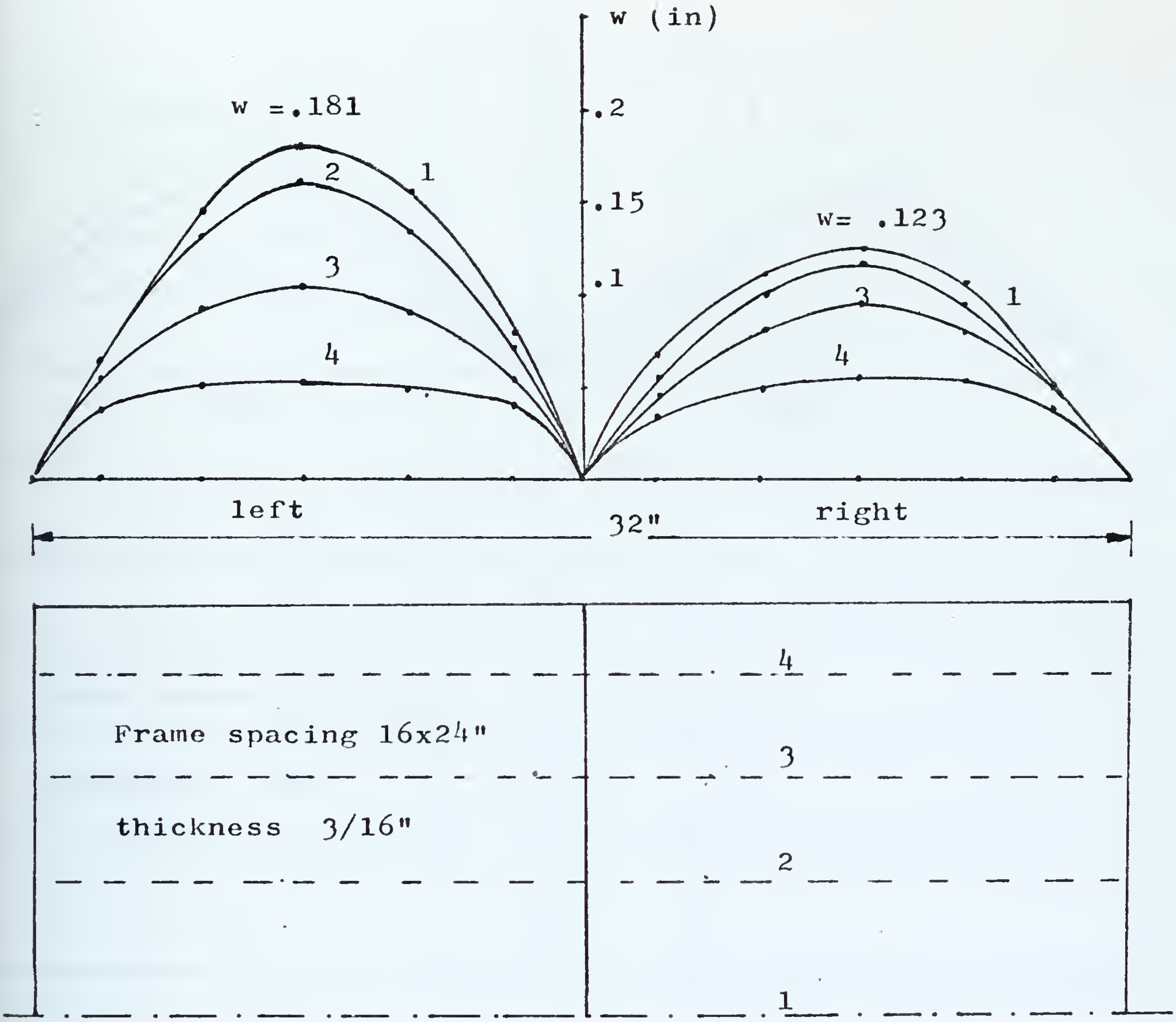

Figure 4.6b- Profile of Plate Displacement w due to Angular Distortion

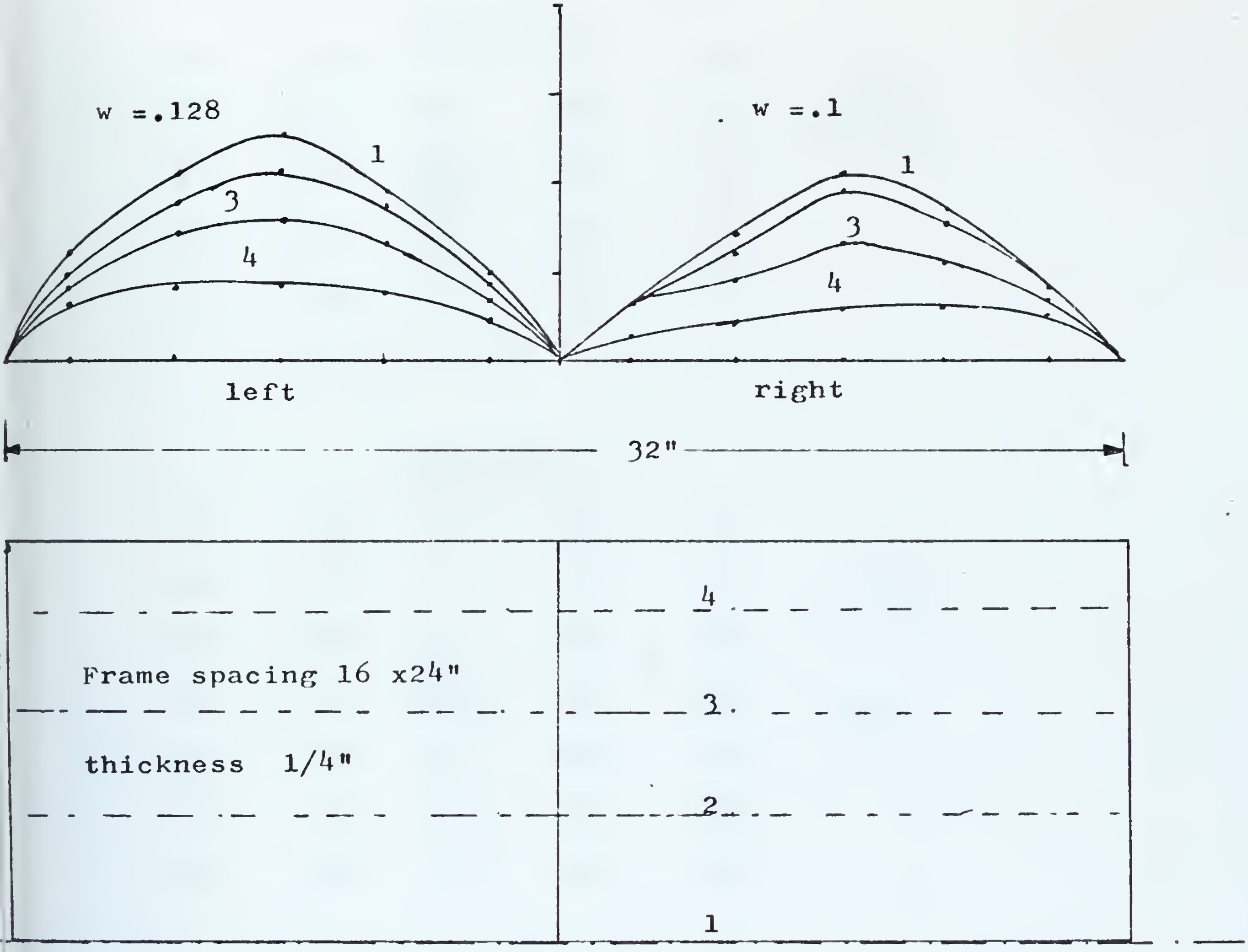

Figure 4.6 c- Profile of Plate Displacement w due to Angular Distortion

Table 4.3

Plate displacement (w) due to distortion
(values in thousandths of inch)

Plate no. 1

50	59	70	67	79	
72	116	148	121	61	1/4" 24 x 24
87	156	192	161	75	
65	117	154	124	67	
47	68	70	69	43	

Plate no. 4

31	51	52	52	50	
53	116	115	100	70	3/16" 16 x 24
62	128	157	133	76	
64	145	181	157	79	left
65	132	159	135	72	
54	93	105	90	54	
38	49	52	47	40	

37	37	44	43	43	
46	66	77	67	60	3/16" 16 x 24
58	93	105	84	60	right
64	111	123	107	49	
56	102	118	94	51	
46	80	94	80	48	
34	48	55	53	40	

Plate no. 3

53	75	91	72	51
77	160	213	163	82
91	210	289	213	92
73	147	203	165	69
55	73	91	74	49

3/16"
24 x 24

Plate no. 2

29	39	47	39	28
46	74	92	72	43
55	88	119	89	43
62	105	128	95	50
47	89	108	87	44
42	72	80	64	36
32	42	43	39	23

1/4"
24 x 16

left

Plate no. 2

15	22	34	28	17
28	50	70	56	29
32	66	100	76	40
34	71	106	84	41
34	60	96	77	41
33	45	64	54	33
14	20	28	31	25

1/4"
24 x 16

right

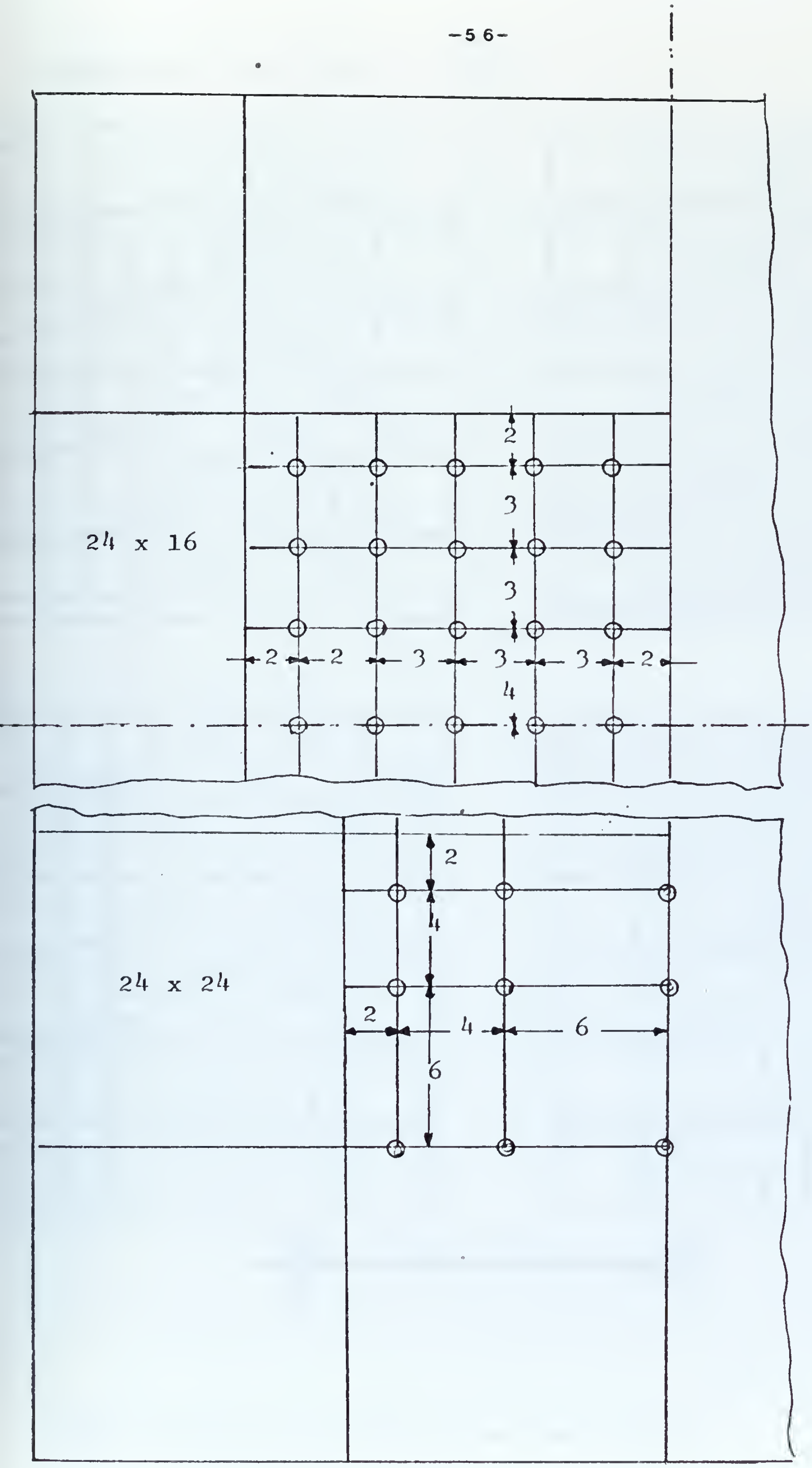
24 x 16
2
3
3
4
2
2
3
3
3
2
24 x 24
2
4
6
2
4
6

Figure 4.7 - Measurement Stations

Plate no. 1 - 24 x24"   1/4"

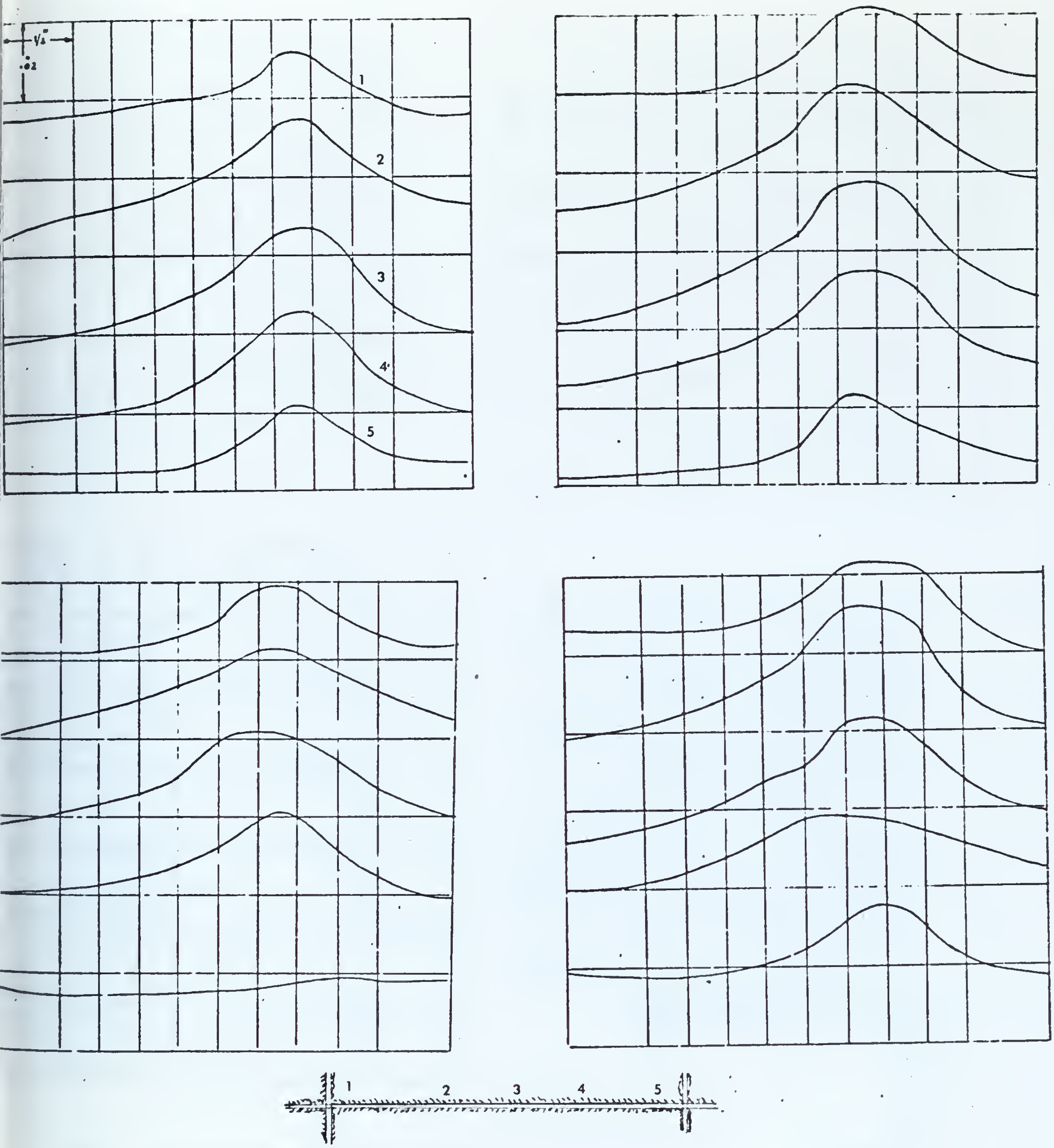

Fig.4.8a Plate profile at the weld lines

Plate no. 2 -16 x24"   1/4"

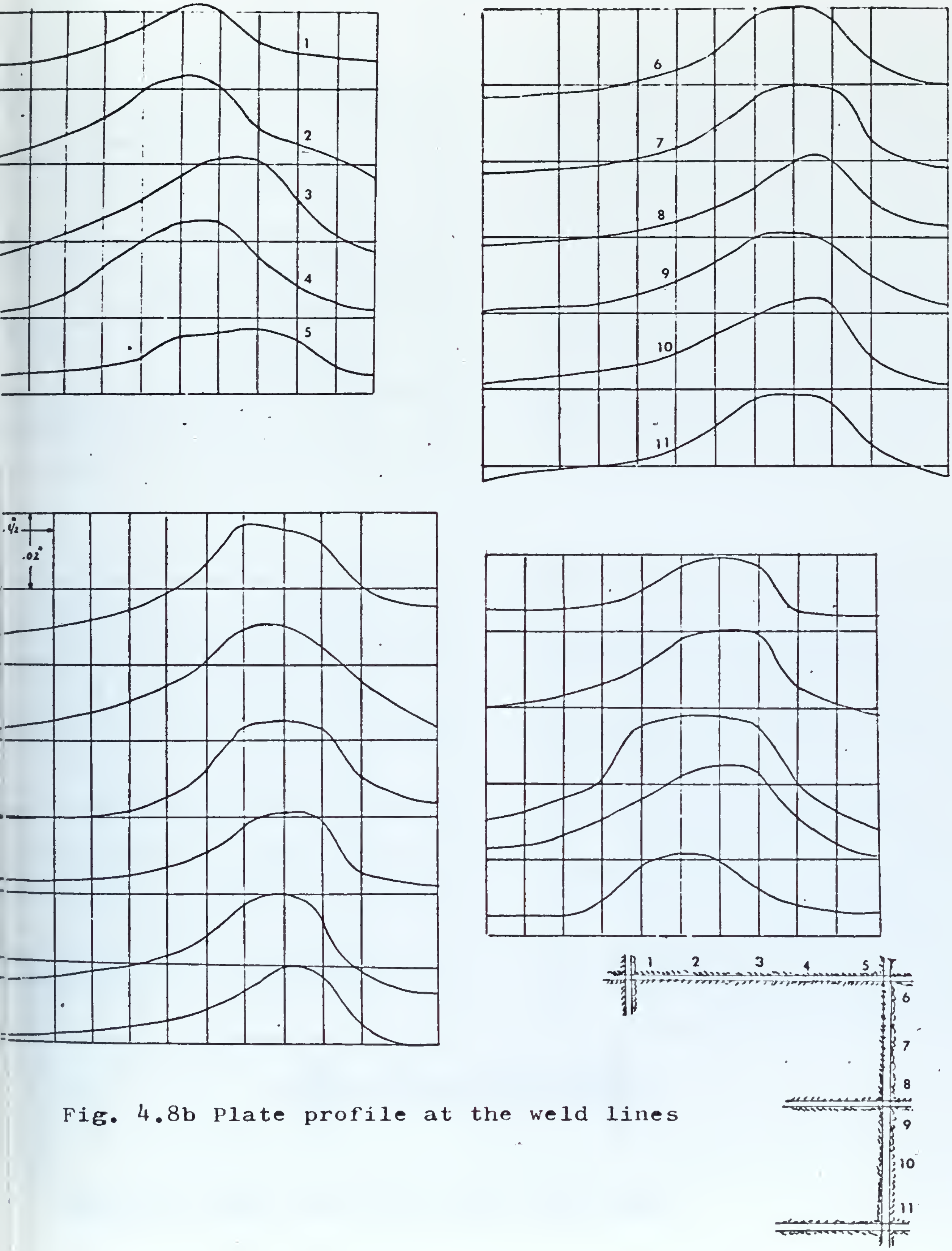

Fig. 4.8b Plate profile at the weld lines

Plate no. 3 - 24 x 24"   3/16"

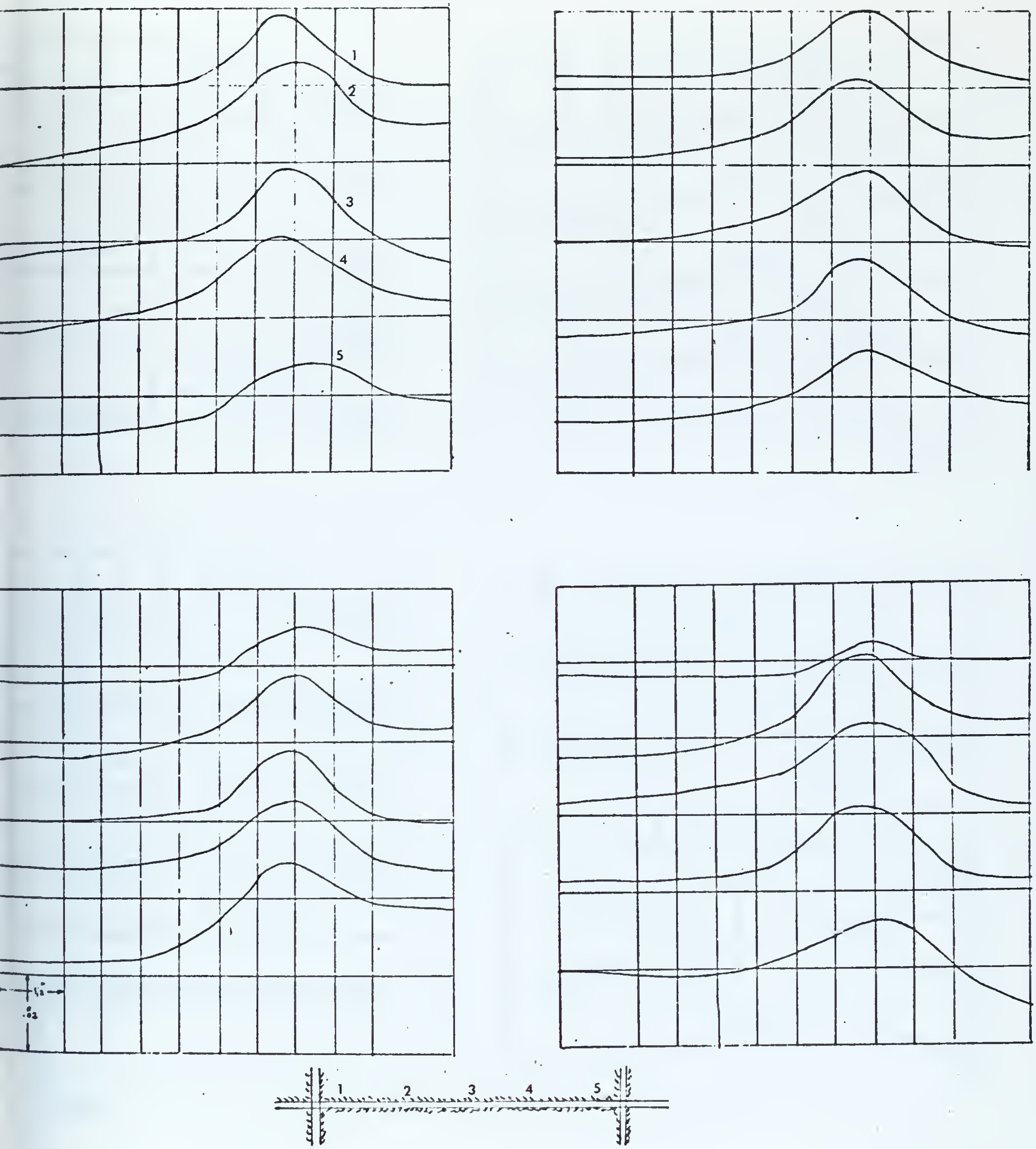

Fig.4.8c Plate profile at the weld lines

Plate no. 4 - 16 x 24" 3/16"

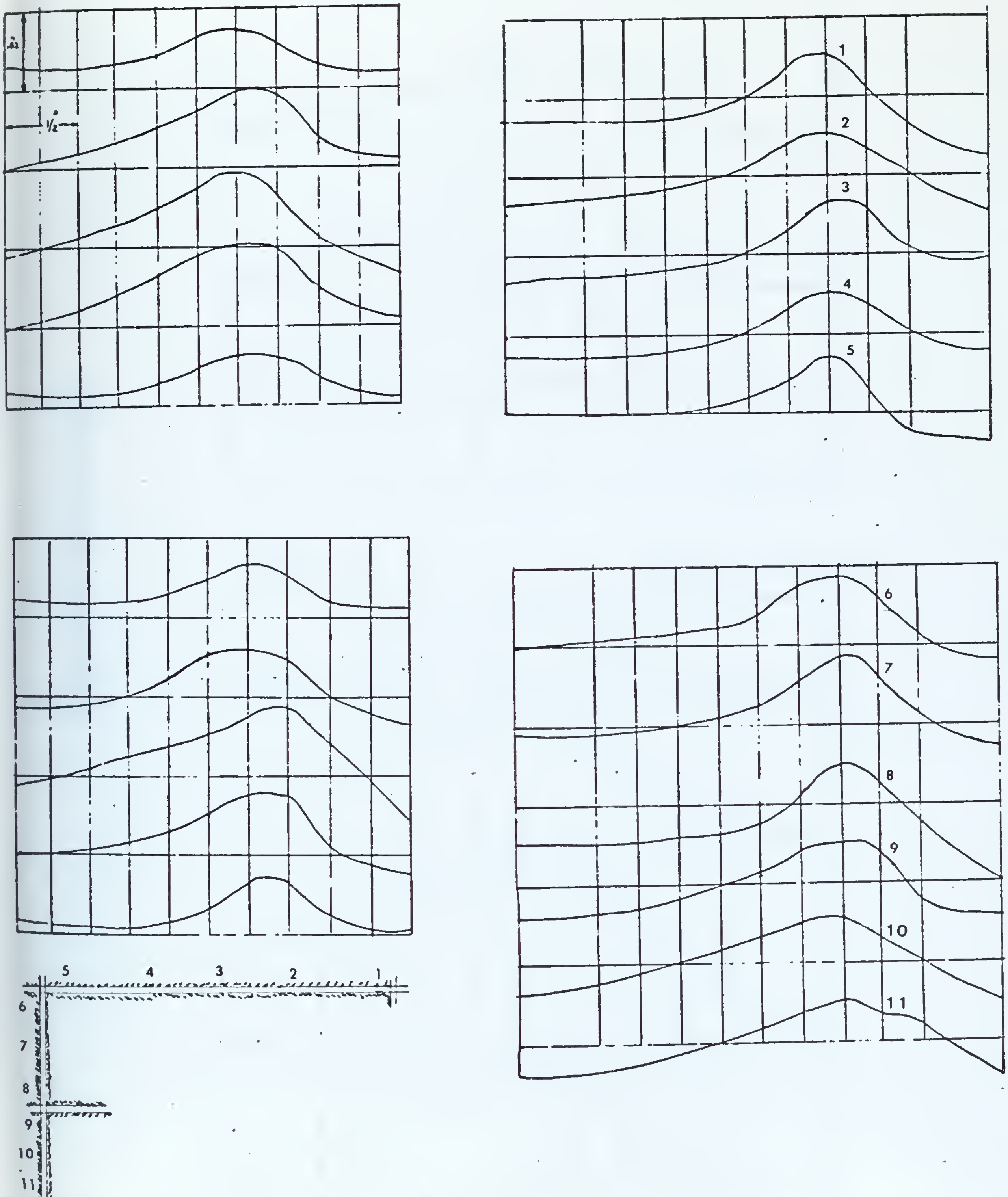

Fig. 4.8d Plate profile at the weld lines

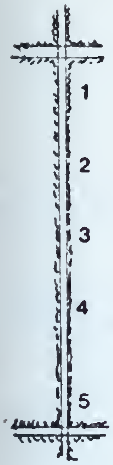

Plate no. 2 middle stiffener

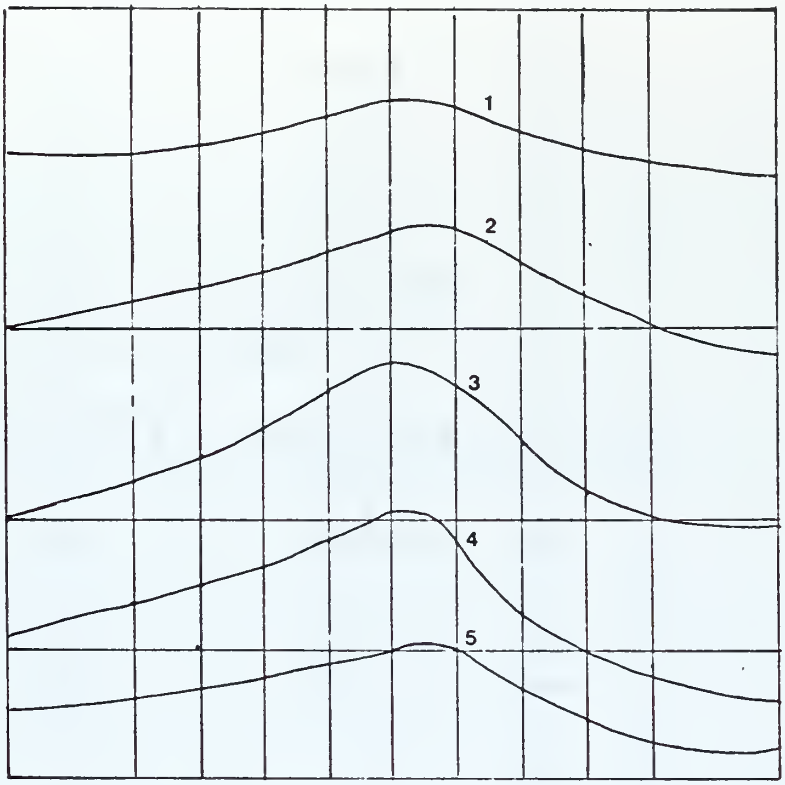

Plate no. 4 middle stiffener

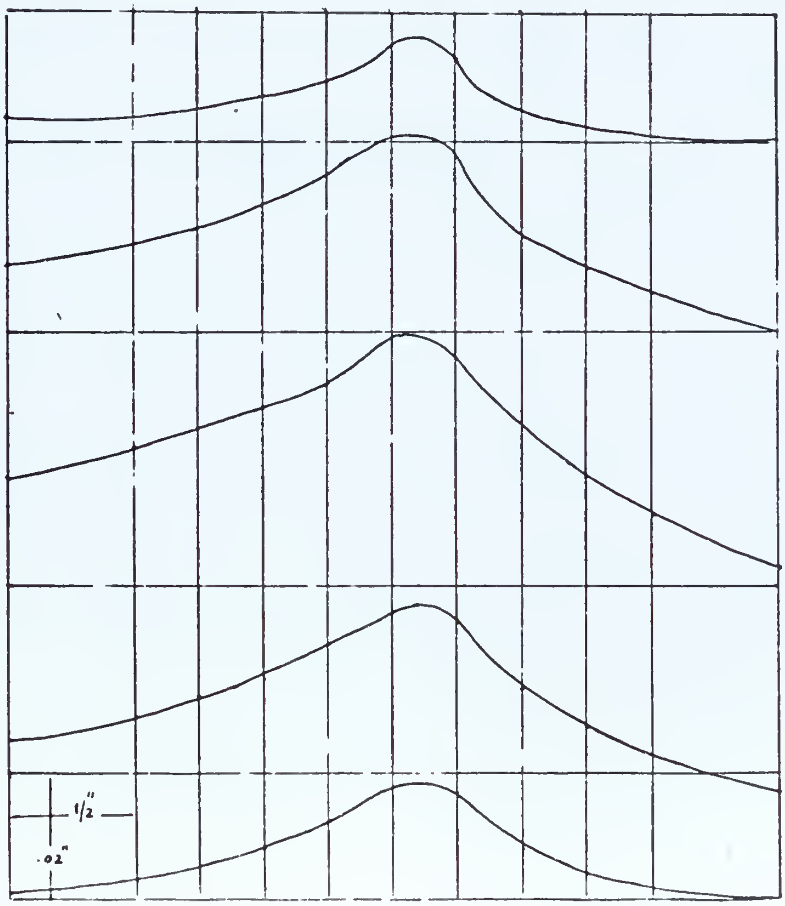

Fig. 4.8e Plate profile at the weld lines

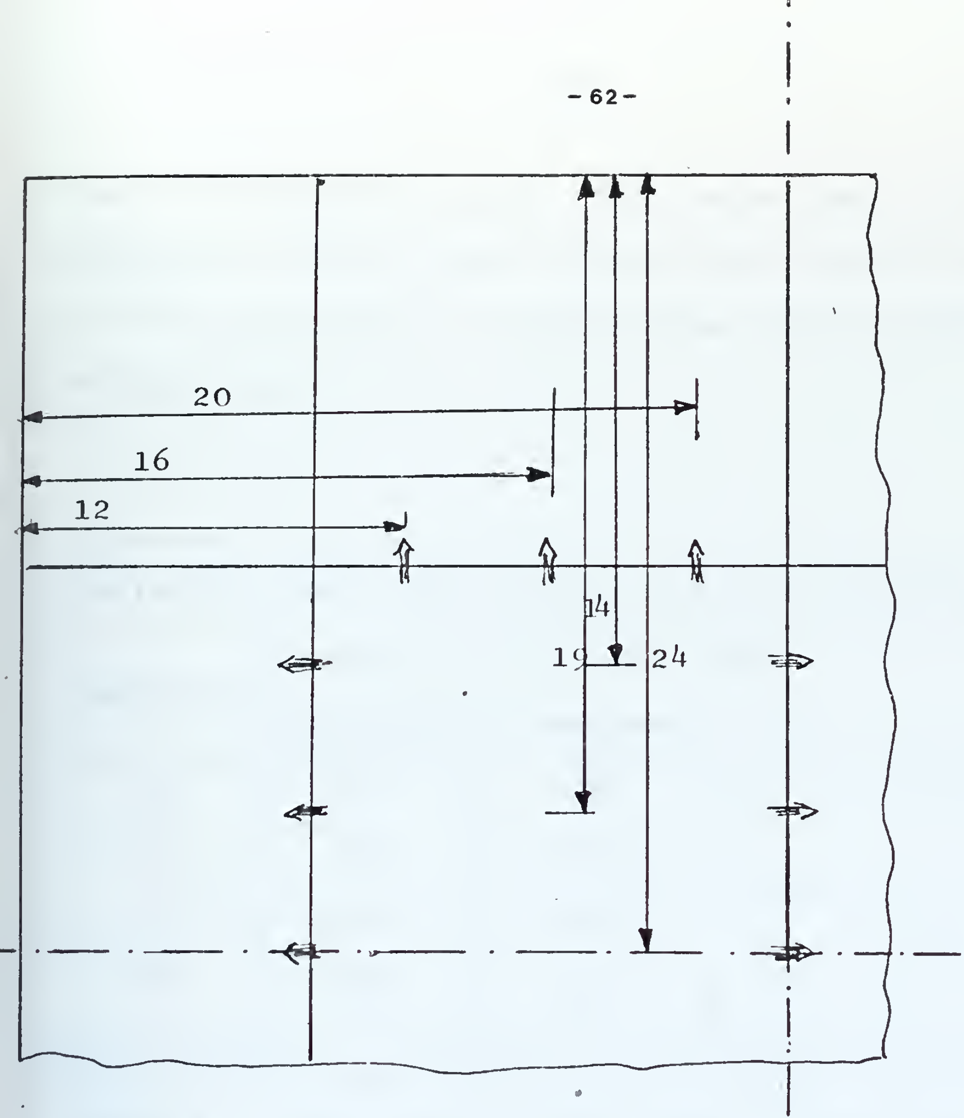
20
16
12
14
19
24

Figure 4.9 - Profile Stations

than for remaining plate. This shows that a plastic deformation occurs near the weld and that for the case of this thin plate, it affects the entire thickness of the plate.

Table 4.4 -Mean value of the steepest angle (rad)

Plate no.	position at the weld line		
	midpoint	extreme	
1	.042	.032	
2	.036	.019	
3	.040	.020	
4	.030	.014	

Table 4.5- Mean value of the angle between the horizontal reference and the secant s (on the weld line)

Plate no.	position at the weld line		
	mid point	extreme	
1	.020	.013	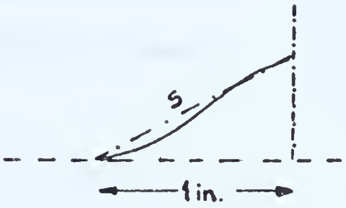
2	.019	.014	
3	.016	.010	
4	.017	.010	

B - PHASE II

This second set of experiments were done for complementing those of Phase I, and to attempt a reduction of distortion by heating the plate before welding.

4.2 - Description and results of the experiment

The set up used was the same as in Phase I. The welding was done at MIT Welding Laboratory, using a semi-automatic GMA welding process.

Experiment no. 5 was done without any kind of preheating. In experiment no. 6, with the same dimensions of no. 5, the plate was heated near the weld line, - figure 4.10, before the weld to be done. The average temperature on the welding site after heating was 200° F.

These two experiments should be done with the same welding conditions, for evaluating the preheating effect on angular distortion, but unfortunately this was not possible, because the manual welding speed was not the same.

Experiment no. 7 was done heating the base plate underneath - figure 4.11 to 160° F (on the top face).

The plate dimensions are indicated in table 4.6.

The welding conditions are collected in table 4.7.

TABLE 4.6

Experiment dimensions (refer to figure 4.1 a and 4.1 b)

Exp no.	A	B	a	b	T	h	H
5	26	24	16	16	4 1/2	3/16	3/16
6	26	24	16	16	4 1/2	3/16	3/16
7	39	15	36 1/2	13 3/16	4 1/2	3/16	3/16

TABLE 4.7

Experiment welding conditions

Exp no.	Voltage Volts	Current Amp	Mean travelling arc speed inch/sec	Mean filler wire consumption lbs/inch	gr/cm
5	23	200	.246	.004625	.825
6	23	200	.3	.00379	.676
7	23	200	.264	.0043	.767

Exp no.	Weldment length L (in)	Gas flow cu ft/hour	Filler wire diameter	Number of passes	Mean wire feed speed inch/sec
5		40	3/64	1	6.8
6		40	3/64	1	6.8
7		40	3/64	1	6.8

Assumed deposition efficiency 95%

Filler wire Al 5356 gas argon

Average ambient temperature 73° F

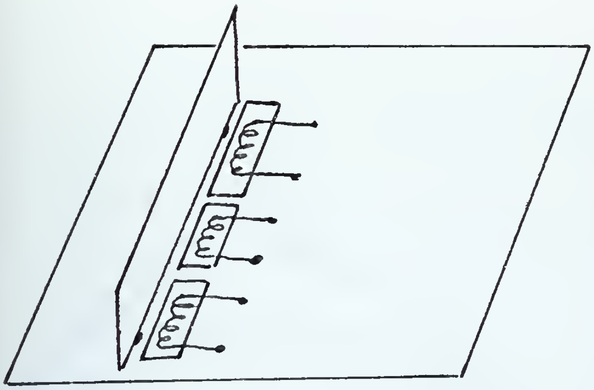

Figure 4.10

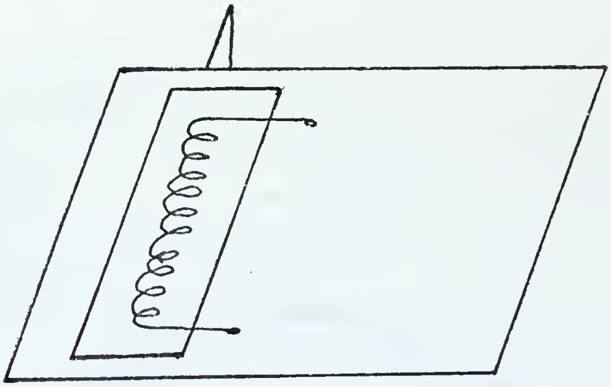

Figure 4.11

Schematic of Plate Pre-heating

The deformation profile of the plates is included in Table 4.8 and figures 4.12 a, b, c.

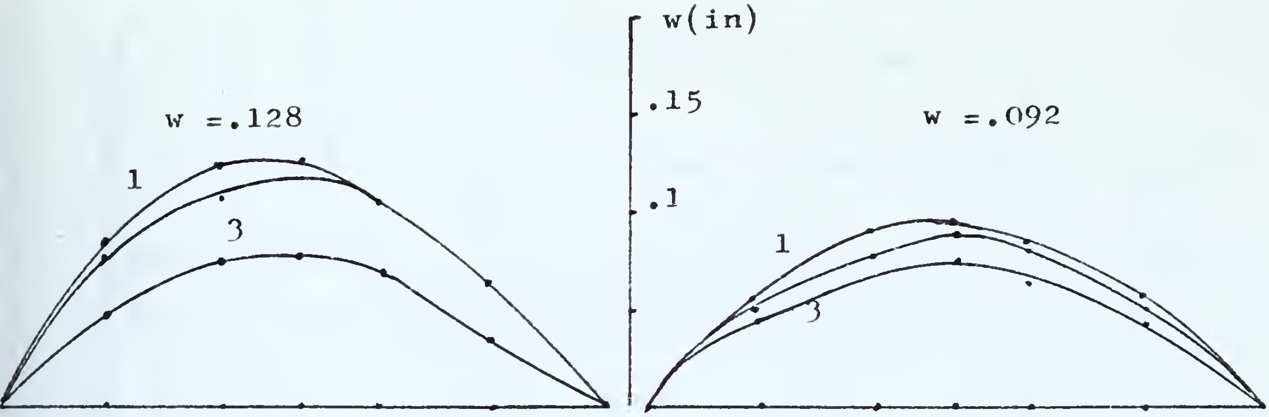

plate no. 5

plate no. 6

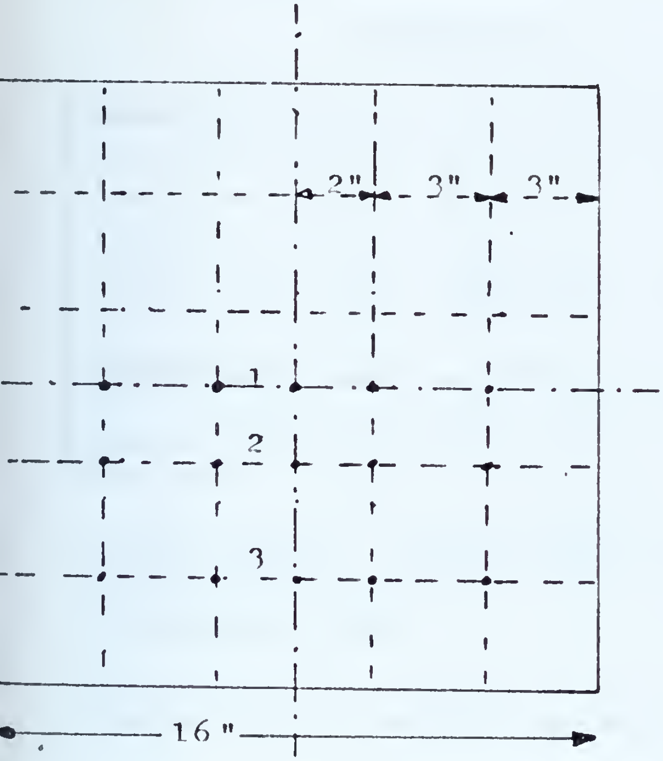

Frame spacing 16"x16"

thickness 3/16"

Figure 4.12 a,b -Profile of Plate Displacement w due to Angular Distortion

maximum deflection w =.077

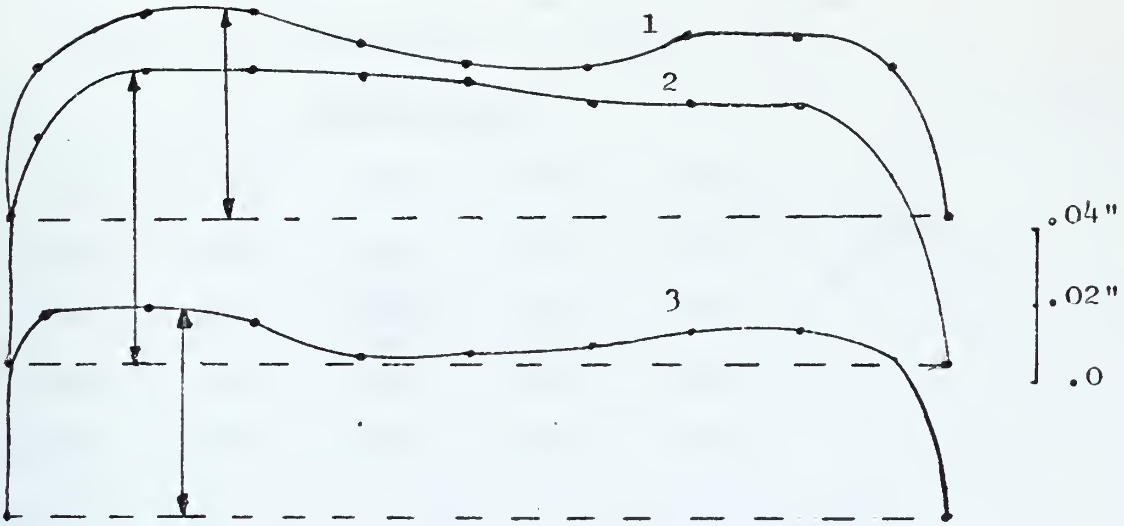

plate no. 7

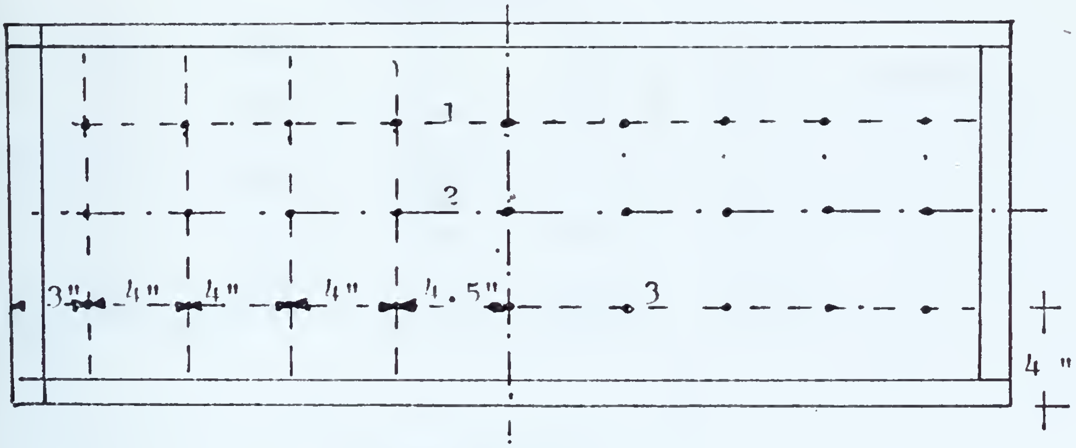

Frame spacing 36 1/2 x 13 3/16 "

thickness 3/16"

Figure 4.12 c- Profile of Plate Displacement w due to Angular Distortion

Table 4.8

Plate displacement (W) due to distortion
(values in thousandths of inch)

Plate no. 5

51	73	80	80	57
70	109	123	112	66
82	119	128	104	64
77	115	127	108	65
45	76	80	70	36

3/16"
16 x 16

Plate no. 6

53	62	64	60	52
53	84	90	84	44
53	90	92	83	55
52	79	92	78	50
44	66	77	64	41

3/16"
16 x 16

Plate no. 7

40	55	55	47	40	40	50	47	40
59	77	77	75	75	70	70	69	51
55	55	52	42	43	42	50	51	42

3/16"
36 x 13

5. ANALYSIS OF OUT-OF-PLANE DISTORTION DUE TO FILLET WELDING IN ALUMINUM ALLOY PLATING

5.1 - Summary of previous work

Analysis of distortion started being done by correlating experimental data in steel. The authors of (9) mentioned that angular change in a base plate due to free fillet welded joints was analogous in nature to angular change in bead on plate. They also found that bending or angular distortion is only produced in the vicinity of welds.

An empirical equation for angular distortion in free fillet joints, analogous to bead on plates was presented in (9)

$$\Phi_o = C_1 \left(\frac{I}{h\sqrt{vh}}\right)^{2.5} \exp\left[-C_2 \left(\frac{I}{h\sqrt{vh}}\right)\right] \qquad (5.1)$$

Φ_o = angular change in radians

h = plate thickness (cm)

I = welding current amp

v = travel speed cm/sec

C_1 , C_2 = are constants depending on the properties of the electrode used, and are obtained from experimental data.

The maximum distortion is verified when $\frac{I}{h\sqrt{vh}} = \frac{2.5}{C_2}$

The equation (5.1) is insensitive to the base material characteristics.

Another relationship was derived if the thickness were larger than 10 m/m

$$\Phi_0 = C_0 \; w \; h^{-1.5} \qquad (5.2)$$

w = weight of weld metal deposited per unit weld length in gr/cm

C_0 = constant depending on the electrode used

Professor Masubuchi, using elastic beam theory and applying the principle of stationary (minimum) strain energy, got a relationship between the angular change Φ_0 due to fillet welding if the joint is unconstrained or free to rotate and Φ when there is a constraint (see figure 5.1). This relationship is derived in references (4, 6, 9, 10) and is as follows:

$$\Phi = \frac{\Phi_0}{1 + \frac{2D}{\ell}\,\frac{1}{C}} \qquad (5.3)$$

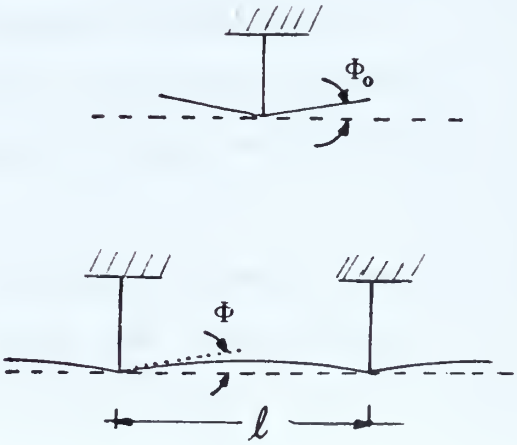

Figure 5.1 - Free and constraint joint

C = a rigidity coefficient

$D = \frac{E\,h^3}{12(1-\nu^2)}$ = flexural rigidity

h = thickness

ν = Poisson's ratio

The rigidity coefficient C is obtained from

experimental data for every base material and it was found to be empirically related to the thickness and to the weight of weld metal deposited per unit weld length in gr/cm.

Taniguchi (4) found values of C for Aluminum as previously they were obtained for steel (9).

The use of the computer allowed the numerical analysis of distortion and more sophisticated analytic models were set up.

Taniguchi (4), assumed that once we had equation 5.3, relating the angular distortion for free and constrained joints, the effort of getting a mathematical model good for out-of-plane distortion should be devoted to finding Φ_o ; using an elasto-plastic analysis he got values of Φ_o smaller than those obtained from experiment.

Shin (10) using the concept of C, did an elastic analysis of orthogonally framed plates, using the variational principle and Finite Element Analysis (FEM). We couldn't get good correlation between analysis and experimental data for steel plate and concluded that the problem was the difficulty of making accurate mesurements of Φ_o and Φ .

A complete analytic model for elastic plastic two dimensional distortion analysis, using FEM, accounting for the transient stress and strain field during weld was done by Dr. Muraki at MIT and finished by 1974.

Agreement between the results obtained using this analytic approach and the experimental data have not yet been satisfactory and the computer program running time makes this analysis very expensive.

A review of these previous works in out-of-plane distortion analysis will allow us to draw the next chart picturing the development of this subject.

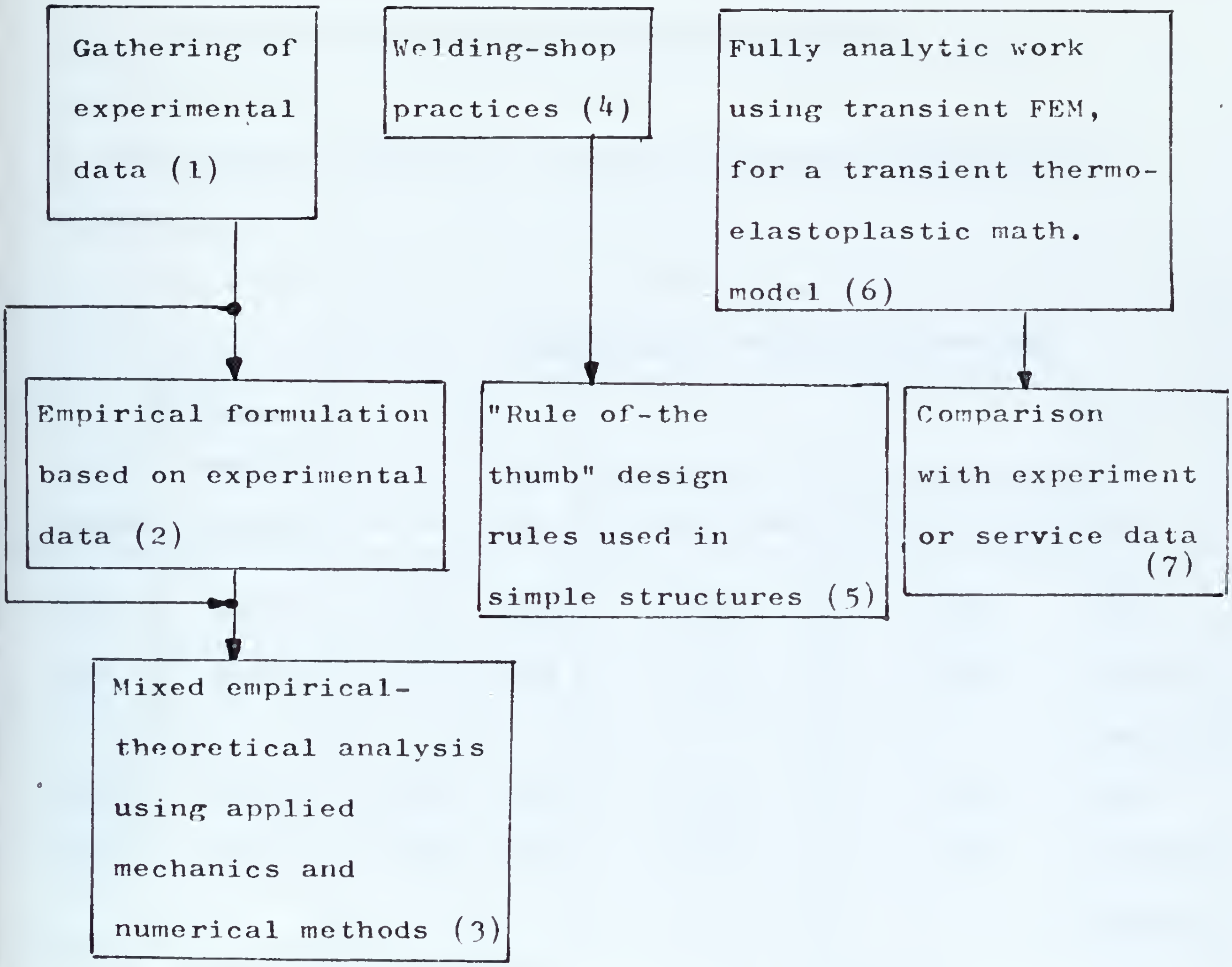
Gathering of experimental data (1)
Welding-shop practices (4)
Fully analytic work using transient FEM, for a transient thermo-elastoplastic math. model (6)
Empirical formulation based on experimental data (2)
"Rule of-the thumb" design rules used in simple structures (5)
Comparison with experiment or service data (7)
Mixed empirical-theoretical analysis using applied mechanics and numerical methods (3)

We will preceed the analysis by doing more work related with blocks 2 and 3.

5.2 - Correlation of data from present experiments with previous analytic models

From the work done by Taniguchi (4), using his rigidity coefficient empirical function $C = 6.35\ h^{(2.67\ -\ .065\ w)}$ (Kg.mm/mm.rad) suitable for Aluminum Alloys, and where

h= thickness mm

w= double fillet weld consumption gr/cm

we can construct table 5.1, based on the data gathered in section 4.

Table 5.1 Welding Parameters

h	Frame spacing	w	Φ_0	C		Φ
inches	inches	gr/cm	rad	Kg mm/mm rad	lb in/in rad	rad
1/4	24x24	2.307	.060	670	1476	.033
1/4	24x16	2.38	.061	670	1478	.033(1)
						.029(2)
3/16	24x24	1.9378	.050	337	743	.030
3/16	24x16	1.7296	.040	344	759	.030(1)
						.020(2)

(1) ℓ= larger frame spacing

(2) ℓ= smaller frame spacing

$$\Phi = \frac{C\ell\,\Phi_0}{C\ell + 2D}$$

Using the values Φ_0 and C shown in table 5.1, we used the Finite Element Computer program developed by Shin (10), and the results are ploted in figures 5.2 a, b, c, d. The angular change at the welding lines is included in table 5.1.a.

We see that the calculated values of the distortion have a similar profile, but they fall behind the values obtained by experiment, specially for 3/16 thickness.

Trying higher values for C, we will get closer distortion values. This is similar with what happened with steel data.

In 5.4 we will develop more about the usefulness and suitability of this Computer Program.

5.3 - Elastic Analysis of Out-of-Plane Distortion After Welding

5.3.1 - General

For analysing the plate after the fillet weld be done, we can consider the plate to behave elastically, as a simply supported plate in which an uniform moment M_0 was applied along the weld lines - figure 5.3, and assuming that no membrane forces are involved (small deflections). We can calculate the moment M_0 and the angles that the plate will make right on the weld lines θ_x and θ_y, using the values of deflection obtained from the experimental data.

Figure 5.1.a

Calculation of the angle at the weld lines, using the FEM computer program (10)

Plate no.	θ_X	θ_Y
1	.029	.029
2	.0173	.0279
3	.026	.026
4	.0172	.0192

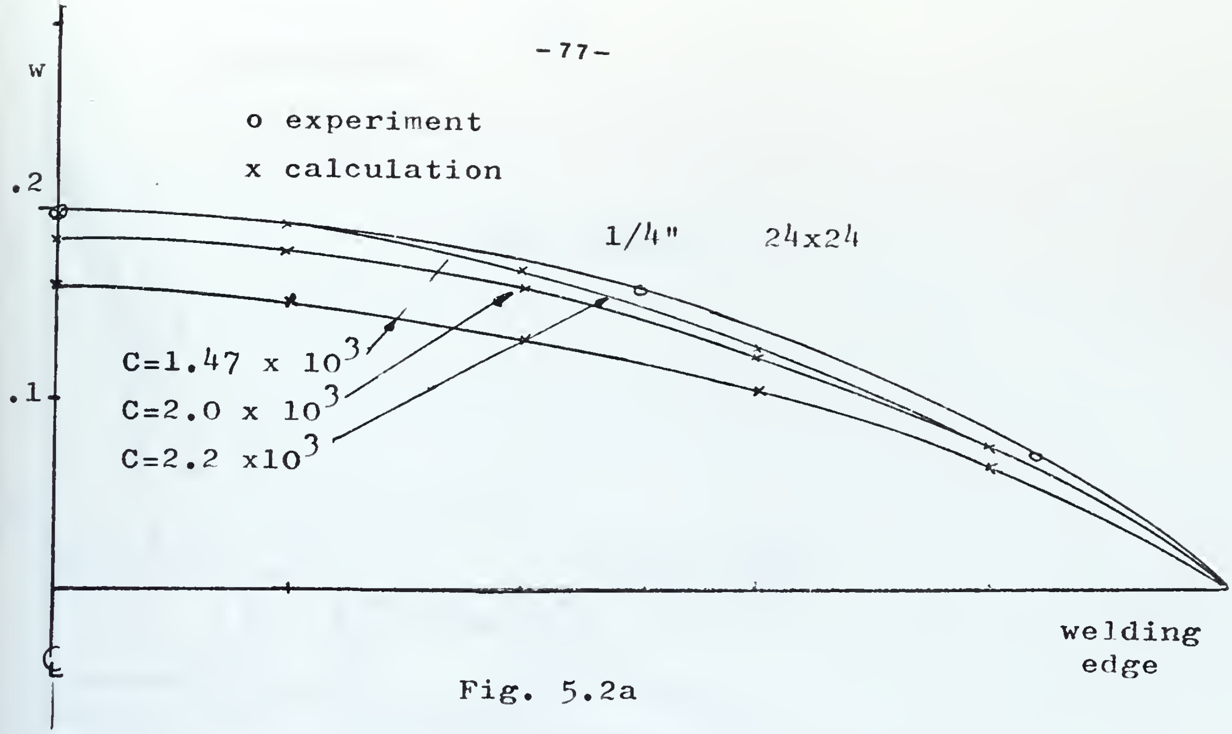

Fig. 5.2a

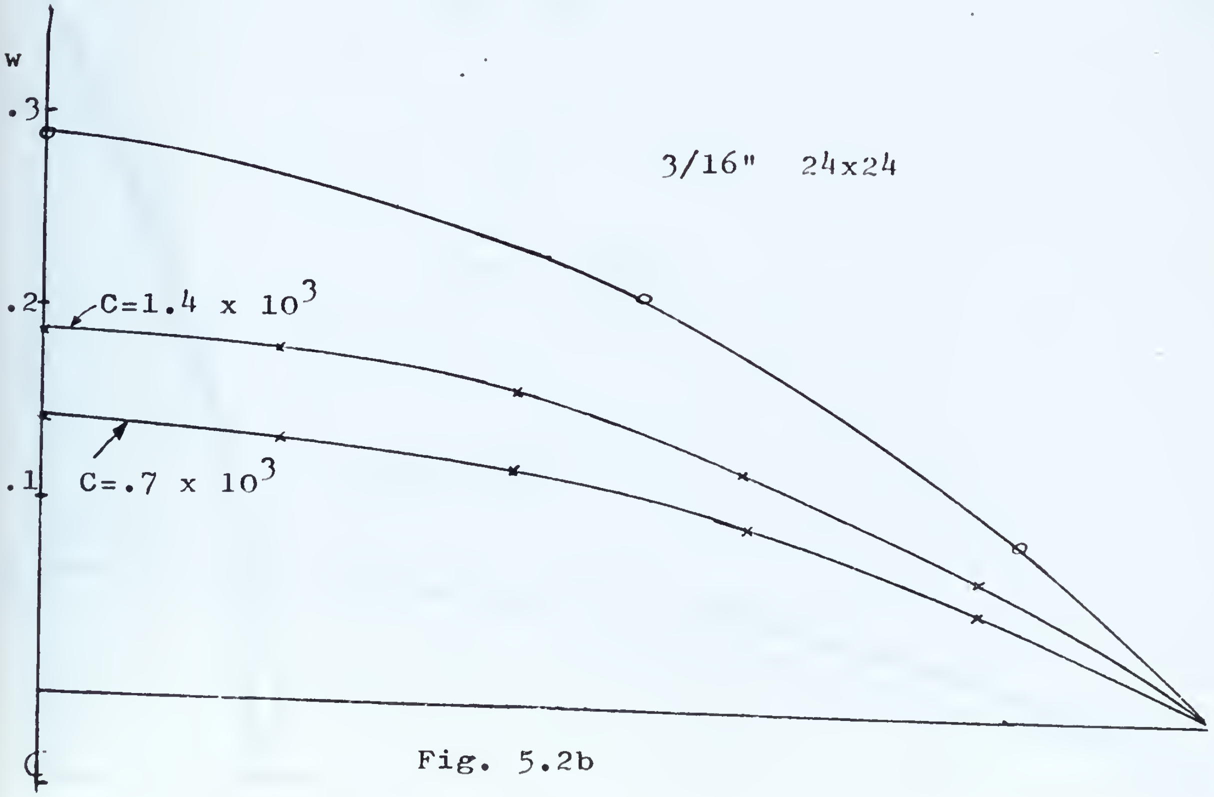

Fig. 5.2b

Experimental and Predicted Deformation

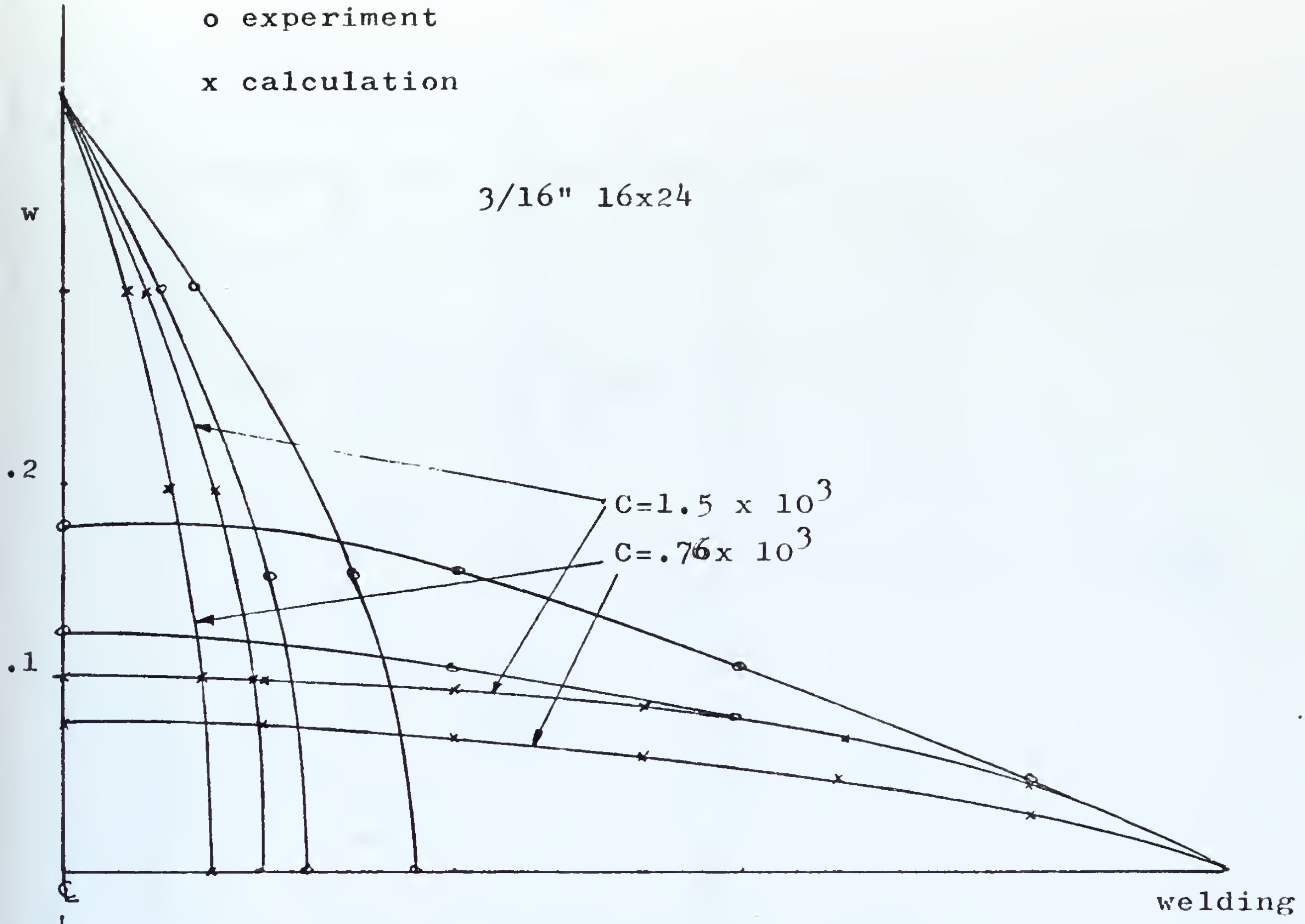

Fig. 5.2c

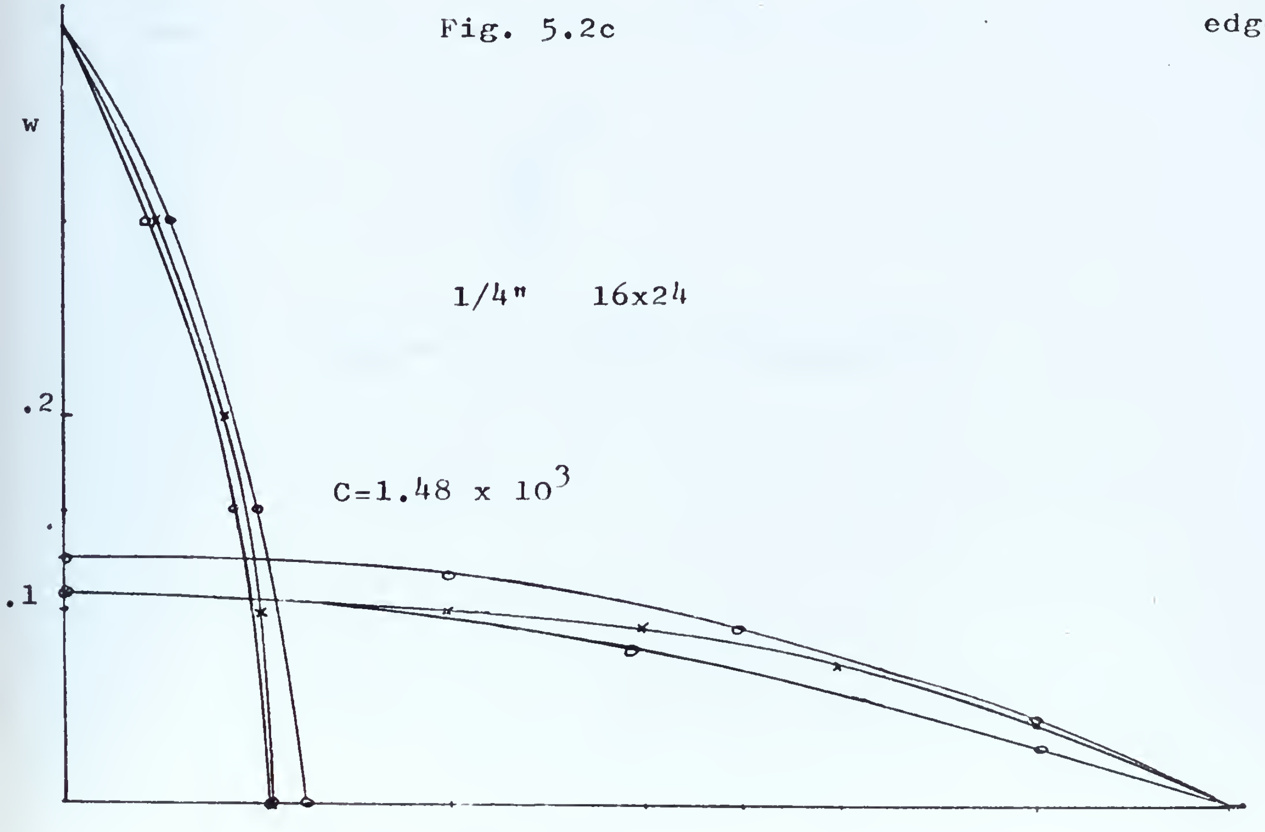

Fig. 5.2d

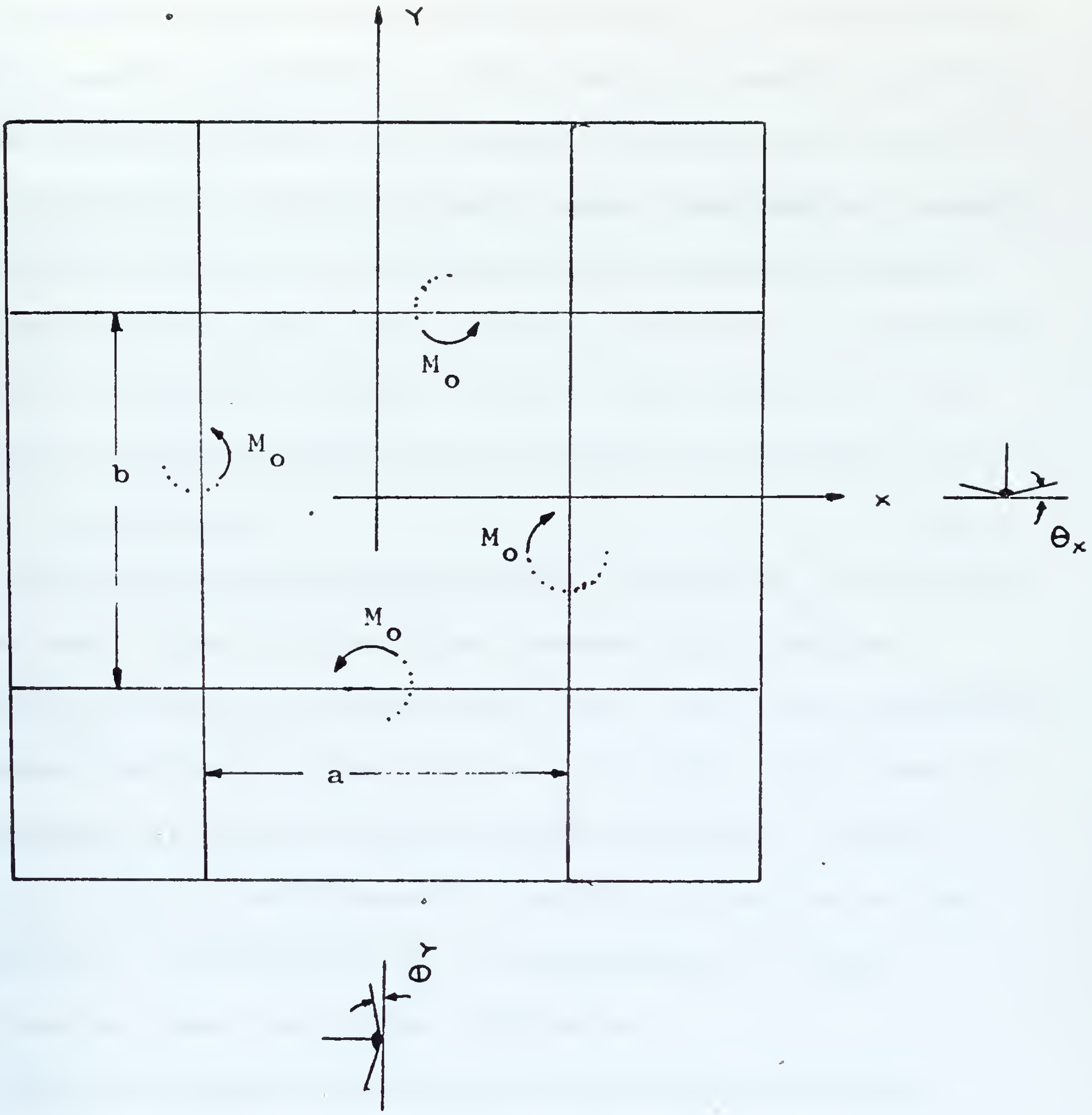
Y
x
M_o
M_o
M_o
M_o
b
a
θ_x
θ_Y

Figure 5.3 - Plate Configuration

We must emphasize that this moment M_o is an uniform elastic moment equivalent to the overall transient effects of the fillet welding, after having cooled down to the room temperature. This approach seems reasonable, because here we are seeking a way of getting an analytic model suitable for designing ship plating and mainly to get the central deformation ($x=y=0$) and not one analysis of the transient welding process which require an elastic-plastic treatment.

The equivalent uniform elastic moment M_o is function of the heat input, filler wire consumption, and the constraint condition at the weld line ; this last constraint condition has to do with the fact of either the plate is continuous, or its extension is not enough to consider the plate fully continuous.(it was the situation of our experiment). The moment M_o is independent of the stiffenning space and plate thickness.

The advantage of using this equivalent uniform elastic moment is that for the continuous plate, it is constant if welding parameters are the same, no matter what plate thickness and frame spacing, therefore it allows the easy prediction of central plate deformation, if welding parameters are known. In actual fabrication and for an existing automatic welding equipment the welding parameters are set fixed for each material and and thickness. This parameters are those likely to give

a sound weld.

Using semi-automatic welding process, this analytic method is not as reliable, because of the human intervention - no two welds are done exactly at the same speed -, but we are convinced that the variation in actual deflection and the one predicted is acceptable.

5.3.2 - Development of a relationship between the equivalent uniform moment M_o induced during fillet weld and the central deflection

Considering the plate in figure 5.3, the application of symmetric uniform moments at the welding edges may be represented (pag. 181 of reference 19) by

$$M_y = \frac{4M_o}{\pi}\sum_{m=1}^{\infty} \frac{1}{m} \sin \frac{m\,(x+a/2)}{2} \qquad \text{at } y = \pm\, b/2 \qquad (5.4a)$$

$$M_x = \frac{4M_o}{\pi}\sum_{m=1}^{\infty} \frac{1}{m} \sin \frac{m\,(y+b/2)}{2} \qquad \text{at } x = \pm\, a/2 \qquad (5.4b)$$

(the origin is at the center of the plate)

The resultant deflection for any arbritary point is:

$$w = \frac{2M_o}{\pi^3 D}\left[a^2 \sum_{m=1,3,5} \frac{\alpha \tanh \alpha}{m^3 \cosh \alpha} \sin \frac{m\,(x+a/2)}{a} + b^2 \sum_{m=1,3,5} \frac{\beta \tanh \beta}{m^3 \cosh \beta} \cdot \sin \frac{m\,(y+b/2)}{b} \right] \qquad (5.5)$$

α, β, and D are defined in appendix 3

$$\theta_y = \left.\frac{dw}{dy}\right|_{\substack{y=b/2\\ x=0}} \qquad \theta_x = \left.\frac{dw}{dx}\right|_{\substack{x=a/2\\ y=0}} \qquad (5.8)$$

Making $\gamma = b/a$,and calculating the central deformation

$$w_o = w \Big|_{\substack{x=0 \\ y=0}}$$

$$w_o = \frac{M\gamma a^2}{\pi^2 D} \sum_{m=1,3,5} (-1)^{(m-1)/2} \frac{1}{m^2} \left(\frac{\tanh \frac{m\pi\gamma}{2}}{\cosh \frac{m\pi}{\gamma 2}} + \frac{\tanh \frac{\gamma m\pi}{2}}{\cosh \frac{m\pi}{2\gamma}} \right) \qquad (5.9)$$

the values of w_o(in), θ_x, θ_y(rad) and M_o (lb in/in) for the experimental data (phase I) are included in table 5.2.

Plotting the term under summation for several values of γ , we get a linear aproximmation - figure 5.4 useful for relating w_o, M_o, and the material characteristics with the plate dimensions.

5.3.3 - Generation of empirical values for the equivalent uniform moment M_o

In 5.3.2 we have assumed that M_o was related to the welding parameters - heat input and welding consumption. The correlation of data for M_o with VI/v and w using a functional approximation allows us to plot this relationship in figure 5.5. Using this figure we can determine empirical values of the equivalent unitary elastic moment due to continuous fillet welding given the welding parameters. The data we have obtained refers to 5052-H32 Aluminum Alloy material using one pass double fillet GMA welding process of continuous orthogonally framed plate.

Sensitivity to specific base material and filler wire properties was not checked by lack of appropriate data.

It is expected that for multiple pass fillet weld the increase in M_o is less sensitive to the increase of weldconsumption or of power input.

Using semiautomatic GMA welding, it is difficult to determine the exact arc travelling speed v, because it depends on how the welder proceeds, his skill, surrounding conditions (wind, humidity), cleanness of the base plate etc., therefore as the arc travelling speed affects the power input, and welding consumption, we may expect some variation on M_o. We have found that for our data points if we have a deviation of $\pm$ 10% in v, it will give a deviation of about 20% in the M_o value. Undoubtly a fully automatic process will give more accurate results.

Once M_o is obtained, for any welding conditions, and for a given plate thickness, material mechanical characteristics and frame spacing, the central deflection of an orthogonally stiffened plate is obtained from figure 5.4 or equation 5.10.

The procedure we have just outlined allows an easy prediction of central deflection due to out-of-plane distortion in fillet welded stiffened plate using one pass GMA welding process.

This method seems to be reliable under the assumptions that were made and that are common to elastic calculations with small deflections, but it only was checked for 3/16

and 1/4" thick plate. For thicker plate its necessary some actual or experimental data to verify whether this can be applied or not.

Table 5.2

Values of M_o for Experimental Data

$\gamma = b/a$	h	$w\big\|_{x=0,\,y=0}$	$\frac{dw}{dy}\big\|_{y=b/2,\,x=0}$	$\frac{dw}{dx}\big\|_{x=a/2,\,y=0}$	M_o lb in / in		
1	1/4	.192	.036	.036	64.55	$M_o = 336.20w$	$M_o = 21515.45\ wh^3$
1	3/16	.289	.055	.055	40.98	$M_o = 141.83w$	
2/3	1/4	.1	.028	.024	59.45	$M_o = 594.55\ w$	$M_o = 38051.5\ wh^3$
2/3	1/4	.128			76.10		
2/3	3/16	.123	.035	.0305	30.85	$M_o = 250.83\ w$	
2/3	3/16	.181			45.4		

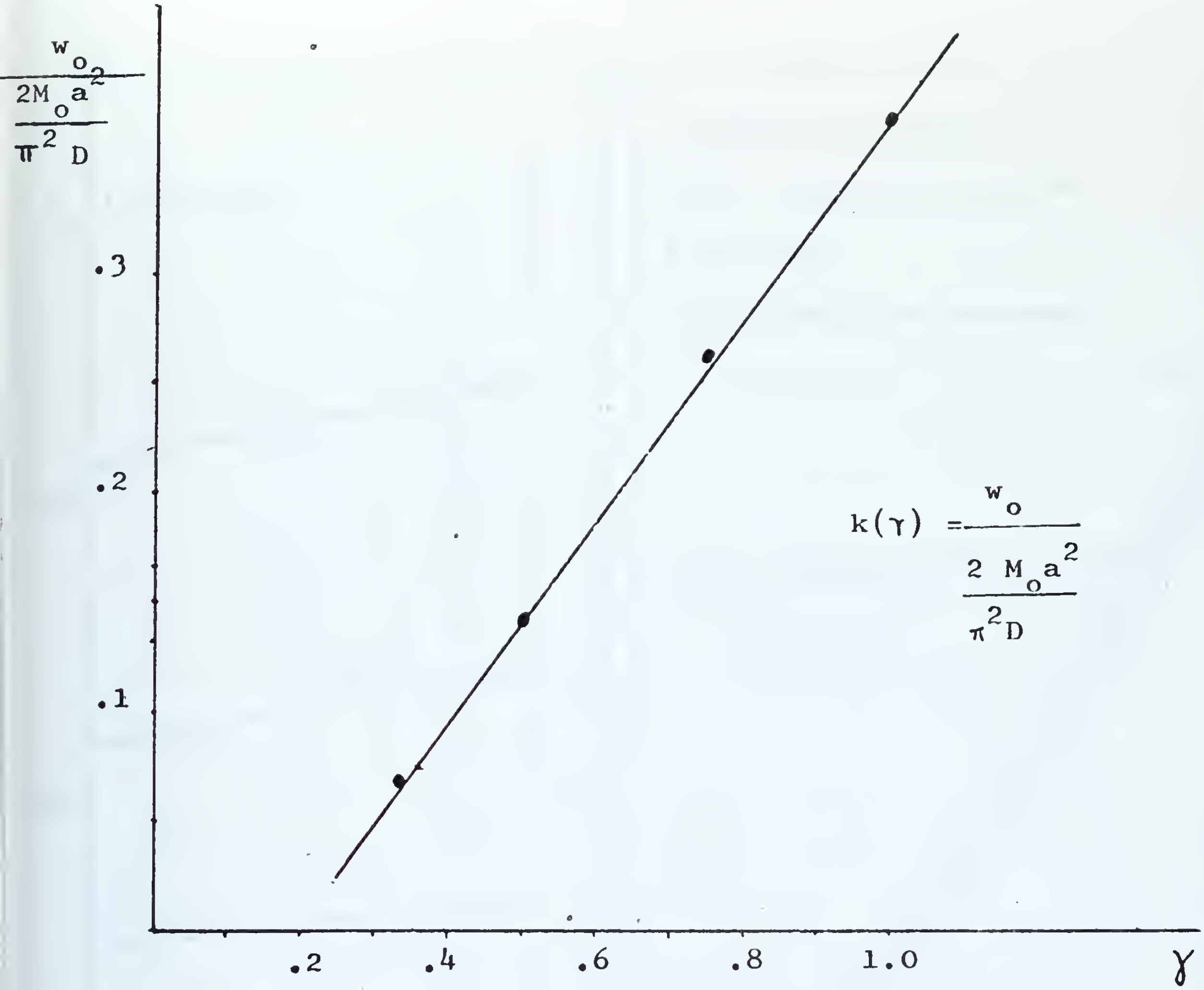

Figure 5.4 - Calculation of k (γ)

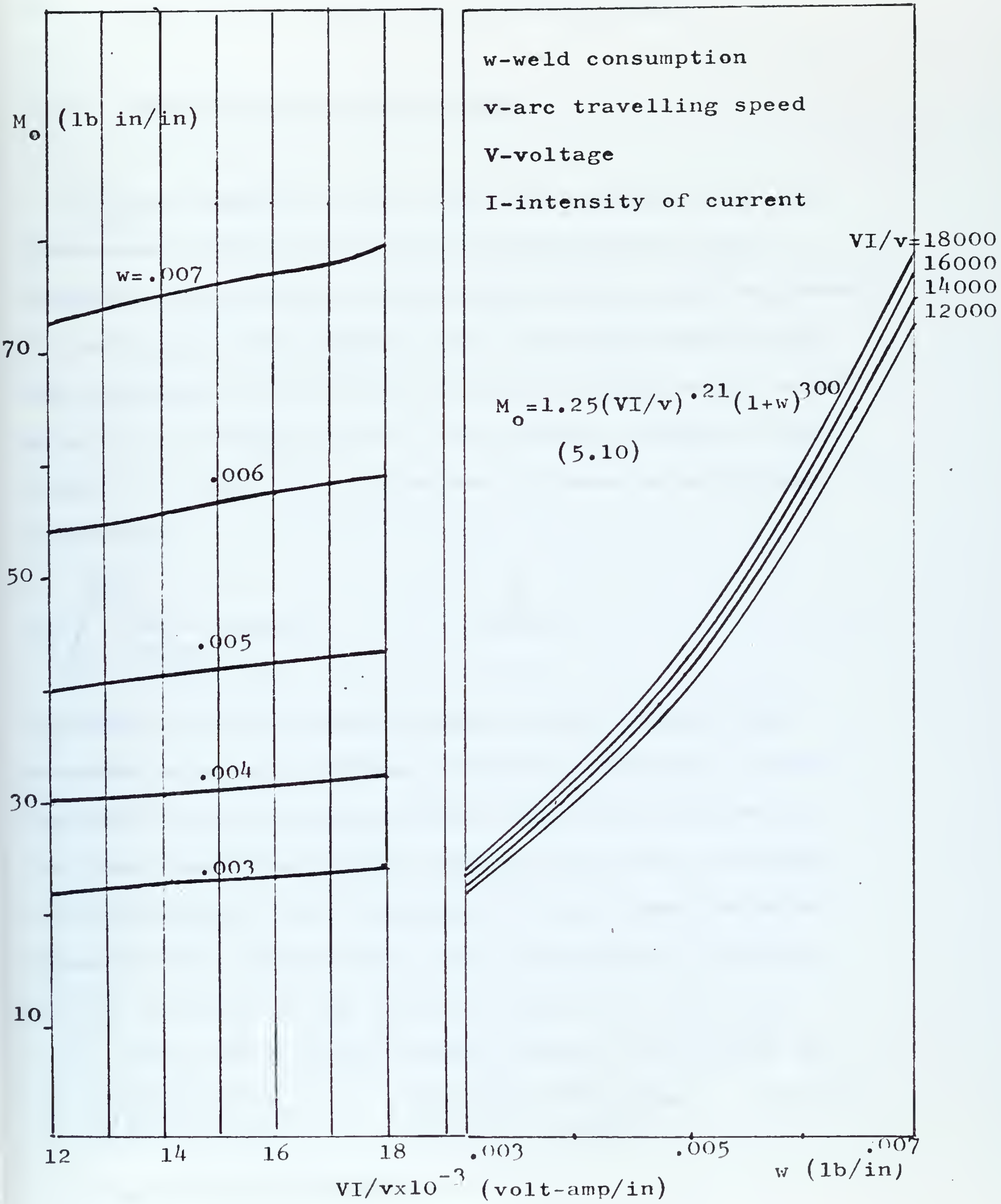

Fig. 5.5 Calculation of M_o

5.4 - Relationship between parameters M_o and C

5.4.1 - Derivation of relationship

Prof. Masubuchi et al, have investigated the one dimensional plate deformation during welding with a minimum strain energy concept using elastic bending theory. Following the same approach for a two dimensional case, and analysing the plate we have been working with, we will proceed by defining first U_w the welding energy per unit length of fillet weld, dispended if there is stiffener constraint

$$U_w = \int_0^{\theta_0 - \theta} \frac{dU_w}{d(\theta_0 - \theta)} \, d(\theta_0 - \theta) \qquad (5.11)$$

in which θ_0 is the angular change at the welding line considering a plate without external constraint; it is assumed that this unconstrained fillet weld is done in the same conditions as the fillet weld of the structure we are studying. The variable θ is the normal angular change at the fillet weld in the constrained structure (it is function of the position along the weld line).

The elastic strain energy stored in the plate is

$$U_s = \frac{D}{2} \iint \left\{ \left(\frac{d^2 w}{dx^2} + \frac{d^2 w}{dy^2} \right)^2 - 2(1-\nu) \left[\frac{d^2 w}{dx^2} \cdot \frac{d^2 w}{dy^2} - \left(\frac{d^2 w}{dxdy} \right)^2 \right] \right\} dxdy \qquad (5.12)$$

D is the flexural rigidity

w is the displacement at the point (x,y)

ν is the Poisson's ratio

Assuming that the ratio of incremental welding energy changes to angular change $(\theta_0 - \theta)$ is linear and given by the equation:

$$\frac{dU_w}{d(\theta_0 - \theta)} = C(\theta_0 - \theta) \qquad (5.13)$$

C -is the rigidity coefficient determined by the weight of deposited material and by the welding process.

Plugging (5.3) into (5.1) becames:

$$U_w = \frac{C}{2}(\theta_0 - \theta)^2 \qquad (5.14)$$

Since θ varies with the position along the weld line we cannot find the minimum energy by differenciating $U_t = \sum_{i=1}^{n} \int U_w + U_s$ with respect to θ and equating it to zero. But assuming that the plate behaves elastically and the deformation is small with respect with the plate thickness $(w \approx 1/2\ h)$ and postulating that the fillet welding, after cooling down, induces an uniform moment M_o acting normally to the weld line, such that the deformation w, due to this moment applied at the four welding lines $(n=4)$ of the considered plate element can be given by

$$w = \frac{2M}{\pi^3 D}\left[a^2 \sum_{m=1,3,5} AA \sin\frac{m\ (x+a/2)}{a} + b^2 \sum_{m=1,3,5}{}' BB \sin\frac{m\ (y+b/2)}{b} \right] \qquad (5.15)$$

AA and BB are dimensional functions defined in appendix 3.

The angle θ is aproximated to $\frac{dw}{dx}$ at $x = \pm\ a/2$ and to $\frac{dw}{dy}$ at $y = \pm\ b/2$

and is function of D, M_o and of the overall plate dimensions.

For a given plate, the variation of Θ implies the variation of M_o, therefore the relationship between C, Θ_o and Θ or M_o necessary for finding the minimum energy is obtained by $\frac{dU_t}{dM_o} = 0$ (5.16)

$$\text{or} \qquad \frac{dU_w}{dM_o} + \frac{dU_s}{dM_o} = 0 \qquad (5.16a)$$

The detailed development of this equation is done in appendix 3.

The final result factoring C is

$$C = \frac{-TT}{AA2 - \frac{\Theta_o}{M_o} AA1} \qquad (5.17)$$

$$M_o = \frac{\Theta_o C \; AA1}{C \; AA2 + TT} \qquad (5.17a)$$

AA1, AA2 and TT are defined in appendix 3.

5.4.2 - Numerical calculations

We have seen in 5.2 that the computer program developed in (10), was not giving satisfactory solutions for predicting out-of-plane distortion if the program input, namely C was obtained from one dimensional analysis model (elastic beam theory).

We have calculated M_o and C, for some discrete frame spacing and plate thickness, using the equations

given in 5.4.1.

The parameters chosen and M_o and C values are presented in table 5.3. The corresponding curves are plotted in figure 5.6, a, b.

Using Θ_0 and M_o obtained from the experimental data, and using these plottings we can get a revised value of C - table 5.4.

Inputing this new set of parameters in Shin's program (10), we can get a better prediction of the distortion - figure 5.7, then those formely obtained in section 5.2. Doing it for other arbitrary values of Θ_o and M_o and comparing with the values C obtained from Taniguchi's (4), we see that the prediction of distortion using the revised C, is closer to the one predict by the theory of elasticity.

Still looking at figure 5.6 and 5.7, we see that besides the welding conditions, C is also dependent on the frame spacing, specially when the plate element becames square.

5.5 - Allowable out-of-plane distortion

5.5.1 - General

Various industrial and military codes and specifications which cover welding fabrication have standards on allowable distortion. Most of these specifications aparently are based upon experience obtained over the years on steels,

Table 5.3

Summary of parameters TT, AA1 and AA2 for several frame spacing (h = 1/4 in).

b	γ	a.b	TT	AA1	AA2
8	1/3	192	13558	45565	10.635
10	5/18	360	21312	85311	25.718
10	5/14	280	21153	66502	19.121
10	1/2	200	21142	47646	12.522
15	15/28	420	47631	100104	38.500
15	3/4	30	48207	71615	24.223
16	4/9	570	54056	137141	57.712
16	4/7	448	54277	106819	42.939
16	2/3	384	54514	91620	34.733
16	1	256	62976	61138	45.693
20	5/9	720	84748	171659	87.110
20	5/7	560	85384	133661	61.552
20	1	400	98400	95527	37.650
24	2/3	864	122680	206166	117.222
24	1	576	141697	137560	65.059
30	5/6	1080	193553	257880	166.412
36	1	1296	318685	309509	219.574

$$C = \frac{TT}{\frac{\Theta_o}{M_o} AA1 - AA2}$$

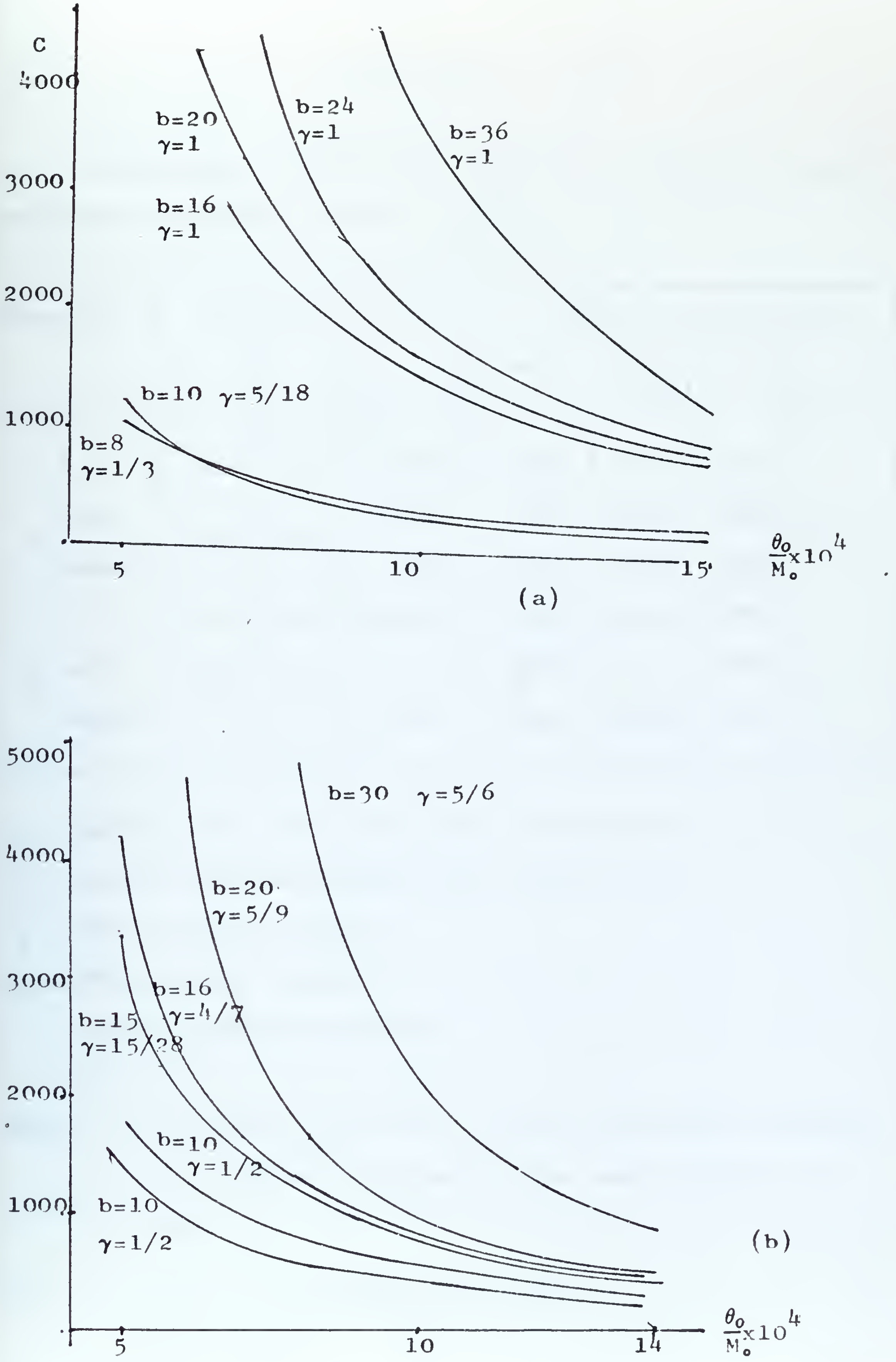

Figure 5.6 - Coefficient C as function of θ_o, M_o, b, γ (h=1/4")

Table 5.4

Calculation of Revised Values of C using the concept presented in section 5.4

Plate no.		Φ_o	C_1	C_2	Central deflection			
					w_1	w_2	w	
1		.060	1476	2256	.155	.191	.192	
2	Left	.061	1478	1410	.100	.098	.128	
	Right			920	.100	.090	.100	
3		.050	743	10380	.148	.290	.284	
4	Left	.040	759	-	.074	-	.181	
	Right			1495	.074	.100	.123	

C_1 = coefficient calculated from reference 10

C_2 = coefficient calculated from section 5.4

w_1 = FEM solution using C_1

w_2 = FEM solution using C_2

w = actual plate deflection

NOTE: for different thickness, TT and AA1 remain constant but AA2 must be calculated from table (h=1/4) as follows

$$AA2 = \frac{(AA2@1/4)\ (1/4)^3}{h_n^3}$$

h_n = new thickness for what we want to calculate AA2

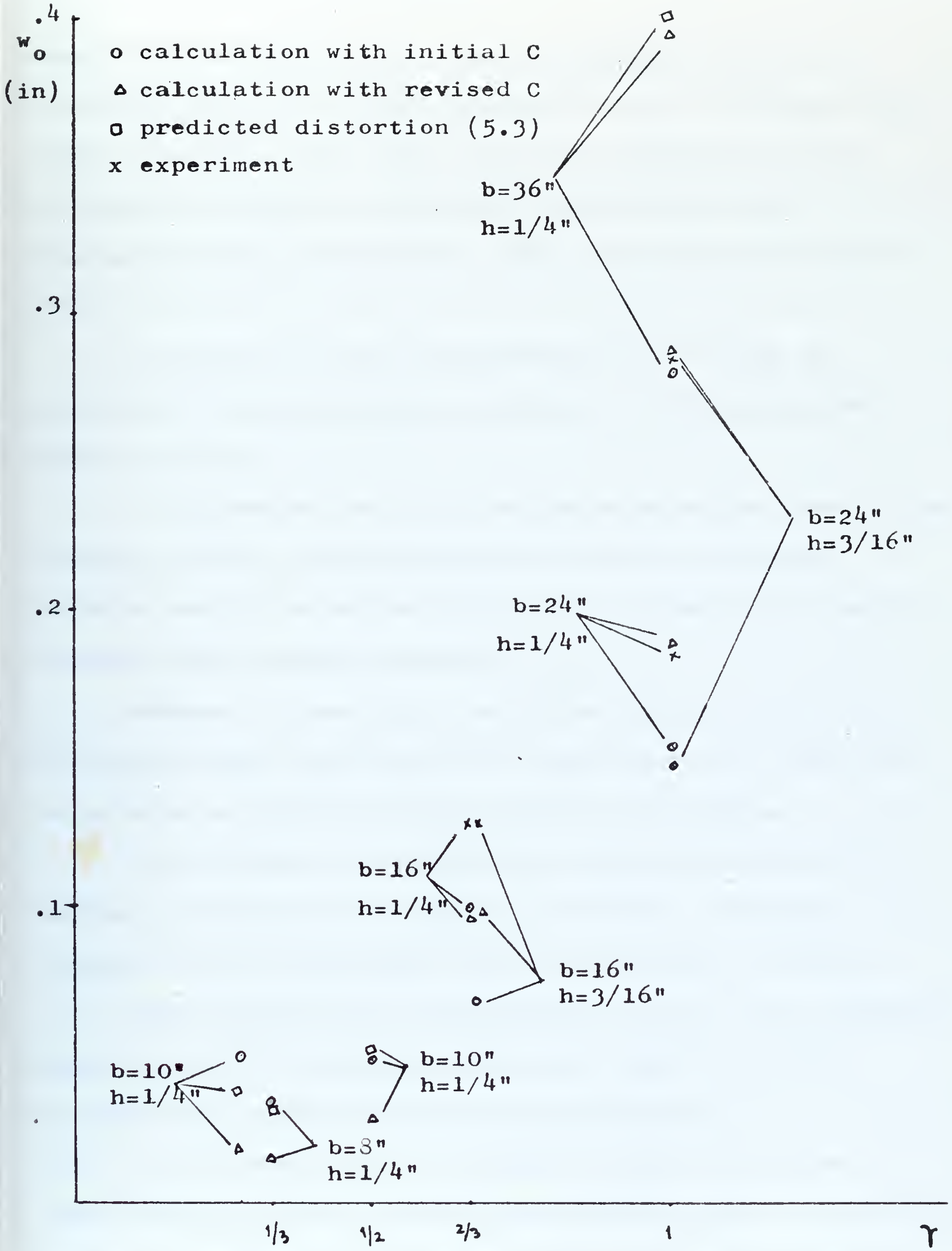

Fig. 5.7-Comparison between calculated, predicted and experimental central plate deflection

specially low carbon steel, and it appears to be costumary pratice to apply the same codes to Aluminum and other materials (17) which may raise questions on the suitability of these standards for materials with characteristics different of those where they were based on.

It seems that the establishing of any kind of allowances for fabrication processes can be approached from two sides:

i) Allowance has to be set up because the fabrication process produces imperfections in spite of the best working conditions and using all the economically feasible current technological advances.

Because of economic reasons, standards have to be different either they refer to high production commercial structures or special purpose unique structures.

ii) Influence of fabrication imperfections on the design calculations (strength, stiffeness, cracking, fatigue, brittle fracture, etc.), and margin of safety.

The standards are established in such a way that the use of current design procedures and margin of safety accounts for the effect of the imperfection.

It is clear that for weight critical structures or very specific cases like high performance ships, since the design is much more refined and factor of safety smaller, the predicted imperfections must be directly inputed into the design procedure.

5.5.2 - Aluminum Structures and the US Navy Permissible Plate Unfairness Standard

Kitamura (23) investigated the effect of out-of-plane distortion in plate buckling, for transversely framed structures and he found that the standards established by the US Navy were not always reallistic in a sense that for some frame spacing and plate thickness, this standard was very difficult to satisfy; on the other side he verified that for most of the plate dimensional characteristics it would reach the yield (uppermost fibers) well below the limit for permissible unfairness. This means that the standards allow permanent set, therefore the plate services in the elasto-plastic range which in almost all structures may be perfectly acceptable.

These USN standards (27) do include different values for plate operation in different places (e.g. bottom, main deck, side shell, secondary decks, etc.), but they do not refer for which stress schedule is the plate going to operate (e.g. orthogonal stiffening, longitudinal framing, hydrostatic load, etc.), therefore we think that the concept mentioned in 5.5.1.ii was only partially accounted for.

Using the data generated in this thesis, we plotted the central deformation on plates no. 1. 2. 3, 4 in figure 5.8, where we see that the values of unfairness are

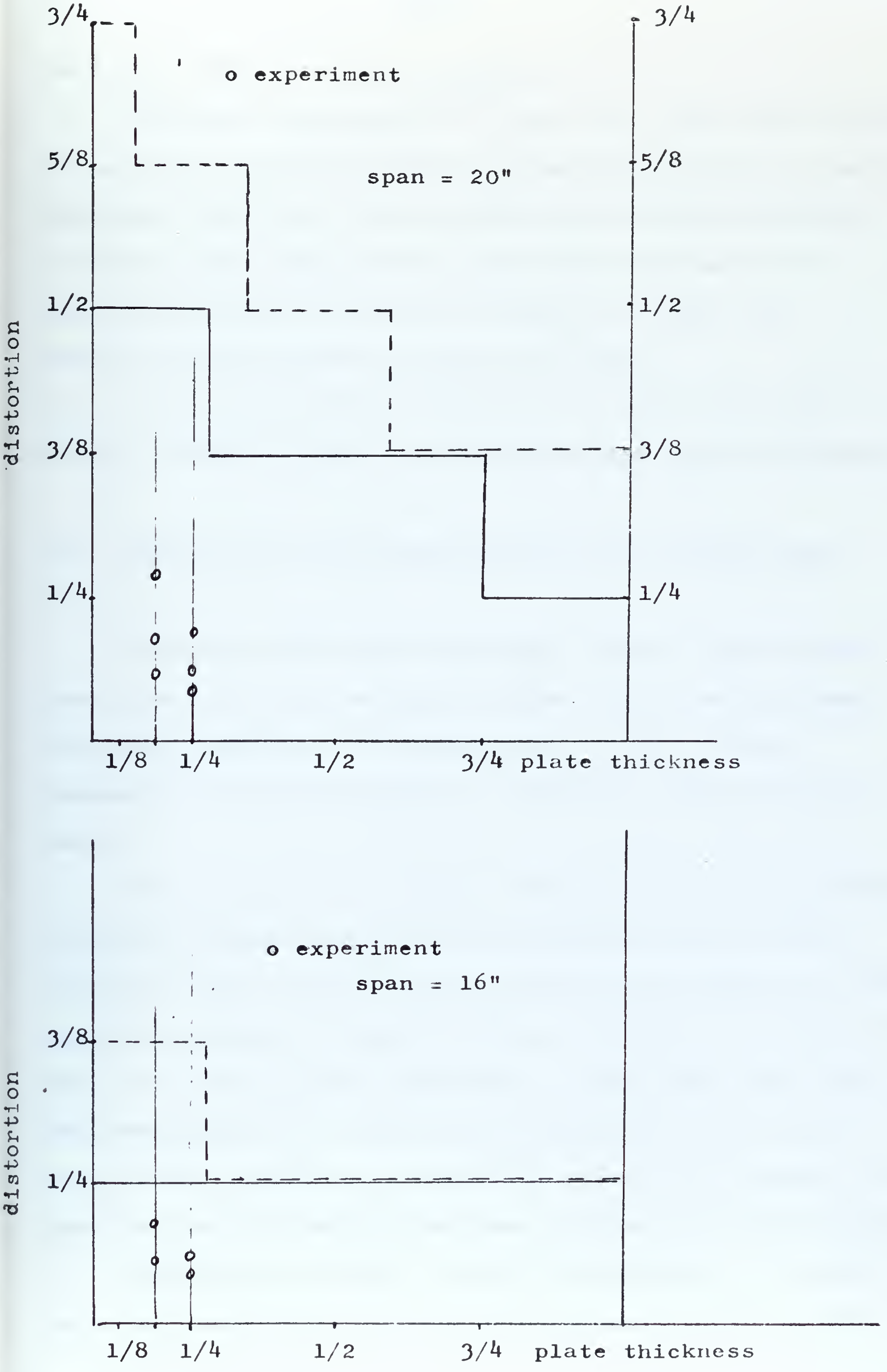

Fig. 5.8 Experimental and Allowable Distortion (27)

well below the permissible ones.

Using the deformation of plate no. 1 and the concept of equivalent uniform moment M_o (section 5.3.3), we could elaborate table 5.5 where we see that as frame spacing increases, the plate central deflection approaches the permissible limit. Also as the plate is wider the deflection gets closer to the same limit.

Later in sections 5.6 and 5.7 we will verify the effect of out-of-plane deformation on the plate efficiency.

5.6 - Design of a Grillage Subjected to a Lateral Load

In some local ship structures (tanks, cargo decks, etc.) the effect of bending stresses on the hull girders is either negligible in comparison with the lateral pressure that the grillage must support or they do not exist.

Using the Limit Analysis Theorems (13) we can get the uniform collapse load p_c on a flat plate and this is a limiting load no matter how we consider the material: elastic perfectly plastic or rigid perfectly plastic (is does not take in account strain hardening). This limit load and the knowledge of the initial deformation for each plate with fillet welded stiffeners will allow us to develop an equation for determining the loss of load carrying capacity.

Knowing the initial central deformation w_o, or the material characteristics and welding conditions, we will

Table 5.5

Welding Distortion (w_o) vs. USN Specs. (tol) -
(M_o = 64.5 lbs in / in, h = 1/4 in)

frame spacing width b	h=1/4" tol (in)	$\gamma=1$		$\gamma=2/3$		$\gamma=1/3$	
		w_o	w_o/tol	w_o	w_o/tol	w	w_o/tol
16	.375	.085	.227	.108	.288	.139	.371
20	.5	.133	.266	.169	.338	.217	.435
24	.625	.192	.244	.244	.390	.313	.500
28	.625	.260	.333	.333	.533	.423	.681
32	.75	.341	.434	.434	.580	.556	.742
36	.75	.432	.550	.550	.733	.704	.936
40	.75	.533	.678	.678	.904	.864	1.152

know the equivalent uniform elastic moment M_o applied at the plate edges (welding lines).

The collapse load is sensitive to the edge conditions, being for the limit cases as follows:

$$p_{c}\,(cl) = \frac{3\,\sigma_o}{\frac{b^2}{h^2}\,(3-2\,\zeta\,)} \qquad \text{(clamped plate)} \qquad (5.18)$$

$$p_{c(ss)} = \frac{3\,\sigma_o}{\frac{2b^2}{h^2}\,(3-2\,\zeta\,)} \qquad \text{(simply supported plate)} \quad (5.19)$$

$$\zeta = (\,\sqrt{3+\gamma^2} - \gamma\,)\gamma \qquad \gamma = b/a \qquad (5.20)$$

$$p_{c(ss)} = p_{c(cl)}/2 \qquad (5.21)$$

A continuous flat plate subject only to lateral load can be considered to have clamped edges, because of symmetry and because a plastic hinge would be formed at the boundaries when the collapse load is applied.

The existence on unfairness, out-of-plane angular distortion, represented by the constraining uniform moment M_o due to fillet welding makes the condition of clamped edges to be droped going towards a simply supported condition as M_o is larger.

If $M_o = M_p$ where M_p is the fully plastic collapse moment

$$M_p = \frac{\sigma_o h^2}{4} \qquad (5.22)$$

We would have a simply support case, if $M_o = 0$ it reduces to a clamped plate.

By analogy with the work of Wood in 1960 we can postulate that the plate with initial deformation will have a collapse load p

$$p = \frac{6M_p \left(2-\frac{M_o}{M_p}\right)}{b^2 \left(3-2\zeta\right)} \qquad (5.23)$$

and the loss in carrying load capacity is:

$$\Delta p = \frac{p_{c(cl)}-p}{p_{c(cl)}} = \frac{12M_p-(12M_p-6M_o)}{12\,M_p}$$

$$\Delta p = \frac{M_o}{2M_p} \qquad (5.24)$$

From figure 5.4

$$M_o = \frac{D\,w_o\,\pi^2}{2a^2\,k(\gamma)}$$

$k(\gamma) \simeq -.0764 + .442\,\gamma$ (figure 5.4)

$$\Delta p = \frac{D\,w_o\,\pi^2}{4a\quad k(\gamma)M_p} = \frac{\pi^2}{12}\,w_o\,\frac{E}{\sigma_o}\,\frac{h}{a\,(1-\nu^2)k(\gamma)} \qquad (5.25)$$

The loss in load carrying is linear with the central deformation for the same plate element.

Equation 5.25 gives a good appreciation of the effect of out-of-plane distortion on the effectiveness of a plate strictly subject to lateral load.

For the initial set of four experiments the loss in carrying capacity would be:

Plate no.	$\Delta p(\%)$
1	7
2(right)	6.3
2(left)	8.1
3	7.8
4(right)	5.9
4(left)	8.6

We may conclude that the prediction of loss in plate efficiency if only lateral uniform pressure is present is independent on the frame spacing, depending only on the welding conditions (M_o), plate thickness and tensile yielding stress.

5.7 - Effect of initial out-of-plane deflection on plate element design, using Marguerre's theory of plates and the equivalent elastic moment concept

5.7.1 - Analysis

Kitamura (23), studied the problem of the maximum

allowable central deformation, due to fillet welding for a continuous transverse framed plate, longitudinally compressed and subjected to a lateral load. Using the Von Mises yield criteria and once the material characteristics, thickness, frame spacing and welding conditions were known, the maximum allowable central deformation for an all elastic plate was found.

We will develop next a somewhat similar procedure that might be a design procedure rather then a parametric analysis. It is based on Marguerre's theory of plates (18), in which the plates are subjected to longitudinal compression σ_A, uniform lateral loading p and an uniform moment M_o applied at the weld lines (plate element edges). In the calculations, the membrane stresses due to large deflections are retained. The plate is simply supported and the edges remain straigth no matter the loads.

For each plate - figure 5.9, with material characteristics ν, E, σ_y, thickness h, plate width b and side ratio b/a, the maximum allowable deformation w_o is calculated using Tresca's yielding criteria for the skin stresses (the Tresca hexagon - figure 5.10 is inscribed in the Von Mises ellipse).

All the calculations are shown in appendix 4.

Since the value of stresses in y direction are independent of the longitudinal compression - equation A4.7a - we started using this equation to find the maximum allowable central deflection to thickness ratio w/t. This equation defines states of stress along line

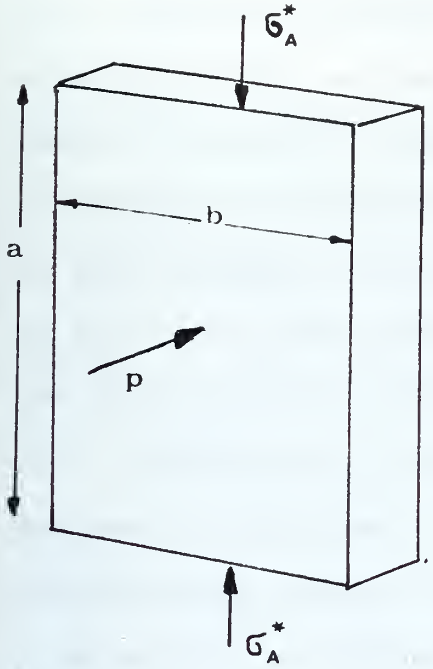

Figure 5.9 - Load and plate configuration

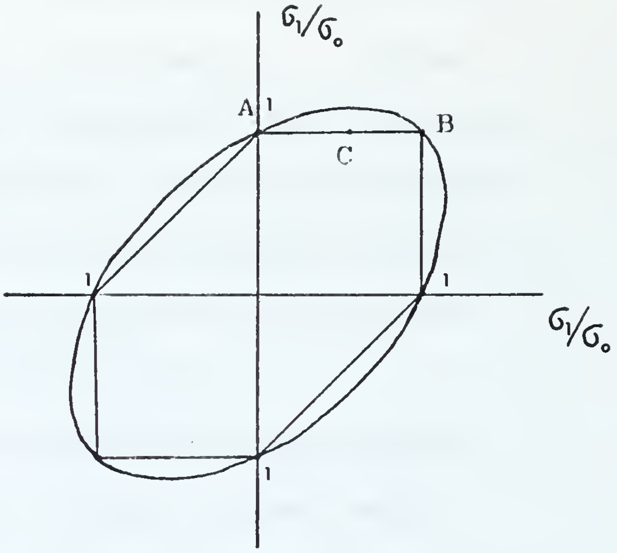
σ1/σ0
A
1
B
C
1
1
σ1/σ0
1

Figure 5.10 - Yielding criterion

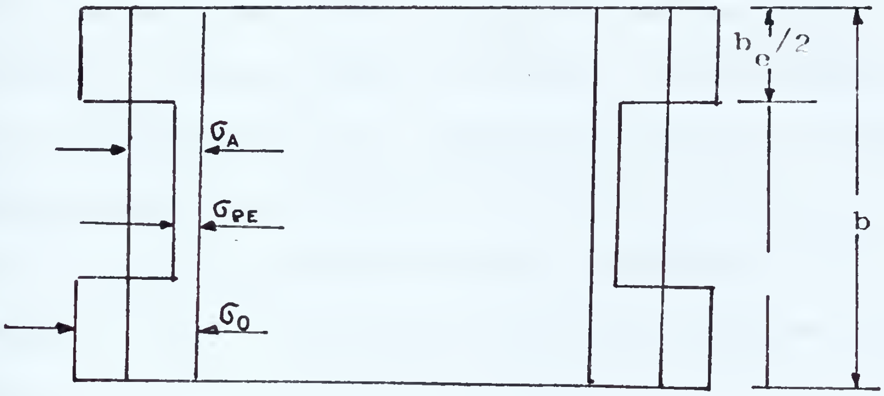
σA
σPE
σ0
be/2
b

Figure 5.11 - Effective width b_e

AB - figure-5.10. Plugging in the central deflection w in equation-A4.7b, we can find the limiting σ_A. These values σ_A and w/h together with equations-A4.7- allow us to define the point C on figure-5.10. As C moves toward B, the strength of the plate is better used and point B is the point where the elastic properties of the plate are fully used (at the plate mid point).

Knowing w/h, using equation-A4.8-and applying the theorem of stationary potential energy, we can draw a relationship between σ_A and p, for each value of b, t, γ, E, σ_o, ν, M_o. σ_A^* has to be less than or equal to σ_A -figure 5.9.

For the same material, thickness and welding conditions (M_o), curves can be plotted for different frame spacing b and side ratio γ. Figures 5.12 a, b, c, d represent σ_A/p relationship for b=16, 20, 24, 26" h=1/4" γ=.8(3), 1, 1.5, M_o=64.55 lb in/in, E=10^7psi, σ_o=30000 psi, ν=.3. The values for these figures are in table 5.6.

This curves are the locus of the most efficient plate dimensions - i.e. plate where the elastic characteristics of the material are better used, for the corresponding frame spacing.

This development includes post buckling plate behavior in a sense that the values of the inplane load are larger than the elastic buckling stress σ_{PE} defined by

Table 5.6

Allowable σ_A and p for several plate dimensions

b	$\gamma=b/a$	w/h	σ_c	σ_A/σ_c			
				p= 0	4	5	7
16	.8(3)	1.47	9123	1.61	1.32	1.25	1.10
16	1	1.40	8826	1.53	1.32	1.26	1.15
16	1.5	1.17	10358	1.43			1.26
20	.8(3)	2.10	5838	2.39	1.89	1.77	1.52
20	1	2.01	5649	2.24	1.87		1.59
20	1.5	1.71	6630	2.045			1.76
24	.8(3)	2.77	4055	3.53	2.75	2.56	2.17
24	1	2.67	3923	3.28	2.70		2.27
24	1.5	2.32	4604	2.99			2.55
26	.8(3)	3.12	3455	4.2	3.07	2.78	2.22
26	1	3.01	3342	3.93	3.23		2.70
26	1.5	2.63	3923	3.60			3.06
30	1	3.71	2511	5.52	4.51		3.75
30	1	3.29					

$b/a > .7$ (buckling in one half wave)

w/h = maximum deformation to thickness ratio before yielding

σ_c = Buckling stress (psi)

p = Lateral pressure (psi)

Bryan's small-deflection theory (13)

$$\sigma_{PE} = \frac{K\ \pi^2}{12(1-\upsilon^2)}\ \frac{\sigma_0}{\beta^2} \quad (5.26)$$

$K \simeq 4$ for long simply supported plates. For post buckling behavior the distribution of inplane loads cannot be considered uniform over the entire section. Von Karman in 1932 (15) postulated that provided the unloaded edges of a long pinned plate (simply supported), remain straigth, the maximum post buckling load the plate can sustain occurs when the edge stress σ_e reaches the yield stress (figure 5.11) , the center portions of the plate will have less compression strain than the portions near the edges because of the larger deflections in the center of the plate. The introduction of this postulate, lead us to verify if the average σ_A will produce yielding at the weld lines. To do so we need to introduce the effective width b_e, or the plate width adjacent to the stiffener and such that $b_e\ \sigma_o = b\ \sigma_A$ (5.27)

Von Karman provided us with the weld known minimum effective width at failure

$$b_e = 1.9\ h\ \sqrt{E/\sigma_o} \quad (5.28)$$

For the Aluminum Alloy we are considering

$$b_e \simeq 34\ h \quad (5.29)$$

The maximum value of the σ_A becomes

$$\sigma_{A(max)} = \sigma_m = \frac{b_e}{b}\sigma_0 = 1.9\ \frac{h}{b}\sqrt{\frac{E}{\sigma_0}} = \frac{1.9}{\beta}\ \sigma_0 \quad (5.30)$$

This equation has been used for longitudinal by framed panels $(a > b)$

For our plate material

$$\sigma_m \simeq 10.35 \times 10^5 \frac{h}{b} \quad (5.31)$$

We have used this last equation to verify the values plotted in figure 5.12, but the values σ_m are smaller than σ_A at the edge lines - equation - table 5.7.

For transversely framed ships it has been shown (15) that if after buckling the middle zone remains stressed at the elastic small deflection buckling stress, for the same boundary conditions

$$\frac{\sigma}{\sigma_0}ym = \frac{a_{em}}{a} = \frac{.9}{\beta^2} + \frac{1.9}{\alpha\beta}\left(1 - \frac{.9}{\beta^2}\right) \quad (5.32)$$

$$\alpha = \frac{a}{b}$$

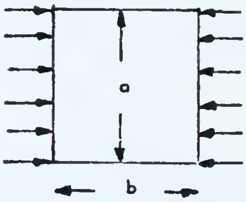

The existence of residual stresses might also be included in the calculation of the limiting σ_A, but in general it is considered (15) that on initial service, residual stresses will be shaken-down and therefore will not constitute problem in future service of the structure unless reverse yielding is achieved, which will produce complete failure of the structure by fatigue.

5.7.2 - Effect of initial distortion on the inplane load and lateral pressure

The relationship between the allowable inplane load

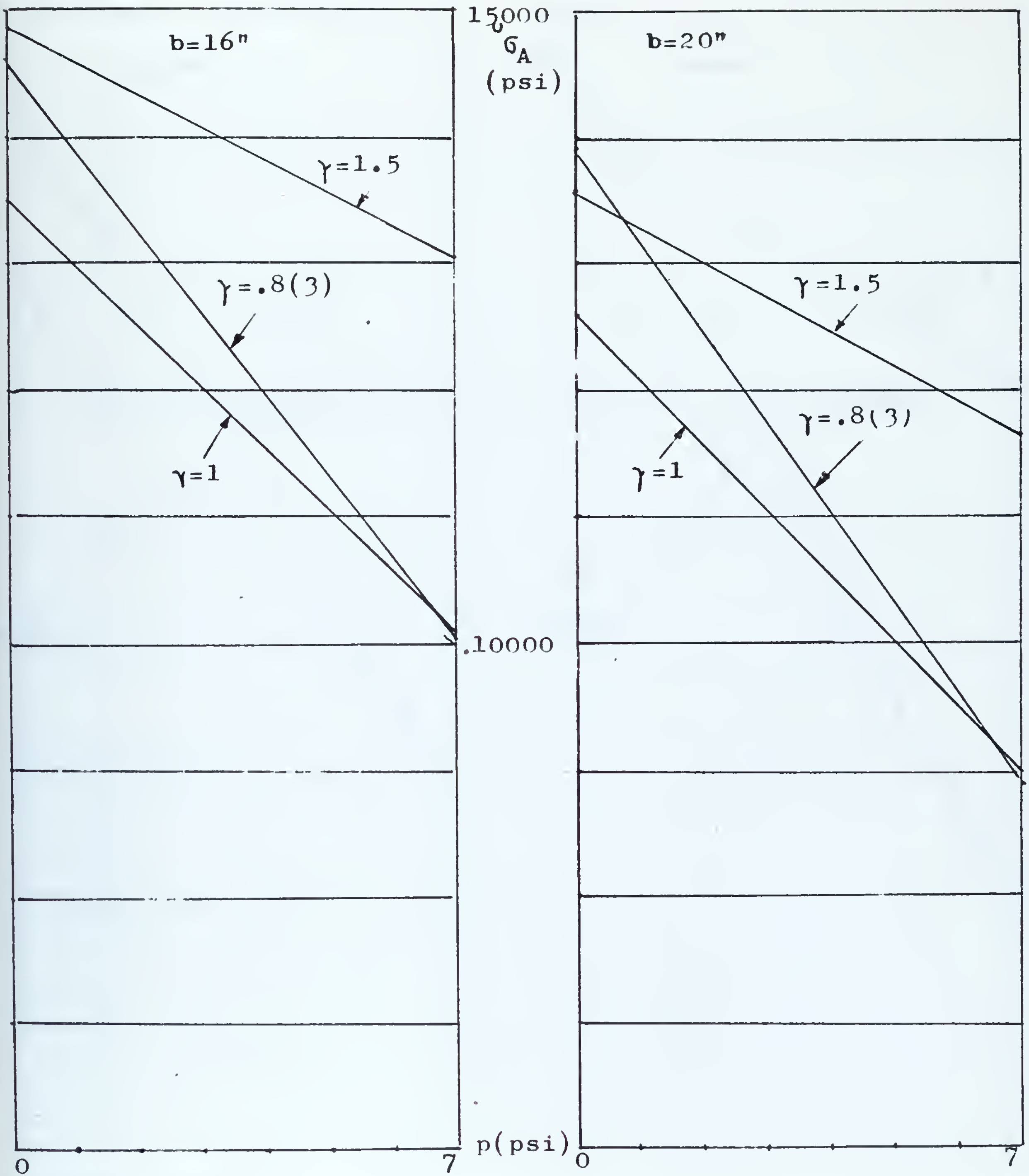

Figure 5.12 a, b - Allowable compressive longitudinal stress in function of lateral pressure and frame spacing.

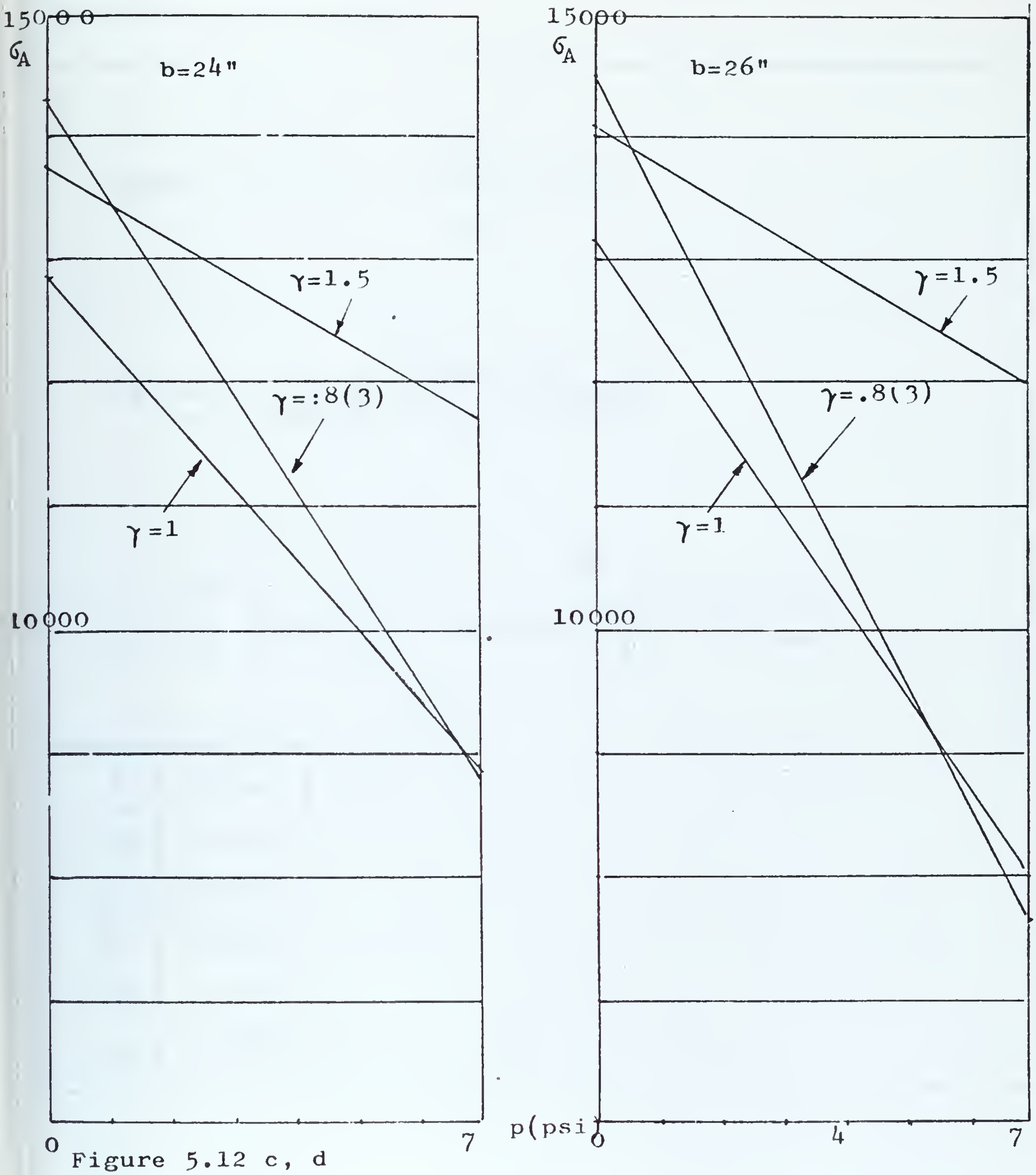

Figure 5.12 c, d

Table 5.7

Calculation of w/ h max.

$$30000 \geq \sigma_{A\ max} + \frac{E\left(\frac{w}{h}\right)^2 \cdot h^2\ \gamma^2}{8b^2}$$

$$w/h\ max = \frac{2b}{\pi \gamma h}\sqrt{\frac{2(30000 - \sigma_{A\ max})}{E}}$$

$$\left.\begin{array}{l} h = .25 \\ E = 10^7 \end{array}\right\}\ w/h\ max = .0011388\ \frac{b}{\gamma}\sqrt{\sigma_0 - \sigma_{A\ max}}$$

b	$\sigma_{A\ max}$
16	15940
20	12750
24	10625
26	9810
30	8500

load whether distortion is present or not will now be developed, by computing the reduction in compressive inplane load due to out-of-plane distortion

$$\varepsilon = \frac{\sigma_A^0 - \sigma_A^1}{\sigma_A^0}$$

σ_A^0 = allowable in plane stress - no out-of-plane distortion $M_o = 0$

σ_A^1 = allowable in plane stress - out-of-plane distortion

From equation (A4.6) we can get

$$\varepsilon = \frac{\frac{128}{\pi^4} b^2 \left(\frac{1+\beta^2}{1+\beta^4}\right) \frac{M_o}{Eh^4}}{\left(\frac{w}{h}\right)^3 + \left(\frac{w}{h}\right) \frac{4}{3} \frac{1}{(1-\nu^2)} \frac{(1+\beta^2)^2}{(1+\beta^4)} - \frac{p}{\pi(1+\beta^4)} \left(\frac{4b}{\pi h}\right)^4 \frac{1}{\varepsilon}}$$

$$w/h = -\frac{2\left(1+\nu \frac{b^2}{a^2}\right)}{(1-\nu^2)} + 4\sqrt{\left(\frac{1+\nu \frac{b^2}{a^2}}{2(1-\nu^2)}\right)^2 + \frac{\sigma_o b^2}{2E\pi^2 h^2}} \qquad \text{(appendix 4)}$$

$$M_o = \frac{w_o D \pi^2}{2a^2 k(\gamma)} \qquad \text{(fig. 5.4)}$$

The complexity of ε does not allow a simple relationship between the parameters involved, however we can conclude that the loss in load carrying capacity ε decreases as the lateral load decreases, being minimum when p=0.

The loss in load for the cases included in figure 5.12

were calculated and presented in table 5.8.

The losses vary with the plate dimensions. In actual design the present procedure could be introduced in the integrated design process, being the best feasible plate dimensions picked up using a systematic search or other.

Table 5.8

Loss in load carrying capacity ε (percentage)

(M_o = 64.55 lb in/in - experiment no. 1)

b	γ =b/a	psi=0	psi=4	psi=7
16	.8(3)	8.6	10	12.1
16	1	8.1	9.3	10.5
16	1.5	8.6	8.9	9
20	.8(3)	6.5	8.2	9.8
20	1	6.2	7.3	8.5
20	1.5	8	8.3	8.6
24	.8(3)	4.9	6.7	7.7
24	1	4.6	5.6	6
24	1.5	7	7.4	7.7
26	.8(3)	4.3	5.4	6.8
26	1	4.1	4.9	5.8
26	1.5	6.6	6.9	7.2

6. CONTROL AND REDUCTION OF DISTORTION

A. - General

The effects of out-of-plane distortion are not desirable as was seen in sections 3 and 5, but since they are present in almost all fusion welding processes, methods of design and fabrication techniques must be developed to help minimize the distortion effect.

We have seen in 5.6 and 5.7 that during the design of a grillage for a determined load carrying capacity, the expected distortion can be inputed in an integrated design system and the best structure under the design criteria (load efficiency, minimum weight) can be found. This is a reduction of distortion effects by appropriate design.

Complementary to the method of design, distortion can be reduced by: proper choice of welding process and welding parameters, joining schedule, prewelding distortion avoidance techniques and postwelding correction mesures.

It is clear that all the measures possible to take before the welding are desirable to post welding repair work.

B. - Methods of Reducing Distortion in Fillet Welding

6.1 - Choice of welding process

Distortion occurs because of the non uniform temperature distribution in the specimen and because of the actual temperatures involved leading to the existence of plastic zones. If all the stresses generated were elastic, no distortion would be felt. Unfortunately this is not so, a plastic zone is inherent to fusion welding.

The best welding process for reducing distortion would be the one that produces a highly concentrated heat source, passing fast enough to avoid high heat input and therefore appreciable heat propagation.

Laser and electronbeam welding are two processes that seem to be suitable for reducing distortion because they have a high power density as they are highly concentrated power sources.

The merits of these two new welding processes namely the electron beam (EBW) are far beyond the distortion problem and are related with the possibility of welding thicker plate with only one or few passes.

Dr. Terai (26) mentioned that in his laboratory using EBW it was recently possible to weld a section of 300 mm thick (11.81 inches) of 5083 Aluminum Alloy with one pass and without distortion for engineering purposes.

For the most common welding processes, used for

Aluminum Alloys - GTA and GMA - it seems that thinner filler wire associated with high power input, high filler wire feed speed and high travelling arc speed, would produce less distortion, but only a metalurgical study of welded specimens, could tell which is the acceptable choice of parameters for achieving simultaneously a sound welding and significative reduction of distortion.

6.2 - Welding sequence

Welding sequence techniques in multipass butt welding were presented in previous works (5, 17).

It seems that for fillet welding of continuous framed plates, welding sequence does not make appreciable difference.

6.3 - Forced cooling

This process requires the contact of a cooling fluid (cryogenic liquid Co_2 or liquid N), immediatly after the passing of the arc.

This alteration of thermal pattern aims drastically to reduce the plastic zone, because the elevation of temperature on most of plate is not so high and the yield strength of the plate is kept in greater values, therefore the plate will behave elastically in larger extension. This process is referred in (5, 17) where is

mentioned that residual stresses can be greatly reduced.

The application of this method to fillet weld of stiffened plate is more difficult to implement than for butt welds, because of the geometry of the joint.

Figure 6.1 show one way of forced cooling using CO_2, mentioned in (5, 17)

6.4 - Plate pre heating

Plate heating before welding has been investigated at MIT by professor K. Masubuchi and several students.

A technique called "differential heating" has been developed, and it consists of heating the stiffener previously to welding, for avoiding the effect of longitudinal shrinkage due to fillet welding which induces stiffener and plate bowing at the weld line.

This bowing reduces the beam column buckling strength of the stiffener and adjacent plate.

In our case, we applied plate heating for tentatively reduce the out-of-plane distortion as we have described in section 4 phase II.

It seems that the effect of fillet welding in angular distortion can be broken down in 2 parts:

i) Effect of the shrinkage due to cooling of the added material and ii) nonuniform shrinkage of the plate cross section, due to a temperature gradient across the plate thickness and to thermal strains induced during the

fast localized temperature increase at welding.

It seems that the first effect is preponderant in thin plate and with material of higher thermal diffusivity, like the Aluminum Structures we are studying.

Plate heating, should reduce the shrinkage effect due to ii), because by the time the welding is done, the thermal strains associated with the temperature increase, are smaller because the temperature difference is smaller, therefore the plastic zone is reduced - more of the plate acts elastically.

Also the temperature gradient across the section verified at welding time can be reduced specially if the plate is heated from the side opposite to the welding. This should be more notorious for thick plate.

Physically, it seems that the plate pre heating will reduce effect ii), but will do nothing to reduce the shrinkage of the added metal.

As we mention in section 4.2 we did not get evidence of reduction of distortion using the heating scheme shown in figure 4.10 ,(plate no. 6), but we feel that the conditions in which this heating was done were not efficient.

However, using the set up shown in figure 4.11 ,(plate no. 7) we got evidence of reduction of angular distortion.

The central deformation was reduced by 35% from what should be predicted using the analytic method we have presented in section 5.3. This value of reduction is only

approximate, because the arc travelling speed of the welding was not constant as it could be if instead it was used an automatic welding system.

For an accurate relationship between plate heating and reduction of distortion, more research should be done, using a simpler structure - e.g. a T joint - and an automatic welding process, where the arc travelling speed could be precisely determined ; table 6.1 represents a summary of the experimental data and analysis done using pre heating.

Table 6.1

Reduction of distortion due to pre heating

Plate no.	VI/v Volt Amp/in	w lb/in	From section 5.3.2 and 5.3.3		Actual central deflection w_o	Reduction of distortion
			M_o	predicted w_o(in)		
6	15330	.0038	30	.093	.092	0
7	17360	.0043	36	.123	.076	-35%

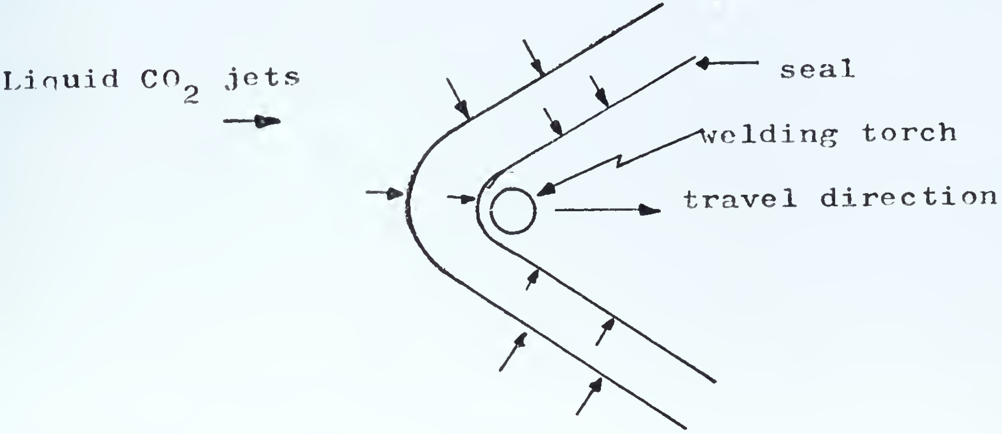

Figure 6.1 - Forced cooling

6.5 - Use of external constraints

6.5.1 - General

The use of holding fixtures are common in thin sheet aluminum welding. Numerous jigging and clamping systems suitable for determined structures are developed and are current practice in welding shops.

Prebowing or prebending has also been subject to research (5) and is also largely applied by the Industry.

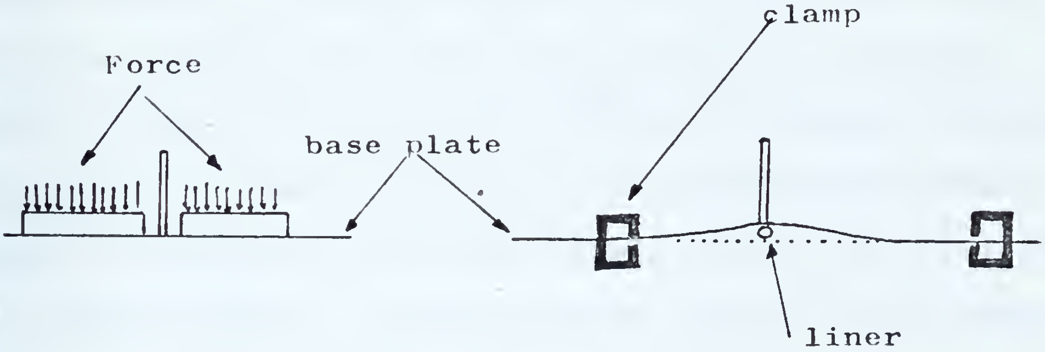

Figure 6.2 - Pre bending systems

6.5.2 - Analysis of distortion reduction in orthogonally framed plates using pre-bending

The use of purely mechanical means for reducing out-of-plane distortion due to fillet welding in flat plates has been studied and results are presented in previous works (5).

These mechanical means can be either complete restraint or pre bending - figure 6.2 . This pre bending solution is good for simple structures and for one dimensional frame spacing. For the case of orthogonaly framed plates, it seems to be difficult the use of this technique and we will present the analysis of another system - figure 6.3 in which a press is used for inducing an initial deformation on the plate, which would remain during the welding of the four lines A, B, C, D, concerning this plate element. An appropriate initial deformation would give a final flat plate.

The analysis will be done assuming that the plate behaves elastically in all the extension but the weld lines.

The plate is considered initially clamped along the boundaries, ($\frac{dw}{dx} = \frac{dw}{dy} = 0$ at the boundaries); an uniform load is applied - figure 6.3, producing a central deformation w^{**} and a moment M_1 is induced at the boundaries. During welding this moment M_1 is locally relieved; as the welding proceeds, the cooling down will produce a local moment M_2. After the all 4 fillet are done, the load is removed and

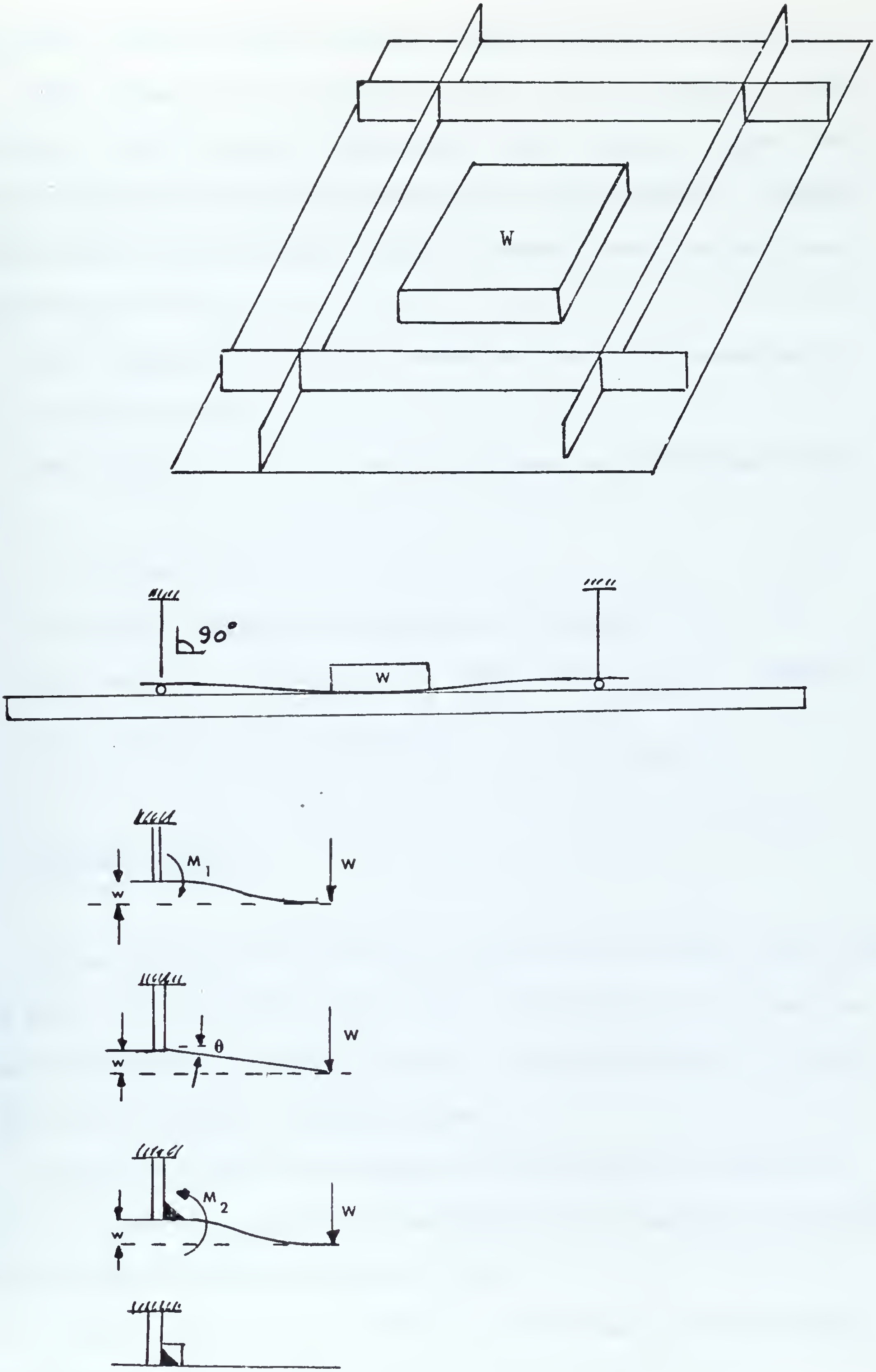
W
90°
W
M1
W
w
θ
W
w
M2
W
w

Figure 6.3 - Prebending system for orthogonally framed plate

the plate will be flat without angles at the boundaries.

The value w^* is approximately the deformation that the plate would acquire under the same welding conditions, without any pre bending operation. This value w^* would be obtained from previous test of other work as the one done in section 5.3.

The derivation of the solution for this problem is done in appendix 5.

The sequence of the calculations are mentioned now:

1. Assume q
2. Solve system of equations (A5.10)
3. Compare $w^{**}\big|_{x=y=0} = w_1 + w_2 + w\big|_{x=y=0}$ with w^*
4. Adjust q for achieving $w^* \sim w^{**}\big|_{x=y=0}$

6.6 - Flame heating

Line heating followed by quenching has been used for long time in shipyards and other fabricators in order to induce curvature in steel plates. This process is like an art and requires skilled labor.

Using the same principle, flame heating could be used for reducing angular distortion in Aluminum, in spite of the higher thermal diffusivity.

Flame heating is a form of localized post-heating. Generalized post heating has been used for stress

relieving as mentioned in The Welding Handbook.

Using an Oxy-acetylene torch, we line heated plate no.3, at the weld lines, on the nonwelded side. The central deformation was continuously verified by a dial gage placed on the center of the plate.

Initially, the central deformation was about .29"; as the heating was proceeding, the central displacement was reduced by about .10", but as soon as we finished heating, the distortion started to increase again and 10 minutes later, the deformation was .31" therefore larger than initially, which was due to plate expansion, since this time the plate was evenly heated.

About two hours later the plate was at room temperature and the central deformation had virtually the initial value.

The effect of line heating followed by fast cooling when the plate reached the least deformation could have reduced it, but this was not tried. The increase of local stresses and metallurgical transformations are questionable points of this process.

6.7 - Other Methods

Other methods of post welding distortion removal and stress relief are mentioned in references 5, 17:

Stress relief annealling

Vibratory stress relief

Electromagnetic hammer

Peening

Some are not feasible for fillet welding and for some materials. In general this processes are developed by the Industry, and enough information is not available.

7. SUMMARY AND CONCLUSIONS

7.1 - Summary

The present thesis work can be summarized as follows:

i) An introductory study of welding defects and their influence in ship design is presented (sections 2 and 3).

ii) Experimental data on out-of-plane distortion due to fillet welding was gathered for 5052-H32 Aluminum Alloy thin plate, orthogonally framed, using semi automatic GMA welding (section 4.).

iii) Using the previous data and linear elastic analysis, we could calculate a functional aproximation, that will allow the prediction of central deflection of a plate once the fillet welding conditions are known (for thin plate and one pass GMA welding). (section 5.3)

iv) The concept developed in (ii) was related with previous analytical work (10), for testing the FEM computer program presented there with Aluminum data. The reasons of the difference between the analytical results and the experiment are studied (section 5.4).

v) The effect of angular distortion on continuous stiffened or framed plate behavior was studied by determining the reduction of plate efficiency if either the plate element is only subjected to uniform lateral load (section 5.6) or to longitudinal uniform compression and

lateral load (section 5.7). It was found that for the present data, the reduction of plate efficiency is on the order of 5 to 10%, depending on the welding conditions, material mechanical characteristics, frame spacing and plate thickness.

vi) The experimental data is checked against the US Navy standards and it was found that the values of distortion we got fall well below of the limiting permissible unfairness (central deflection) (section 5.5).

vii) Experiments on reduction of distortion were done using preheating and post heating, and it was found evident reduction of distortion by the preheating of the plate underneath at the welding lines. The reduction of central deflection was by 35% (sections 4.2, and 6.4 and 6.6).

viii) A prebending system for reducing the values of angular distortion is proposed and its analytical solution is presented, but it was not tried because with the existing facilities would be difficult to implement (section 6.5).

7.2 - Conclusions

The conclusions that we may draw from the present thesis work, and concerning the out-of-plane distortion due to fillet welding of T joints in Aluminum plate, and its effect on ship plating are as follows:

i) The effects of welding using current techniques are highly complex, and the deformations and residual

stresses induced must be considered on the prediction of plate behavior and buckling mechanisms;however, not all the different types of fabrication imperfections (i.e. deformation and locked-in stresses) have the same importance in considering a grillage or a panel and their stress schedule. Out-of-plane distortion directly affects the buckling of each plate element, but has a secondary effect either on beam-column type buckling (where stiffener longitudinal bending is more important) or on tripping or on complete grillage collapse.

ii) The prediction of out-of-plane distortion by a fully analytic model requires an accurate temperature distribution and must account for the different elasto-plastic and thermal material characteristics at different temperatures, otherwise the results can't be satisfactory and an empirical-analytic treatment is preferible.

iii) An empirical-analytic model like the one we have developed in section 5.3, can be readily applied in actual fabrication but the empirical functions must be obtained from data concerning the welding machine and working conditions as the ones in practice.

iv) Reduction of distortion or of its effects, can be achieved either by new welding processes - the Electron Beam Welding is one example of welding process virtually distortion free - or by an integrated design systems, in which the several forms of pertinent distortion is inputed and will be traded-off with all the other design parameters, for achieving the best structure under the design criterion.

Using the conventional welding processes for Aluminum - GTA and GMA - where angular distortion is always present, base plate preheating seems to reduce this distortion and must be further investigated, using simple T models and different heating temperatures.

Reduction of distortion by prebending, using a press and mobile jacks should be feasible in shipyards and should be of easy and inexpensive operation.

LIST OF REFERENCES

1. S. R. Heller Jr. - Structural Design of Ship Plating Subjected to Uniform Lateral Load -Int. Shipb. Prog.1974
2. A. W. Pense and R. D. Stout - Influence of Weld Defects on the Mechanical Properties of Aluminum Alloys Weldments WRC Bulletin 152
3. D. Faulkner - A Review of Effective Plating for Use in the Analysis of Stiffened Plating in Bending and Compression - Journal of Ship Research - March 1975 Vol. 19 no.1
4. C. Taniguchi - Out-of-Plane Distortion Caused by Fillet Welds in Aluminum - OE Thesis - MIT - Department of Ocean Engineering - 1972
5. R. Henry - Reduction of Out-of-Plane distortion in Fillet Welded High Strength Aluminum - MS Thesis MIT - Department of Ocean Engineering - 1974
6. K. Masubuchi et al - Analysis of Thermal Stresses and Metal Movements of Weldments: a Basic Study Toward Computer Aided Analysis and Control of Welded Structure - Paper no.6 Presented at the SNAME - Annual Meeting 1975
7. W. Eggington and N. Kobitz - The Domain of the Surface Effect Ship - Paper no.11 Presented at the SNAME annual meeting 1975

8. A. E. Mansour - Post Buckling Behavior of Stiffened Plate with Small Initial Curvature under Combined Loads - MIT - Department of Ocean Engineering - Report 70-18, 1970

9. H. Kihara et al. - Researches on Welding Stress and Shrinkage Distortion in Japan - Vol. 4 Chap. 9 - published by the Society of Naval Architects of Japan, 1959

10. D. B. Shin - Finite Element Analysis of Out-of-Plane Distortion of Welded Panel Structures OE Thesis - 1972 MIT - Department of Ocean Engineering

11. C. S. Smith - Compressive Strength of Welded Steel Ship Grillages - The Naval Architect - October 1975

12. H. A. Shade - The Effectiveness Breath of Stiffened Platting Under Bending loads - Transations SNAME, Vol. 59, 1951 and Vol. 61, 1953

13. N. Jones and R. M. Walters - Large Deflections of Rectangular Plates - Journal of Ship Research - V. 15 no. 2 June 1971

14. D. Clark & W. Varney - Physical Metallurgy for Engineers pg 515 - ed D. van Nostrand Company

15. J. Harvey Evans (ed) - Ship Structural Design Concepts - AD 782 - 198, 1974 (NTIS)

16. - Structural Design Studies for Surface Effect Ships - Final Report, Phase I, 1969 - Bell

Aerosystems Report no. 7363 - 950001

17. K. Masubuchi - Residual Stresses and Distortion in Welded Aluminum Structures and Their Effects on Service Performance-WRC Bulletin 174

18. Bleich & Ramsey - Buckling Strength of Metal Structures pg 480 - Mc Graw-Hill Book Co 1952

19. S. Timoshenko et S. Woinowsky-Krieger - Theory of Plates and Shells - Mc Graw-Hill Book Company 1959

20. Kuriyama et al - Prevention of Porosity in Al. Alloys Welds IHI. Engineering Review vol. 8 no.3 Sept. 1975

21. K. Masubuchi - "Lecture Notes and Text on Ocean Engineering Material", subject 13.17 J, MIT 1973

22. - Welding Handbook - section 4 - Metals and Their Weldability - American Welding Society 1972

23. K. Kitamura - Special Report on Out-of-Plane Distortion of Welded Panel Structures - MIT - Department of Ocean Engineering - MIT DSR no. 82558 - July 1975

24. N. W. Murray - Analysis and Design of Stiffened Plates for Collapse Load - The Structural Engineer - March 1975 no. 3 volume 53

25. B. Aalami and J. C. Chapman - Large Deflection Behavior of Ship Panels Under Normal Pressure and Inplane Loading. Transactions of R.I.N.A., 1972

26. K. Terai - Recent Progresses on Electron Beam Welding in Japan - Lecture given at MIT - course 13.38, March 18, 1976

27. NAVSHIPS 0900-000-1001 - Fabrication, Welding and Inspection of Ship Hulls, Department of the Navy, June 1969.

Appendix 1

Materials used in experiments and their properties

a) Aluminum - magnesium structural alloy 5052-H32

(strain hardened, non-heat treatable)

The characteristics and properties of the material are as follows:

1. Typical chemical composition

Elements	Mg	Mn	Cr	Cu	Zn	Si-Fe	Al
Percentage %	2.2-2.8	.10	.15-.35	.10	.10	.45	Remainder

2. Physical properties @ standard temperature (15° C)

Density	.097 lb/in^3 ($2.68\ gr/cm^3$)
Specific heat	.23 BTU/lb °F
Liquidus temperature	1120°F approx.
Thermal conductivity	$.185 \times 10^{-2}$ BTU/in sec°F
Thermal diffusivity	$8.2 \times 10^{-2}\ in^2/sec$

3. Mechanical properties @ standard temperature

Modulus of elasticity (E)	10.2×10^6 psi
Modulus of rigidity (G)	3.8×10^6 psi

Min tensile strength (σ_o)	33	x 10^3psi
Min yield strength (σ_y)	28	x 10^3psi
Poisson's ratio (ν)	.334	

b) Electrode filler wire - Alloy 4043

Typical chemical composition

Elements	Mn	Zn	Mg	Cu	Si	Fe	Ti	Al
Percentage %	.05	.10	.05	.30	4.5-6.0	.80	.20	Remainder

Electrode filler wire - Alloy 5356

Typical chemical composition

Elements	Mn	Zn	Mg	Cu	Si-Fe	Cr	Ti	Al
Percentage %	.12	.10	5.00	.10	.50	0.12	0.15	Remainder

Appendix 2

Guidelines for GMA Welding Process

- following the Welding Handbook (published by the American Welding Society)

Advised welding conditions for the current experiment

Plate thickness	no. of passes	electrode wire diameter	Reverse polarity direct current	Voltage
3/16	1	3/64	180-210	22-26
1/4	1	3/64 or 1/16	170-240	24-28

Plate thickness	argon gas flow cfh	arc travel speed inch/min	approximate filler wire consumption lb/100ft
3/16	30	24-30	4.5
1/4	40	24-30	7.

The Deposition Efficiency for GMA is one of the highest, generally greater than 95%, because of the absense of spatter or oxidation of the transferring metal.

Suggested filler wires for welding 5053-H32 aluminum alloy:

i) for strength color matching after anodizing and least crack tendency should use Al 5356

ii) for ductility should use Al 5654

iii) for saltwater corrosion resistence should use Al 5554

iv) Al 4043 is the most weldable

Appendix 3

Relationship between M_o and C

(the theory for developing this analysis was taken from chapter 6 reference 19)

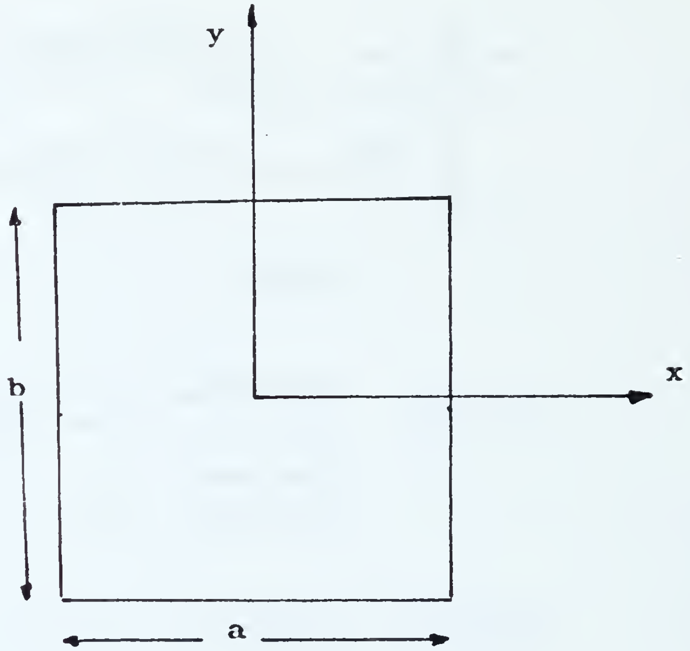

$$\alpha = \frac{m\pi b}{2a} \qquad (A3.1)$$

$$\beta = \frac{m\pi a}{2b} \qquad (A3.2)$$

$$D = \frac{E h^3}{12(1-\nu^2)} \qquad (A3.3)$$

$$AA = \frac{1}{m^3 \cosh\alpha}\left(\alpha \tanh\alpha \cosh\frac{m\pi y}{a} - \frac{m\pi y}{a}\sinh\frac{m\pi y}{a}\right) \qquad (A3.4)$$

$$BB = \frac{1}{m^3 \cosh\beta}\left(\beta \tanh\beta \cosh\frac{m\pi x}{b} - \frac{m\pi x}{b}\sinh\frac{m\pi x}{b}\right) \qquad (A3.5)$$

$$w = \frac{2M_o}{\pi^3 D}\left[a^2\sum_{m=1,3,5} AA \sin\frac{m\pi(x+a/2)}{a} + b^2\sum_{m=1,3,5} BB\sin\frac{m\pi(y+b/2)}{b}\right]$$

(A3.6)

$$\frac{dw}{dx} = \frac{2M_o}{\pi^3 D}\left[a\sum_{m=1,3,5} m\pi AA \cos\frac{m\pi(x+a/2)}{a} + b\sum_{m=1,3,5}\frac{\pi}{m^2\cosh\beta}\cdot\right.$$

$$\left.\left(\beta\tanh\beta \sinh\frac{m\pi x}{b} - \sinh\frac{m\pi x}{b} - \frac{m\pi x}{b}\cosh\frac{m\pi x}{b}\right)\sin\frac{m\pi(y+b/2)}{b}\right]$$

(A3.7)

$$\frac{dw}{dx} = \frac{2\ M_0}{\pi^3 D} W_x \qquad (A3.7a)$$

$$\frac{dw}{dy} = \frac{2\ M_0}{\pi^3 D} W_y \qquad \left(\text{similar to } \frac{dw}{dx} \text{ where } \begin{array}{c} AA \longleftrightarrow BB \\ \alpha \longleftrightarrow \beta \\ a \longleftrightarrow b \\ x \longleftrightarrow y \end{array}\right) \qquad (A3.8)$$

$$\frac{d^2w}{dx^2} = \frac{2\ M_0}{\pi^3 D}\left[\sum_{m=1,3,5} -m\,\pi^2 AA\ \sin\frac{m\pi(x+a/2)}{a} + \sum_{m=1,3,5} \frac{\pi^2}{m\ \cosh\beta}\,\cdot\right.$$

$$\left.\left(\beta \tanh\beta\ \cosh\frac{m\pi x}{b} - 2\cosh\frac{m\pi x}{b} - \frac{m\pi x}{b}\sinh\frac{m\pi x}{b}\right)\right]\cdot$$

$$\sin\frac{m\pi(y+b/2)}{b} = \frac{2\ M_0}{\pi^3 D} W_{xx} \qquad (A3.9)$$

$$\frac{d^2w}{dy^2} = \frac{2\ M_0}{\pi^3 D} W_{yy} \qquad \left(\text{similar to } \frac{d\ w}{dy} \text{ where } \begin{array}{c} AA \longleftrightarrow BB \\ \alpha \longleftrightarrow \beta \\ a \longleftrightarrow b \\ x \longleftrightarrow y \end{array}\right. \qquad (A3.10)$$

$$\frac{d^2w}{dxdy} = \frac{2\ M_0}{\pi^3 D}\left[\sum_{m=1,3,5} \frac{\pi^2}{m\ \cosh\alpha}\left(\alpha \tanh\alpha\ \sinh\frac{m\pi y}{a} - \sinh\frac{m\pi y}{a} -\right.\right.$$

$$\left. -\frac{m\pi y}{a}\cosh\frac{m\pi y}{a}\right) + \sum_{m=1,3,5} \frac{\pi^2}{m\ \cosh\beta}\left(\beta \tanh\beta\ \sinh\frac{m\pi x}{b} -\right.$$

$$\left.\left. -\sinh\frac{m\pi x}{b} - \frac{m\pi x}{b}\cosh\frac{m\pi x}{b}\right) \cos\frac{m\pi\,(y+b/2)}{b}\right] = \frac{2\ M_0}{\pi^3 D} W_{xy} \qquad (A3.11)$$

Energy Equations

$$U_t = \sum \int U_w + U_s \qquad (A\ 3.12)$$

$$\frac{dU_t}{dM_0} = \frac{d}{dM_0}\left(\sum \int U_w\right) + \frac{d}{dM_0} U_s = 0 \qquad (A\ 3.13)$$

$$\frac{dU}{dM_o}w = \frac{d}{dM_o}\left[2\int\frac{C}{2}\left(\theta_o-\frac{dw}{dx}_{x=a/2}\right)^2dy+2\int\frac{C}{2}\left(\theta_o-\frac{dw}{dy}_{y=b/2}\right)^2dx\right] \quad (A3.14)$$

$$\frac{dU}{dM_o}s=\frac{d}{dM_o}\left\{\iint\left\{\left(\frac{d^2w}{dx^2}+\frac{d^2w}{dy^2}\right)^2-2(1-\nu)\left[\frac{d^2w}{dx^2}\,\frac{d^2w}{dy^2}-\left(\frac{d^2w}{dxdy}\right)^2\right]\right\}dxdy\right\}\frac{D}{2} \quad (A3.15)$$

Plugging (A3.7) through (A3.11) into (A3.14) and (A3.15), (A3.13) becames:

$$C\left[-\frac{4\theta_o}{\pi^3D}\left(\int W_xdy+\int W_ydx\right)+\frac{8M_o}{\pi D}\left(\int W_x^2\,dy+\int W_y^2\,dx\right)\right]=-\frac{D\;8M_o}{2\,\pi^6D^2}\cdot$$

$$\cdot\iint\left[(W_{xx}+W_{yy})^2-2(1-\nu)(W_{xx}W_{yy}-W_{xy}^2)\right]dxdy \quad (A3.16)$$

Making

$$TT=\iint\left[(W_{xx}+W_{yy})^2-2(1-\nu)(W_{xx}W_{yy}-W_{xy}^2)\right]dxdy$$

$$AA1=\left(\int W_xdy+\int W_ydx\right)\pi^3$$

$$AA2=\frac{2}{D}\left(\int W_x^2\,dy+\int W_y^2\,dx\right)$$

We will get:

$$C=\frac{-TT}{AA2-\frac{\theta_o}{M_o}AA1} \quad (A3.17)$$

Appendix 4

Plate behavior under longitudinal compression and lateral pressure

Assume that a plate under uniform lateral load p and longitudinal compression σ_A ,and with an uniform moment M_o applied at the edges,can be expressed with sufficient accuracy by:

$$w^* = w \cos\frac{\pi x}{a} \cos\frac{\pi y}{b} \qquad (A4.1)$$

The deflection w can be determined from the Theorem of Stationary Potential Energy as follows:

The strain energy $V=V_s+V_b$, where V_s is the strain energy due to membrane stresses (large deflections allowed) and V_b is the strain energy due to bending.

V is given by : (18)

$$V=\frac{Eabh}{1-\nu^2}\left[\frac{\epsilon_1^2+\epsilon_2^2}{2}+\nu\epsilon_1\epsilon_2-\frac{\pi^2 w^2}{8\ b^2}\left[\epsilon_1\left(\frac{b^2}{a^2}+\nu\right)+\epsilon_2\left(1+\nu\frac{b^2}{a^2}\right)\right]+\frac{\pi^4 w^4}{256b^4}\right. \cdot$$

$$\left.\cdot\left[(3-\nu^2)\left(1+\frac{b^4}{a^4}\right)+4\nu\frac{b^2}{a^2}\right]+\frac{\pi^4 h^2 w^2}{96b^4}\left(1+\frac{b^2}{a^2}\right)^2\right] \qquad (A4.2)$$

ϵ_1,ϵ_2 are mean strains in the x and y directions

$$\epsilon_1 E = \sigma_A+\frac{E\pi^2 w^2}{8a^2}$$

$$(A4.3,a,b)$$

$$\epsilon_2 E = -\nu\sigma_A+\frac{E\pi^2 w^2}{8b^2}$$

The potential energy U_w is due to the external generalized forces σ_A, M_o, p.

For the longitudinal compression the P.E. is:

$U_w = -\sigma_A hab\epsilon_1$

For the lateral load

$$U_w = -\iint pw\ dxdy = -\frac{4pabw}{\pi^2}$$

For the uniform moment

$$U_w = -\left[2\int M_o \frac{dw}{dx}_{x=a/2} dy + 2\int M_o \frac{dw}{dy}_{y=b/2} dx\right] = -2M_o w\left(\frac{a}{b}+\frac{b}{a}\right)$$

The condition $\frac{d(V+\sum U_w)}{dw}=0$,leads to

$$\frac{Eabh}{(1-\nu^2)}\left\{-\frac{\pi^2 w}{4b^2}\left[\epsilon_1\left(\frac{b^2}{a^2}+\nu\right)+\epsilon_2\left(1+\nu\frac{b^2}{a^2}\right)\right]+\frac{w^3\pi^4}{64b^4}\left[(3-\nu^2)\left(1+\frac{b^4}{a^4}\right)+4\nu\frac{b^2}{a^2}\right]+\frac{\pi^4 h w^2}{48b^4}\cdot\left(1+\frac{b^2}{a^2}\right)\right\}=\frac{4pab}{\pi^2}+2M_o\left(\frac{a}{b}+\frac{b}{a}\right) \qquad (A4.4)$$

Assuming that the side ratio $\frac{b}{a} > .7$, the plate buckles elastically in one half wave and the critical stress σ_C for longitudinal compression in x direction is

$$\sigma_C=\frac{\pi^2 E}{12(1-\nu^2)}\left(\frac{h}{b}\right)^2\left(\frac{a}{b}+\frac{b}{a}\right)^2 \qquad (A4.5)$$

Plugging (A4.3) and (A4.5) into (A4.4) and putting in nondimensional form,we will get:

$$\left(\frac{w}{h}\right)^3-\frac{4}{3(1-\nu^2)}\frac{(1+\beta^2)}{(1+\beta^4)}\left(\frac{\sigma_A}{\sigma_C}-1\right)\frac{w}{h}-\frac{256\ b^2}{(1+\beta^4)Eh^4}\left[b^2p+\frac{\pi^2 M_o}{2}(1+\beta^2)\right]=0$$

$$\beta=\frac{b}{a} \qquad (A4.6)$$

The definition of stresses is as follows :

$\sigma_x=\sigma_{xb}+\sigma_{xm}$

$\sigma_y=\sigma_{yb}+\sigma_{ym}$

The subscript b means stress due to bending on the extreme fibers $z=\pm\frac{h}{2}$ and the subscript m means membrane stress over the entire section.

$$\left.\begin{array}{ll}\sigma_{xm}=\sigma_A-\dfrac{E\pi^2 w^2}{8\ a^2} & (x=y=0)\\[2ex] \sigma_{ym}=-\dfrac{E\pi^2 w^2}{8b^2} & (x=y=0)\end{array}\right\}\begin{array}{l}+\ \text{compression}\\[2ex] -\ \text{tension}\end{array}$$

$$\sigma_{xb} = \pm \frac{\pi^2 Ehw}{2(1-\nu^2)a^2}\left(1+\nu\frac{a^2}{b^2}\right) \quad @ \quad x=y=0$$

$$\sigma_{yb} = \pm \frac{\pi^2 Ehw}{2(1-\nu^2)b^2}\left(1+\nu\frac{b^2}{a^2}\right) \quad @ \quad x=y=0$$

$$\sigma_o \geq \sigma_{ym} + \sigma_{yb} \qquad \text{(tension)} \qquad (A4.7a)$$

$$\sigma_o \geq \sigma_{xm} + \sigma_{xb} \qquad \text{(compression)} \qquad (A4.7b)$$

Calculation of σ_A

$$\sigma_A = \sigma_C \left\{ 1 + \frac{\left(\frac{w}{h}\right)^3 - \frac{256\ b^2}{\pi^6(1+\beta^4)\ Eh^4}\left[b^2 p + \frac{\pi^2 N_o}{2}\ (1+\beta^2)\right]}{\frac{w}{h}\left[\frac{4}{3(1-\nu^2)}\ \frac{(1+\beta^2)^2}{(1+\beta^4)}\right]} \right\} \qquad (A4.8)$$

Appendix 5

Analysis of Distortion Reduction on Orthogonaly Framed Plate, Using Pre-bending

The objective of this appendix is the calculation of a pressing system-a load applied on an arbritary rectangle, fig. 6.3 -for bending a plate element previous to welding. Starting with the predicted angular distortion, the value of the load q is found by iteration. A pressing system like this allows clear space for the welding operation, because the load can be applied at an arbritary rectangle or in the limit case at one point. (the theory for developing this analysis was taken from section 44 reference 19)

w_1-deflection due to symmetric moments applied at edges $y=\pm\ b/2$

w_2-deflection due to symmetric moments applied at edges $x=\pm a/2$

w-deflection of a simply supported plate subjected to an uniform load q appied on a rectangle of dimensions u,v.

(Note: the origin of coordinates is at the center of the plate)

$$w_1=-\frac{a^2}{2\pi^2 D}\sum_{m=1,3,5}\frac{E_m(-1)^{(m-1)/2}}{m^2\cosh\alpha}\cos\frac{m\pi x}{a}\left(\frac{m\pi y}{a}\sinh\frac{m\pi y}{a}-\alpha\tanh\alpha\cosh\frac{m\pi y}{a}\right) \qquad (A5.1)$$

$w_2=$ similar to w_1 changing

$$\begin{array}{c} x\leftrightarrow y \\ a\leftrightarrow b \\ E_m\leftrightarrow F_m \\ \alpha\leftrightarrow\beta \end{array} \qquad (A5.2)$$

$\alpha=m\pi b/2a$ $\quad\beta=m\pi a/2b$ $\quad\gamma=m\pi v/4a$

$$w=\frac{4qa^4}{d\pi^5}\sum_{m=1,3,5}\frac{(-1)^{(m-1)/2}}{m^5}\sin\frac{m\pi u}{2a}\left\{1-\frac{\cosh\frac{m\pi y}{a}}{\cosh\alpha}\left[\cosh(\alpha-2\gamma)+\gamma\sinh(\alpha-2\gamma)+\alpha\frac{\sinh 2\gamma}{2\cosh\alpha}\right]+\frac{\cosh(\alpha-2\gamma)}{2\cosh\alpha}\frac{m\pi y}{a}\sinh\frac{m\pi y}{a}\right\}\sin\frac{m\pi(x+a/2)}{a}\qquad(A5.3)$$

We will assume that the angular change is very small and equal to the derivative of the displacement. We must also assume an initial value for q .

$$\left.\frac{dw_1}{dy}\right|_{y=b/2}=-\frac{a}{2\pi D}\sum_{m=1,3,5}E_m\frac{(-1)^{(m-1)/2}}{m}\cos\frac{m\pi x}{a}\left(\tanh\alpha+\frac{\alpha}{\cosh^2\alpha}\right)\qquad(A5.4)$$

$$\left.\frac{dw_1}{dx}\right|_{x=a/2}=\frac{a}{2\pi D}\sum_{m=1,3,5}E_m\frac{1}{m\cosh\alpha}\left(\frac{m\pi y}{a}\sinh\frac{m\pi y}{a}-\alpha\tanh\alpha\cosh\frac{m\pi y}{a}\right)$$

$$\left.\frac{dw_2}{dx}\right|_{x=a/2}=\text{similar to (A5.4)}\qquad(A5.5)\quad(A5.6)$$

$$\left.\frac{dw_2}{dy}\right|_{y=b/2}=\text{similar to (A5.5)}\qquad(A5.7)$$

changing $x\longleftrightarrow y$, $a\longleftrightarrow b$, $E_m\longleftrightarrow F_m$, $\alpha\longleftrightarrow\beta$

$$\left.\frac{dw}{dx}\right|_{x=a/2}=-\frac{4qa^3}{D\pi^4}\sum_{m=1,3,5}\frac{(-1)^{(m-1)/2}}{m^4}\sin\frac{m\pi u}{2a}\;W\qquad(A5.8)$$

W is the term under $\{\ \}$ in (A5.3)

$$\left.\frac{dw}{dy}\right|_{y=b/2}=\frac{4qa^4}{D\pi^5}\sum_{m=1,3,5}\frac{(-1)^{(m-1)/2}}{m^5}\sin\frac{m\pi u}{2a}\left\{1-\tanh\alpha\left[\frac{\cosh(\alpha-2\gamma)}{2}+\gamma\sinh(\alpha-2\gamma)+\alpha\frac{\sinh 2\gamma}{2\cosh\alpha}\right]+\alpha\cosh(\alpha-2\gamma)\right\}\sin\frac{m\pi(x+a/2)}{a}\qquad(A5.9)$$

At any point of the boundary, the angle is zero, therefore the following condition must be satisfied:

$$\left.\begin{aligned}\frac{dw}{dy}+\frac{dw_1}{dy}+\frac{dw_2}{dy}&=0\quad\text{at } y=b/2\\ \frac{dw}{dx}+\frac{dw_1}{dx}+\frac{dw_2}{dx}&=0\quad\text{at } x=a/2\end{aligned}\right\}\qquad(A5.10)$$

The solution of (A5.10) for three arbitrary points of each boundary ($x=a/2$,$y=b/2$) , gives us the values of the unknowns E_1 ,E_3 ,E_5 ,F_1 ,F_3 ,F_5 .

We can now calculate w, w_1, w_2

$w^{**}= w+ w_1+ w_2$ at $x=y=0$ must be compared with the predicted deflection w^* induced by welding.

The value of q must be adjusted and a new iteration must be done up to the point where $w^{**} \approx w^*$ (A5.11) ,being this final value of q,the pre-bending load.

Appendix 6

Parameters included in figure 3.3

(from reference 8)

$$D_x = \frac{E_x h^3}{12(1-\upsilon_x \upsilon_y)} \qquad D_y = \frac{E_y h^3}{12(1-\upsilon_x \upsilon_y)}$$

G= modulus of elasticity in shear $= \frac{E}{2(1+\upsilon)}$

D_{xy} = effective torsional rigidity of the orthopedic plate

$$2 D_{xy} = \frac{4Gh^3}{12} + \upsilon_x D_y + \upsilon_y D_x$$

$$\rho = \frac{a}{b}\sqrt[4]{\frac{D_y}{D_x}} \qquad J_y = \frac{1}{h} E_x$$

$$\eta = \frac{D_{xy}}{\sqrt{D_x D_y}} \qquad J_x = \frac{1}{h} E_y$$

$$\gamma = \frac{J_{xy}}{\sqrt{J_x J_y}}$$

$$q^* = \frac{\overline{q}\, b^4}{\pi^4 h D_y}$$

$$N^* = \frac{\overline{N}_y b^2}{\pi^2 D_y}$$

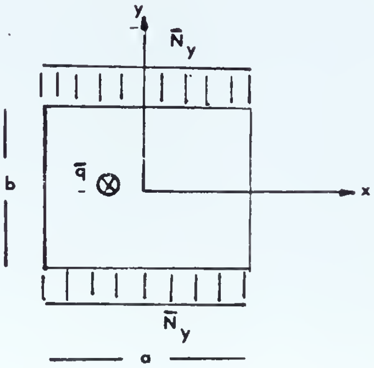

Appendix 7

Computer program developed to calculate the dimensional parameters AA1, AA2, TT, used in section 5.4 and appendix 3, (Fortran language).

Example of inpute required:

Column no.	5 — 12	13 — 24	25 — 36	37 — 48
data card	10.0E+06	24.	16.	.25
	E	a	b	h

one card for each plate ...

last card of data deck BLANK

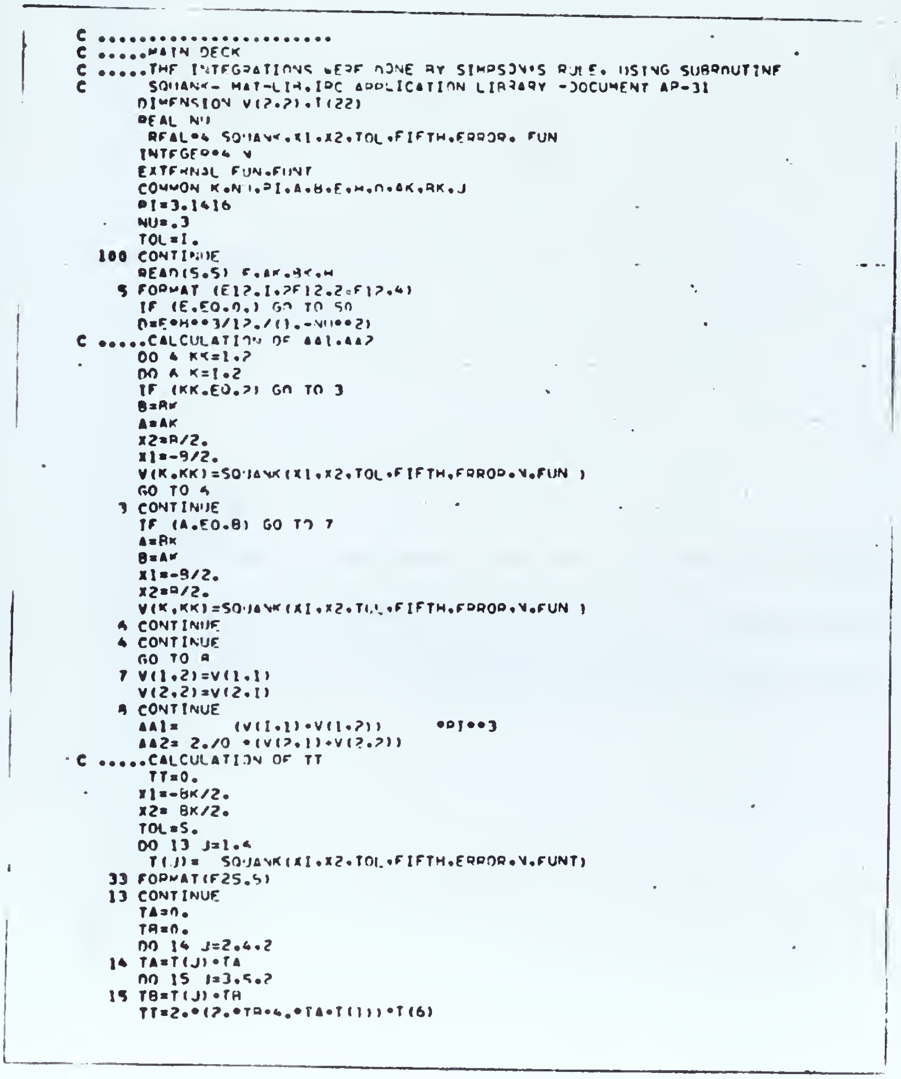

```
C ......................
C .....MAIN DECK
C .....THE INTEGRATIONS WERE DONE BY SIMPSON'S RULE, USING SUBROUTINE
C        SQUANK- MAT-LIB.IPC APPLICATION LIBRARY -DOCUMENT AP-31
      DIMENSION V(2,2),T(22)
      REAL NU
       REAL*4 SQUANK,X1,X2,TOL,FIFTH,ERROR, FUN
      INTEGER*4 N
      EXTERNAL FUN,FUNT
      COMMON K,NU,PI,A,B,E,H,D,AK,BK,J
      PI=3.1416
      NU=.3
      TOL=1.
  100 CONTINUE
      READ(5,5) E,AK,BK,H
    5 FORMAT (E12.1,2F12.2,F12.4)
      IF (E.EQ.0.) GO TO 50
      D=E*H**3/12./(1.-NU**2)
C .....CALCULATION OF AA1,AA2
      DO 4 KK=1,2
      DO 6 K=1,2
      IF (KK.EQ.2) GO TO 3
      B=BK
      A=AK
      X2=B/2.
      X1=-B/2.
      V(K,KK)=SQUANK(X1,X2,TOL,FIFTH,ERROR,N,FUN )
      GO TO 6
    3 CONTINUE
      IF (A.EQ.B) GO TO 7
      A=BK
      B=AK
      X1=-B/2.
      X2=B/2.
      V(K,KK)=SQUANK(X1,X2,TOL,FIFTH,ERROR,N,FUN )
    6 CONTINUE
    4 CONTINUE
      GO TO 8
    7 V(1,2)=V(1,1)
      V(2,2)=V(2,1)
    8 CONTINUE
      AA1=      (V(1,1)+V(1,2))       *PI**3
      AA2= 2./D *(V(2,1)+V(2,2))
C .....CALCULATION OF TT
       TT=0.
      X1=-BK/2.
      X2= BK/2.
      TOL=5.
      DO 13 J=1,6
       T(J)=  SQUANK(X1,X2,TOL,FIFTH,ERROR,N,FUNT)
   33 FORMAT(F25.5)
   13 CONTINUE
      TA=0.
      TB=0.
      DO 14 J=2,4,2
   14 TA=T(J)+TA
      DO 15 J=3,5,2
   15 TB=T(J)+TB
      TT=2.*(2.*TB+4.*TA+T(1))+T(6)
```

```
      TT=A/30.*TT
C .....PRINTING
      WRITE (6,10) AA1,AA2,TT
   10 FORMAT (3F25.5)
      GO TO 100
   50 STOP
        END
      FUNCTION FUN(Y)
      REAL*4 Y
      REAL NU
      COMMON K,NU,PI,A,B,E,H,D
      WX1=0.
      WX2=0.
      X=A/2.
      DO 1 M=1,5,2
      AL=M*PI*B/2./A
      BE=M*PI*A/2./B
      AA=1./M**3/COSH(AL)*(AL*TANH(AL)*COSH(M*PI*Y/A)-M*PI*Y/A*SINH(M*
     1 PI*Y/A))
      W11=M*PI*AA*COS(M*PI*(X+A/2.)/A)
      W22= PI/M**2/COSH(BE)*(BE*TANH(BE)*SINH(M*PI*X/B)-SINH(M*PI*X/B)
     2 -M*PI*X/B*COSH(M*PI* X/B)) *SIN(M*PI /B*(Y+B/2.)  )
      WX1=WX1+W11
      WX2=WX2+W22
    1 CONTINUE
      FUN=             (A*WX1+B* WX2)
      IF (K.EQ.1) GO TO 2
      FUN=FUN**2
    2 CONTINUE
      RETURN
       END
      FUNCTION FUNT(Z)
      REAL NU
      COMMON K,NU,PI,A,B,E,H,D,AK,BK,J
       XY=0.
      XX=0.
      YX=1.
      DO 11 K=1,2
      A=AK
      B=BK
      Y=Z
      X=-A/2.+(FLOAT(J)-1.)*A/10.
       IF (K.EQ.1) GO TO 12
      IF (A.EQ.B) GO TO 32
      Y=-A/2.+(FLOAT(J)-1.)*A/10.
      X=Z
      A=BK
      B=AK
   12 CONTINUE
      WX1=0.
      WX2=0.
      WXY=0.
      DO 1 M=1,5,2
      BE=M*PI*A/2./B
      AL=M*PI*B/2./A
      AA=1./M**3/COSH(AL)*(AL*TANH(AL)*COSH(M*PI*Y/A)-M*PI*Y/A*SINH(M*
     1 PI*Y/A))
       W1=-M*PI**2*AA*SIN(M*PI/A*(X+A/2.))
      W2=PI**2/M/COSH(BE)*(BE*TANH(BE)*COSH(M*PI*X/B)-2.*COSH(M*PI*X/B)
     1  -M*PI*X/B*SINH(M*PI*X/B))*SIN(M*PI/B*(Y+B/2.))
       WA=PI**2/M/COSH(AL)*(AL*TANH(AL)*SINH(M*PI*Y/A)-SINH(M*PI*Y/A )
     2 -M*PI*Y/A*COSH(M*PI*Y/A))*COS(M*PI*(X+A/2.)/A)
       WX1=WX1+W1
      WX2=WX2+W2
      WXY=WXY+WA
    1 CONTINUE
   32 CONTINUE
      XX=XX+WX1+WX2
      XY=XY+WXY
      YX=(WX1+WX2)*YX
   11 CONTINUE
      FUNT=  XX**2-2.*(1.-NU)*(YX-XY**2)
      RETURN
      END
C ......................
```

165500

Thesis
B8089 Brito
Reduction of distortion in welded aluminum frame structures.

DISPLAY

3 SEP 76

Thesis
B8089 Brito
Reduction of distortion in welded aluminum frame structures.

165500

thesB8089
Reduction of distortion in welded alumin

3 2768 002 08107 7
DUDLEY KNOX LIBRARY